ACTA UNIVERSITATIS CAROLINAE

AUC **GEOGRAPHICA**

57
1/2022

CHARLES UNIVERSITY • KAROLINUM PRESS

ISSN 0300-5402 (Print)
ISSN 2336-1980 (Online)

Rainfall thresholds of the 2014 Smutná Valley debris flow in Western Tatra Mountains, Carpathians, Slovakia

Tereza Dlabáčková*, Zbyněk Engel

Department of Physical Geography and Geoecology, Faculty of Science, Charles University, Czechia
* Corresponding author: tereza.dlabackova@natur.cuni.cz

ABSTRACT

An extensive debris flow occurred, in the Smutná valley, Western Tatra Mts. in Slovakia on 15 May 2014. The aim of this study is to describe the morphology of the observed debris flow and to evaluate the conditions that preceded its formation as well as the previous activity of debris flows on this path. The observed debris flow is among the most extensive ones in terms of morphometric characteristics in the Roháčská valley and its tributaries (e.g., the length of the erosion-accumulation zone of ~600 m, volume >1200 m^3). However, compared to previous studies from the Western Tatra Mts., it belongs to the average sized debris flows, or a minor event in terms of the general size classification based on the volume of debris flows. A similarly extensive debris flow was recorded on this track in the early 1970s after which only two additional minor events have been recorded there until 2014. The monthly precipitation totals in the 2013/2014 winter season were low compared to the long-term average. The main triggering factor for debris flow initiation was continuous rainfall that lasted 29 hours resulting in ~120–135 mm of precipitation. Most of the derived global empirical thresholds for debris flow initiation were exceeded as well as rainfall thresholds suggested by the published studies for the Western Tatra Mts.

KEYWORDS

debris flow; rainfall thresholds; morphometric analysis; Western Tatra Mts.; Carpathians; Slovakia

Received: 3 September 2021
Accepted: 19 January 2022
Published online: 10 February 2022

Dlabáčková, T., Engel, Z. (2022): Rainfall thresholds of the 2014 Smutná Valley debris flow in Western Tatra Mountains, Carpathians, Slovakia. AUC Geographica 57(1), 3–15
https://doi.org/10.14712/23361980.2022.1

1. Introduction

Debris flows are fast-moving masses of poorly sorted sediments saturated with water, which are among the most frequent slope processes in mountain areas (Iverson et al. 1997; Jakob and Hungr 2005). Steep slopes and the presence of an unconsolidated regolith accumulated in bedrock gullies or stream channels are essential for the occurrence of debris flows (Kotarba et al. 2013). These mass movements are triggered by an intense rainfall which reaches or exceeds certain thresholds (Wieczorek and Glade 2005; Guzzetti et al. 2008). These so-called rainfall thresholds can be defined by the intensity, duration, or amount of rainfall measured over a certain period of time. A rainfall-threshold model based on the intensity and duration of a specific rainfall event (intensity-duration, ID) is most commonly used to evaluate the conditions that preceded the debris flow event (e.g. Caine 1980; Jibson 1989). On the contrary, a model based on the amount of rainfall measured during a rainfall event (event-duration, ED) is used especially when the precipitation intensity is unknown (Caine 1980; Innes 1983; Zezere and Rodrigues 2002). Other types of rainfall thresholds are defined by the total event rainfall (e.g. Corominas and Moya 1996; Pasuto and Silvano 1998) or the intensity of rainfall during the precipitation event (event-intensity, EI; e.g. Jibson 1989; Aleotti 2004). Rainfall thresholds are commonly defined on global (Caine 1980; Innes 1983; Rebetez et al. 1997), regional (e.g. Sandersen et al. 1996; Kanji et al. 2003), or local scales (e.g. Wilson et al. 1992; Annunziati et al. 2000). Global rainfall thresholds represent a general minimum level below which debris flows do not occur irrespective of geology, land-use, or regional rainfall patterns (Guzzetti et al. 2007). By contrast, local rainfall thresholds are site-specific and thus are poorly known in many regions including the Tatra Mts., Western Carpathians.

The research on the precipitation that initiates debris flows in the Tatra Mts. is limited despite the fact that the extensive debris flows occur once in 15–20 years (Krzemień 1988) or even once per 2–3 years in the case of debris flows in the apex of the slope (Kotarba 1991). The research on this phenomenon started in the 1970s (e.g. Ingr and Šarík 1970; Krzemień 1988; Kotarba et al. 1987; Kotarba 1989, 1992, 1997, 1998) but only a few studies focused on the rainfall thresholds for debris flow initiation (e.g. Kotarba 1997) or rainfall conditions preceding the debris flows events (Kotarba 1998). Currently, debris-flow research mostly focuses on changes of debris-flow accumulation zones using aerial imagery (Kapusta et al. 2010; Kedzia 2010) or debris-flow dating by the dendrochronological analysis (e.g. Šilhán and Tichavský 2016, 2017).

In this study, we evaluate the topographic controls and rainfall conditions of the extensive debris-flow event that occurred on 15 May 2014 on the north-eastern slope of Plačlivé peak (2125 m a.s.l.) in the Smutná valley, Western Tatra Mts. as well as the previous activity of debris flows in this path. We compared the obtained threshold values with those established for the Western and High Tatra Mts. in order to obtain more robust threshold values for the region. Finally, we examine the validity of globally defined empirical thresholds for debris flow initiation in this region.

2. Study area

The Tatra Mts. are the highest part of the Carpathian range (Gerlachovský štít peak, 2654 m a.s.l.). The mountains consist of a Paleozoic crystalline basement composed of metamorphic (micaschist, gneiss, migmatite, amphibolite) and igneous rocks (granitic rocks) overlain by late Permian to Cretaceous sedimentary sequences and nappes (limestone, sandstone; Králiková et al. 2014). A tectonic uplift of the Tatra Mts. along the sub-Tatra fault system started in the Middle to early Late Miocene (~12–9 Ma) forming an asymmetrical horst structure surrounded by the Liptov, Poprad, and Podhale basins (Králiková et al. 2014).

Despite their limited extent, the Tatra Mts. represent a barrier for the north-south transport of air masses, which causes steep climate gradients (Niedźwiedź 1992). The mean annual air temperature (MAAT) in the northern foothills is 6 °C, while it is 8 °C in the southern ones. The highest elevations show MAAT of −2 °C (Niedźwiedź et al. 2014; Żmudzka et al. 2015). Similarly, the mean annual precipitation is influenced by prevailing north-west air flow that causes higher precipitation amounts on the northern slopes in comparison to the southern ones (Niedźwiedź 1992). The highest mean annual precipitation of 1600–1900 mm thus occurs on the northern slopes between 1400–2000 m a.s.l. Maximum monthly precipitation falls mainly in June and July when it reaches 240–260 mm and 220–250 mm, respectively (Niedźwiedź 1992). The duration of snow cover varies from 60–140 days in the foothills to about 220 days in the highest parts of the ridge (Ustrnul et al. 2015).

The Smutná valley is one of the side valleys of the more extensive Roháčská valley, Western Tatra Mts. It is located on the northern side of the main ridge of the Western Tatra Mts. (Figure 1) and it is surrounded by the Tri Kopy (2136 m a.s.l.), Ostrý Roháč (2088 m a.s.l.), Volovec (2063 m a.s.l.) and Rákoň (1876 m a.s.l.) peaks. The ridge is built of biotite to two-mica diorites and granites, whereas the valley is filled with Quaternary sediments of taluses, moraines, or rock glaciers (Nemčok 1994; Piotrowska et al. 2015). The investigated debris flow extends from the north-eastern foot of Plačlivé peak (2125 m a.s.l.) to the valley bottom (1503 m a.s.l.).

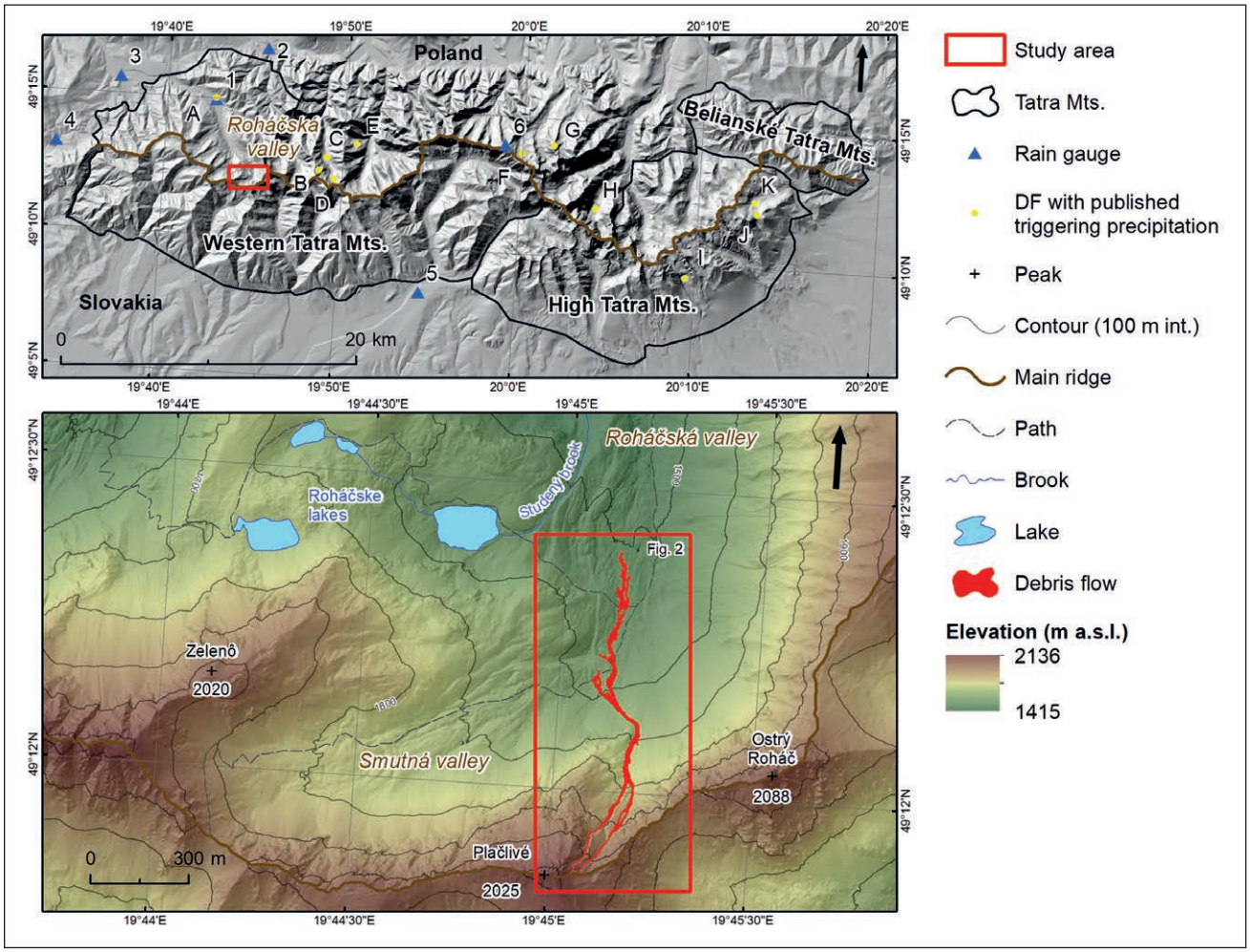

Fig. 1 Location of the study area, selected rain gauges and locations of debris flows with published triggering precipitation in the Tatra Mts. Note: (1) Zuberec-Zverovka (ZZ), (2) Vitanová-Oravice (VO), (3) Zuberec (ZU), (4) Huty (HU), (5) Podbanské (PB), (6) Kasprowy Wierch (KW), (A) Zverovka, (B) Dudowy cirque, (C) Staroróbocianska valley, (D) Staroróbocianski cirque, (E) *Žleb* Piszczałki, (F) Zielony Staw Gasieicowy, (G) *Žółta* Turnia, (H) Morskie Oko lake, (I) Velická valley, (J) Kežmarský *Štít* Peak, (K) Dolina Zeleného plesa, (DF) Debris flow.

3. Methods

3.1 Morphometric analyses of the debris flow

Geomorphological mapping of the debris flow was performed using orthophotomaps from 2015 (Eurosense), a detailed digital elevation model (DEM) with the horizontal resolution of 1 m (ÚGKK SR 2019) and verified by field mapping. The source zone of the debris flow was delineated based on the DEM using the Watershed tool in ArcMap 10.6 (Esri, Inc. 2018) and then manually adjusted, whereas the erosion-accumulation zone was delineated by manual vectorization at a scale of 1 : 500 based on the orthophotomaps. The area and length of the source and erosion-accumulation zones were determined based on the DEM using the 3D analyst - Add surface information tool in ArcMap 10.6 (Esri, Inc. 2018) to avoid inaccurate calculation due to the steep slopes. A minimal volume of debris transported by the debris flow was also derived from the difference between DEM and reconstructed surface before the event.

The spatial extent of the source and erosion-accumulation zones was verified in the field using GPS (Garmin GPSmap 60CSx) and a laser rangefinder (Stanley TLM 210) in July 2015. The field mapping also included measurements of the height of the lateral levees of the debris flow and the size of 5 largest clasts carried by the flow in three segments of erosion-accumulation zone. Temporal changes of the debris flow since 1973 were evaluated using manual vectorization of the erosion-accumulation zone of the debris flow based on the orthorectified aerial photographs from 1973, 1986, 2003 (TOPÚ 2016), and the orthophotos from 2015 (Eurosense). Based on this data the average recurrence interval of debris flow events in this track path was estimated.

3.2 Precipitation analysis

Data from five closest rain gauges and one more distant station operated by the Slovak Hydrometeorological Institute (SHMI 2014) and the Institute of

Tab. 1 Basic characteristics of selected rain gauges.

Weather station	Latitude (N)	Longitude (E)	Elevation (m a. s. l.)	Distance from debris flow (km)
Zuberec-Zverovka (ZZ)	49°14'59"	19°42'42"	1,030	5.8
Vitanová-Oravice (VO)	49°16'57"	19°45'26"	853	8.7
Zuberec (ZU)	49°15'38"	19°37'18"	763	11.3
Huty (HU)	49°13'80"	19°33'54"	808	13.6
Podbanské (PB)	49°08'24"	19°54'38"	972	13.6
Kasprowy Wierch (KW)	49°13'59"	19°58'58"	1,987	17.2

Meteorology and Water Management (NOAA 2016) were used to analyse the rainfall totals that preceded the formation of the debris flow (Table 1). The nearest station Zuberec-Zverovka (ZZ) located only ~6 km from the source zone of the debris flow was considered the most representative as it is also in the north-facing valley of the Western Tatra Mts. and at elevation of 1030 m a.s.l. The Podbanské station (PB) is the only one representing the southern flanks of the mountains. It was chosen because of its relatively small distance from the debris flow (~14 km) and its position at an elevation of almost 1000 m a.s.l. Because some of the closest meteorological stations do not provide continuous precipitation records without measurement failures, additional calculations were done using continuous time series of one more distant station Kasprowy Wierch (KW) located 17 km from the debris flow (NOAA 2016). Daily precipitation data were available for all selected weather stations operated by SHMI, providing accumulated rainfall totals recorded at 7 a.m. In contrast, 6-hour rainfall data are available from Kasprowy Wierch.

Precipitation conditions from the beginning of a climatological winter to the formation of the debris flow (December 2013 to May 2014) were assessed for an overall evaluation of soil saturation, which may have played a role in the initiation of the debris flow. 10-day precipitation sums recorded at all the six stations were analysed and monthly precipitation totals were also calculated for the same period and compared to long-term monthly precipitation averages recorded in the period of 1985–2014 (SHMI 2014; NOAA 2016). For a more detailed analysis of precipitation totals immediately prior to the formation of the debris flow, data recorded at all the weather stations were used. Daily precipitation sums for the period of 1 May to 15 May were analysed, as well as precipitation totals for 24 hours before the debris flow formation (considering the 5 hours from 15 May when the debris flow occurred in the morning hours and 19 hours from 14 May) were calculated.

Global threshold values for debris flow initiation based on the duration of precipitation during the whole rainfall event were derived (ED; Caine 1980, $E = 14.82 \times D^{0.61}$; Innes 1983, $E = 4.93 \times D^{0.504}$). The variable E [mm] in the ED threshold models indicates the amount of precipitation during a given event and the D [h] denotes the duration of the event. These equations indicate rainfall amounts above which debris flows are likely to occur. On the contrary, 4σ method provides a statistically defined threshold for the formation of debris flows that defines relatively extreme values based on long-term precipitation records (Rebetez et al. 1997). In this case cumulative precipitation over three consecutive days in the period of May, June and July 1989–2014 based on KW long-term data series was chosen (Rebetez et al. 1997; Engel et al. 2011). The threshold value for spring/summer period with potential debris flows occurrence was derived. Subsequently, it was compared with the observed 3-day precipitation sums before the Smutná valley debris flow measured at KW station.

4. Results

4.1 Debris flow morphology

The source zone of the debris flow is located at 1657–2013 m a.s.l. on the north-eastern slope of Plačlivé peak and covers the area of 147 570 m^2 (Table 2). It consists of chutes that are from a few decimetres up to a few meters deep, and two small detachment zones with a recently exposed bedrock that are a few decimetres deep and the material of which was probably removed during the debris-flow event (Figure 2 and Figure 3).

The erosion-accumulation zone extends at 1503–1657 m a.s.l. and has the total length of 593 m. The volume of the debris material transported and accumulated during the event is estimated at >1200 m^3. The debris flow runs in the northerly direction along the Mt. Plačlivé ridge, then it sharply changes direction to the northwest and enters the open slope of the debris flow fan. Here, the track is 2–2.4 m deep (Figure 2), ~10 m wide, and reaches an average slope of 25°. Significant lateral levees along the debris flow are 0.2–0.5 m high and generally tend to become higher down the slope. The maximum size of the blocks transported by the debris flow reaches 1.5–3.5 m. The side track of the debris flow diverges in the fan area, which is probably the original straight track of the debris flow formed during the initial phase of the event. The side track was subsequently

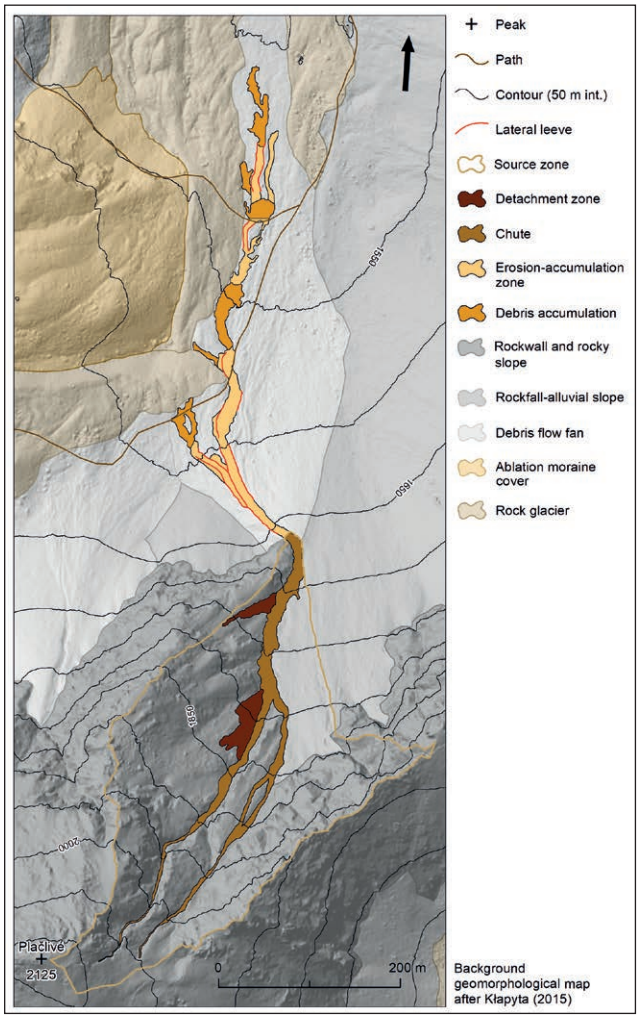

Fig. 2 Geomorphological map of the debris flow in the Smutná valley.

blocked by a stronger surge of the debris flow that deepened the track towards the north.

In the next segment the debris flow undulates slightly in front of a rock-glacier terminus. In this section, the track is ~13 m wide and only 1–1.5 m deep. There is an accumulation of debris inside the track, so it takes on a convex shape, with an average slope of 18°. There is a significant accumulation of debris at an elevation of 1560–1549 m a.s.l. The debris flow here takes on a predominantly convex shape, with the width of about 12 m and the average slope of 12°. This part of the debris flow is already entirely located on the surface of a rock glacier. In the following segment, the debris flow passes through several previously eroded troughs 4–9 m wide that were grassed before the formation of the debris flow. There are lateral levees approximately 0.2 m high. The maximum size of the transported debris is mostly 15 cm and the slope of this part of the track reaches 11°. In the last section of the track, there is only a flat accumulation of the fine-grained debris ~7 cm in size mixed with a sandy matrix. The average width of this final part of the debris flow is 10 m and the average slope is ~8°.

Tab. 2 Morphometric characteristics of the investigated debris flow in the Smutná valley.

Characterictic	Source zone	Erosion-accumulation zone
Area (m²)	147,570	9,687
Length (m)	785	593
Widht (m)	300	13
Maximum elevation (m a.s.l.)	2,123	1,657
Minimum elevation (m a.s.l.)	1,657	1,503
Mean elevation (m a.s.l.)	1,892	1,564
Elevation range (m)	466	156
Maximum slope (°)	88	37
Mean slope (°)	47	19

4.2 Long-term precipitation conditions prior to the debris flow

The most significant snowfall of the 2013/2014 winter season was recorded in the first decade of December 2013 (Figure 4). At that time heavy snowfall occurred mainly in the northern windward areas of the Tatra Mts., bringing up to a few decimetres of snow. By contrast, there was little precipitation for the rest of the month (Figure 4). Overall, monthly precipitation totals lower by 26% (PB) to 59% (ZZ) were recorded in December 2013 compared to the long-term average for 1985–2014 (SHMI 2014). In January 2014, even lower (up to 70% at ZZ station) precipitation totals were recorded compared to the long-term average as no significant snowfall occurred until the second decade of January. During February 2014, precipitation totals were also lower compared to the long-term monthly average with the maximum decrease of 36% at the PB station. The lowest precipitation were recorded mainly in the last decade of the month. On the contrary, precipitation totals in March 2014 were above the long-term average at all the stations by an average of 20%. Increased precipitation was also recorded in April 2014, especially in its second decade when it was up to 30% above the long-term average. Precipitation in May 2014 was also well above the average for 1985–2014 (up to 167% at ZZ station). The highest 10-day precipitation was recorded in the second decade of May when the debris flow occurred (Figure 4).

4.3 Precipitation totals immediately prior to the debris flow

Low daily precipitation totals mostly below 7 mm (ZZ of 2. 5. 2014) were recorded at the weather stations in early May 2014. The exception was PB where the total of 31 mm d^{-1} occurred on 3 May. Precipitation decreased between 8 May to 10 May, with daily totals below 3 mm. After a subsequent short-term increase to ~25 mm d^{-1}, precipitation reached immeasurable amounts. On 14 May, precipitation increased sharply to

Fig. 3 A view of the individual parts of the debris flow.
Note: (1) recently exposed bedrock in the detachment zone, (2) erosion-accumulation zone of the debris flow, (3) debris flow track in the debris flow fan area, (4) debris flow accumulation.

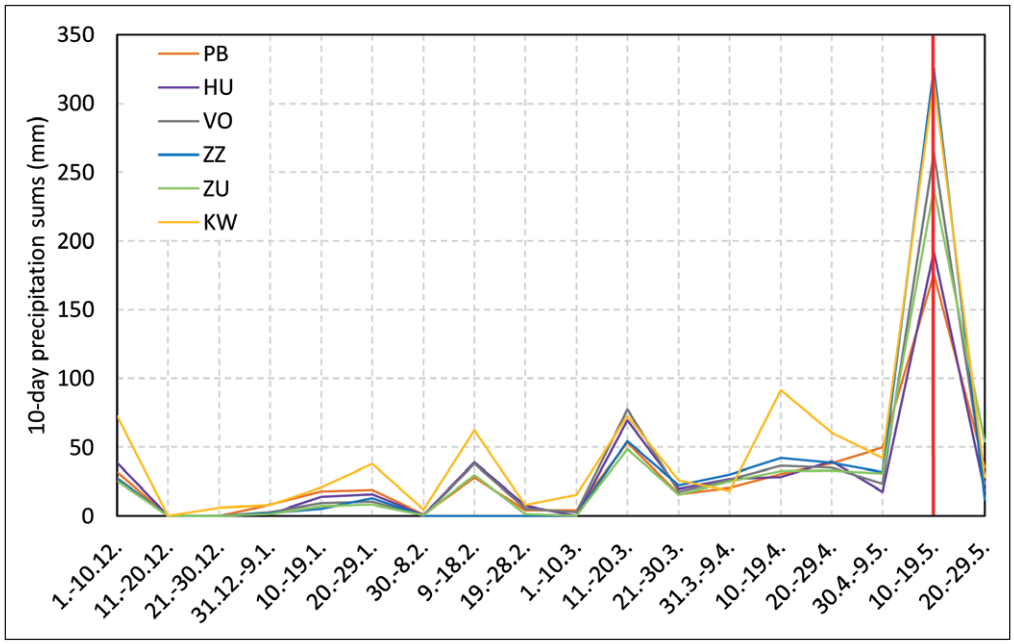

Fig. 4 10-day precipitation sums measured from 1 December 2013 to 29 May 2014.
Note: Red line indicates the occurrence of the debris flow.

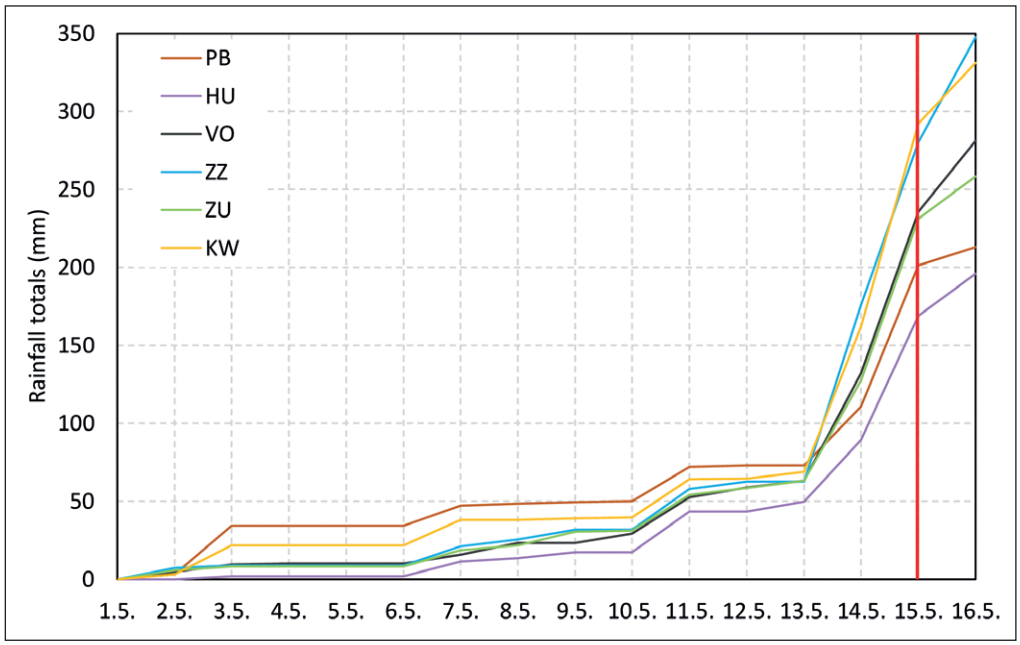

Fig. 5 Cumulative precipitation totals in May 2014.
Note: Red line indicates the occurrence of the debris flow.

>60 mm d^{-1} at the VO and ZU stations or to >90 mm d^{-1} at the KW station. The ZZ station showed the highest total of 113 mm d^{-1} (Figure 5, Table 3). The precipitation was even higher during the following day when the totals >100 mm d^{-1} were recorded at the KW (130 mm), ZZ (104 mm), ZU (104 mm), and VO (103 mm) stations. The debris flow occurred in the morning hours of 15 May 2014. The 24-hour precipitation prior to its formation ranged between 48 mm (HU) and 111 mm (ZZ).

Tab. 3 Precipitation totals before the debris flow formation (15 May 2014).

Station	13 May (mm)	14 May (mm)	15 May (mm)	24 h prior formation (mm)
Zuberec-Zverovka	0	113	104	111
Vitanová-Oravice	5	69	103	76
Zuberec	5	64	104	72
Huty	6	40	80	48
Podbanské	0	38	91	49
Kasprowy Wierch	4	93	130	101

4.4 Rainfall thresholds derived using global rainfall models

Continuous precipitation prior to the formation of the debris flow started at all the weather stations at 7 a.m. on 14 May and continued to 12 a.m. on 15 May. Over 29 hours, 56–135 mm of precipitation was recorded at these stations (Table 4). Corresponding threshold values of 116 mm and 27 mm were derived using the event-duration models proposed by Caine (1980) and Innes (1983), respectively. The threshold value based on the statistical 4σ method (Rebetez et al. 1997) was set at 131 mm.

Tab. 4 Threshold values and precipitation totals derived for the study area.

Station	3-day precipitation (mm)	Threshold value after Rebetez et al. (1997; mm)	Continual event precipitation totals (mm)	Duration of continual precipitation (h)	Threshold value by Caine (1980; mm)	Threshold value by Innes (1983; mm)
Kasprowy Wierch	228	131	***120***	29	116	27
Zuberec-Zverovka	–	–	***135***			
Vitanová-Oravice			*90*			
Zuberec			*86*			
Huty			*56*			
Podbanské			*57*			

Note: The values in bold indicate rainfall totals higher than the Caine's (1980) threshold for debris flow initiation. The rainfalls that exceeded the threshold proposed by Innes (1983) are indicated in italic. Threshold value set by Rebetez et al. (1997) was derived based on the long-term precipitation records for 1989–2014 available only for the Kasprowy Wierch station.

4.5 Temporal changes of the debris flow track

The analysis of historical aerial photographs identified four debris flow events in the investigated track between 1973 and 2015 (43 years), including the debris flow described in this study (Figure 6). The most extensive debris flow over the entire period was recorded in the 1973 aerial photograph (the erosion-accumulation zone was by ~14% larger than in 2015). The front of this accumulation extended ~355 m from the foot of the slope, whereas it was ~330 m in 2015. The length of the whole erosion-accumulation zone was ~624 m in 1973 as opposed to ~593 m in 2015. In contrast, aerial photographs from 1986 and 2003 show a new debris flow extending only to the foot of the slope. An extensive debris flow path from 15 May 2014 is recorded on the 2015 orthophotos. Based on the remotely sensed data, the recurrence interval of the debris flows is nearly 11 years.

5. Discussion

5.1 Morphology of the debris flow

The extent of the source and erosion-accumulation zone of the Smutná valley debris flow is greater than that of other debris flows in the Roháčská valley and its tributary valleys (including the Smutná valley; Dlabáčková 2018). As one of the few debris flows in the Roháčská valley area, it extends from the debris flow fan to the valley floor filled with the body of a rock glacier. However, it is rather an average debris flow in the Western Tatra Mts. in terms of the elevation of the source and erosion-accumulation zone or the volume of the transported material (Kotarba et al. 2013; Kotarba 1992). Its source zone located at 1657–2123 m a.s.l. is within the elevation range of 1293–2217 m a.s.l. of source zones of debris flows in the Western Tatra Mts. set by Kotarba et al. (2013). Similarly, the average elevation of the source zone of 1892 m a.s.l. is close to the average elevation of 1817 m a.s.l. reported by Kotarba et al. (2013). The head of the debris-flow erosion-accumulation zone, situated at an elevation of 1503 m a.s.l., is among the lower debris-flow heads, but also within the interval of the average values (1213–2095 m a.s.l.) determined for the Western Tatra Mts. (Kotarba et al. 2013). Slightly above average is the compound elevation range of the source and erosion-accumulation zone of the debris flow of 620 m compared to the average value of ~500 m reported for the Western Tatra Mts. (Jurczak et al. 2012; Kotarba et al. 2013). By contrast, the length of the debris-flow erosion-accumulation zone of 593 m is well above the average length in the Western Tatra Mts. estimated at 200 and 166 m by Kotarba et al. (2013) and Jurczak et al. (2012), respectively. Yet, the observed length of the debris-flow erosion-accumulation zone falls into the most common debris-flow lengths in the Western Tatra Mts. set by Midriak (1993) at 500–1000 m. Likewise, the average path width of the debris flow erosion zone of 12 m is also within the interval of average debris-flow widths set by Midriak (1993). The estimated volume of the

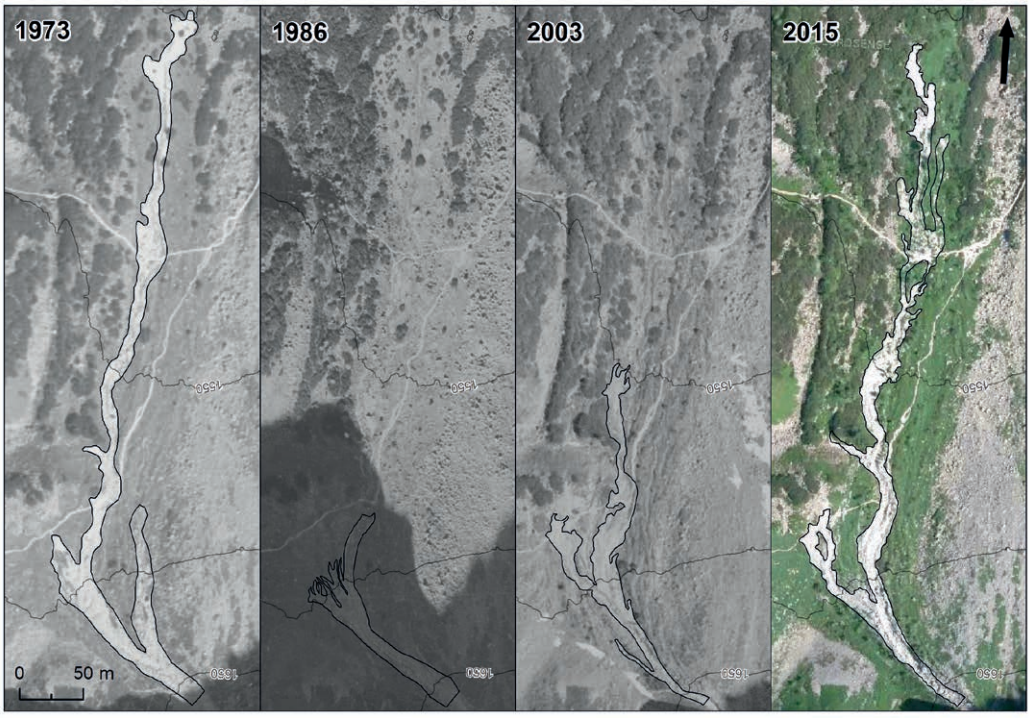

Fig. 6 Temporal changes in the erosion-accumulation zone of the Smutná valley debris flow in the period 1973–2015.

transported material of >1200 m^3 is consistent with the volume estimates for recent debris flows in the Tatra Mts. (Kotarba 1992), representing minor debris-flow events (sensu Jakob 2005). The volume estimates for the largest debris flows in the Tatra Mts. range from 2500 to 5000 m^3 (Ingr and Šárik 1970; Kotarba 1994).

5.2 Triggering precipitation

The rainfall threshold of 27 mm derived using the global event-duration model proposed by Innes (1983) was exceeded at all regional stations. In contrast, the value of 116 mm determined using the event-duration model by Caine (1980) was exceeded only at the stations ZZ and KW (Table 4). These two stations seem to be the most relevant for describing the conditions immediately prior to the 2014 debris flow as both are located at elevations above 1000 m a.s.l. The low precipitation values recorded at other stations are a result of their low elevation, a large distance from the debris flow (HU, PB, and ZU), or the leeward effect of the mountain range (PB). The precipitation threshold of 131 mm derived by the 4σ method (Rebetez et al. 1997) from the KW data proved to be valid as the measured 3-day rainfall total was 228 mm.

Overall, the models proposed by Caine (1980) and Rebetez et al. (1997) are valid for the Tatra Mts. area. On the contrary, model set by Innes (1983) does not seem to be valid for the Tatra Mts. region as the threshold value of 27 mm is too low. Precipitation greater than 27 mm d^{-1} has occurred at KW station approximately 5 times per year during the period 1989–2014 in the months of May to July. This contrasts with the average frequency of one small debris flow per 2–3 years (Krzemień 1988) or one large debris flow event per 15–20 years (Kotarba 1991). The occurrence of debris flows 5 times per year in the Tatra Mts. region thus seems unlikely. In contrast, precipitation exceeding 116 mm d^{-1} occurred approximately once every ten years during the same period, which is close to the published data on the frequency of the formation of debris flows, and information derived from aerial photographs of the monitored debris flow in the Smutná valley. Similarly, 3-day rainfall greater than 131 mm occurred on average once per 2–3 years during this period, which is also consistent with the published data on the frequency of debris flows in the Tatra Mts.

The observed debris flow in the Smutná valley occurred in the morning on 15 May 2014 according to local people. The 6-hour rainfall data from the KW station show that the lowest rainfall of the day (only of 27 mm) was recorded between 6 a.m. and 12 p.m. In contrast, the highest precipitation of 39 mm was recorded between 12 and 6 p.m. (Figure 7). These data indicate that the debris flow may not have occurred during the most intense rainfall.

The precipitation total that led to the 2014 Smutná valley debris flow fits into the rainfall ranges of 60–164 mm d^{-1} and 62–224 mm d^{-1} published for the Western and High Tatra Mts. (Table 5). It was higher compared to the well-described debris flow event on Babia Góra, Poland (>40 mm d^{-1}; Łajczak and Migoń 2007), or debris flows in Southern Carpathians, Romania (74–91 mm d^{-1}; Ilinca 2014). However, it was lower compared to the threshold values of 111–234 mm d^{-1} suggested by Šilhán and Pánek (2010) for the flysch Western Carpathians, Czechia. Outside the Carpathians, debris flows might be triggered after 100 mm d^{-1} in the Jizerské hory

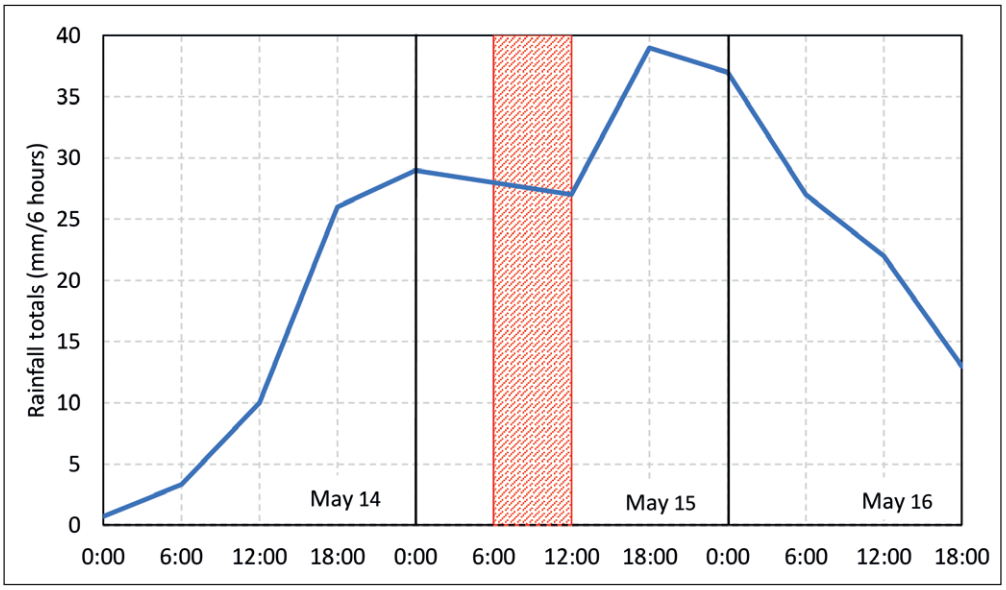

Fig. 7 6-hour precipitation totals recorded at the KW station in 14 May to 16 May.
Note: The approximate time of the debris flow occurrence is indicated by the red hatched area.

Tab. 5 Rainfall thresholds for historical debris flows in the Tatra Mts.

Triggering Rainfall	Location	Date	Author
Western Tatra Mts.			
60–61 mm d^{-1}	Dudowy cirque	20 July 1985	Krzemień (1988)
82.3 mm d^{-1}	Staroróbocianski cirque	26 July 1982	Krzemień (1988)
91.6 mm d^{-1}	Staroróbocianski cirque	23 July 1980	Krzemień (1988)
215.5 mm $2d^{-1}$ (61 mm d^{-1} and 154.5 mm d^{-1})	Zverovka	19 June 1970	Ingr and Šarík (1970)
up to 135 mm $29h^{-1}$ (111 mm $24h^{-1}$)	Smutná valley	15 May 2014	This study
164 mm d^{-1}	Staroróbocianski cirque	June 1973	Krzemień (1988)
73.8 mm $5h^{-1}$	Żleb Piszczałki	4 June 1993	Krzemień et al (1995)
High Tatra Mts.			
62 mm d^{-1} (26 mm h^{-1})	Kežmarský Štít Peak	15 July 1933	Záruba, Mencl (1969)
100 mm d^{-1}	Morskie Oko lake	August 2001	Ferber (2002)
118.7 mm d^{-1} (44 mm h^{-1})	Zielony Staw Gasieicowy	16 August 1988	Kotarba (1994)
223.5 mm d^{-1} (330.3 mm $5d^{-1}$)	Żółta Turnia	8 July 1997	Kotarba (1998)
41.4 mm $1.5h^{-1}$	Morskie Oko lake	23 August 2011	Kotarba et al (2013)
60 mm h^{-1}	Żółta Turnia	9 August 1991	Kotarba (1998)

Tab. 6 Overview of the general rainfall intensity thresholds for debris flow (DF) initiation for the Tatra Mts. region.

Threshold value	Region	Debris flow specification	Reference
50–80 mm d^{-1}	Western Tatra Mts.	DF of various sizes occurring between the end of May – end of July (snow patches occurence)	Krzemień (1988)
80–100 mm d^{-1}	Western Tatra Mts.	DF of various sizes occurring in the period of July–October	Krzemień (1988)
60–135 mm $29h^{-1}$	Western Tatra Mts.	DF over the full length of slope	This study
80–100 mm d^{-1}	High Tatra Mts.	DF over the full length of slope	Kotarba (1997)
35–40 mm h^{-1}	High Tatra Mts.	DF over the full length of slope	Kotarba (2007)
25 mm h^{-1}	Tatra Mts.	Small-scale DF (apex area of talus slope)	Kotarba (1991)
50 mm h^{-1}	Tatra Mts.	DF over the full length of slope	Kotarba (1991)

Mts., Czechia (Smolíková et al. 2016), having similar geological conditions as the study area in the Western Tatra Mts. Similarly, daily rainfall totals exceeding 50–100 mm can trigger debris flows in the Hrubý Jeseník Mts., Czechia, built by metamorphic rocks (Tichavský et al. 2017). The 24-hour rainfalls that triggered the 2014 debris flow are higher than the threshold of 50–80 mm d^{-1} based on long-term observations of debris flows in the May-July period in the presence of snow patches on slopes. The triggering rainfalls are even higher than the rainfall threshold of 80–100 mm d^{-1} for the initiation of debris flows of various sizes in the Western and High Tatra Mts. (Table 6).

5.3 Temporal changes of the debris flow track

The erosion-accumulation zone of the investigated debris flow from May 2014 was among the most extensive ones in the last 43 years (Figure 6). A larger area of debris flow erosion-accumulation zone occurred at this site only in the early 1970s when shallow landslides occurred frequently in the Tatra Mts. (Kotarba 2004; Gądek et al. 2016). By contrast, only one short debris flow was identified in the same track between 1973 and 1986. The observed decrease in the debris flow surface area confirms the timing of a reduced debris-flows activity reported by Kapusta et al. (2010) from the Dolina Zeleného plesa in the High Tatra Mts. (Figure 1). In contrast, these authors did not detect any significant changes in the area of debris flows in the Velická valley in the High Tatra Mts. Krzemień (1988) states that the number of debris-flow events in the Staroróbocianska valley, the Western Tatra Mts., was stable since the 1950s to the mid-1980s.

Aerial photographs taken in 2003 show another debris flow accumulation within the observed track. This debris flow was shorter than the one from the early 1970s but extended to the foot of the slope. Since the mid-1980s to the early 21st century, there was an increase in the area of debris flow erosion-accumulation zones in the High Tatra Mts. (Kapusta et al. 2010; Kedzia 2010). According to Kotarba (1997),

this increase may be attributed to more frequent and intense rainfalls in the summer season. The record from the KW station confirms the frequent occurrence of intense rainfall events in the study area during the period 1986–2003. Precipitation >80 mm d^{-1} was recorded at the KW station 15 times over the 18-year period, 8 of which were even >100 mm d^{-1}.

In the period of 2003–2015, the number of days with rainfalls exceeding the threshold value of 80–100 mm d^{-1} decreased to seven at the KW station. Despite the lower frequency of heavy rainfalls, the rainfall totals higher than 130 mm d^{-1} occurred in August 2009 and May 2014. As a result of fewer rainfall events, there was no increase in the area of debris flows at the study site until 2014. Similarly, Kedzia (2010) reported no significant changes of debris flows in the Żółta Turnia, High Tatra Mts., between 2003 and 2009. By contrast, a significant increase in the area of debris-flows in the Velká Studená valley, High Tatra Mts., between 2004 and 2014 is reported by Šilhán and Tichavský (2017).

6. Conclusion

The debris flow in the Smutná valley, Western Tatra Mts., was initiated on 15 May 2014 after continuous precipitation that lasted 29 hours. A corresponding rainfall ranged from ~120 to 135 mm and exceeded the threshold values for debris flow initiation derived from global event-duration models (27 and 116 mm). A 4σ threshold of 131 mm for the accumulated precipitation on three consecutive days prior to the debris flow initiation was also exceeded. The 24-hour rainfall amount of 101–111 mm recorded prior the debris flow is rather high compared to the reported values from the Tatra Mts., Babia Góra, and the more distant Southern Carpathians.

The debris flow that was formed in the Smutná valley in 2014 is one of the largest debris-flow accumulations in the northern part of the Western Tatra Mts. The erosion-accumulation zone extends far to the valley floor, stretching over the length of ~600 m. A similarly long debris flow was identified in this track only in the early 1970s. Two other debris flows deposited in this track between 1986 and 2003 only reached the foot of the slope.

Acknowledgements

The research was funded by the Grant Agency of Charles University (project no. 1528119). The Tatra National Park Administration is thanked for providing permission to work in the region. The authors are grateful to Jana Kovářová for her assistance with fieldwork and to Tomáš Uxa for his comments on an earlier version of the manuscript.

References

Aleotti, P. (2004): A warning system for rainfall-induced shallow failures. Engineering Geology 73, 247–265, https://doi.org/10.1016/j.enggeo.2004.01.007.

Annunziati, A., Focardi, A., Focardi, P., Martello, S., Vannocci, P. (2000): Analysis of the rainfall thresholds that induced debris flows in the area of Apuan Alps – Tuscany, Italy (19 June 1996 storm). In: Proceedings EGS Plinius Conference on Mediterranean Storms, Maratea, Italy, 485–493.

Caine, N. (1980): The Rainfall Intensity: Duration Control of Shallow Landslides and Debris Flows. Geografiska Annaler 62A(1–2), 23–27, https://doi.org/10.1080/04353676.1980.11879996.

Corominas, J., Moya, J. (1996): Historical landslides in the Eastern Pyrenees and their relation to rainy events. In: J. Chacon, C. Irigaray, T. Fernandez (Eds.), Landslides. A.A. Balkema, Rotterdam, 125–132.

Dlabáčková, T. (2018): Geomorfologické podmínky murových procesů v centrální části Západních Tater. Diploma thesis, Department of Physical Geography and Geoecology, Faculty of Science, Charles University, Prague.

Engel, Z., Česák, J., Escobar, V. R. (2011): Rainfall-related debris flows in Carhuacocha Valley, Cordillera Huayhuash, Peru. Landslides 8(3), 269–278, https://doi.org/10.1007/s10346-011-0259-7.

Ferber, T. (2002): The age and origin of talus cones in the light of lichenometric research. The Skalnisty and Zielony talus cones, High Tatra Mountains, Poland. Studia Geomorphologica Carpatho-Balcanica 36, 77–89.

Gądek, B., Grabiec, M., Kędzia, S., Rączkowska, Z. (2016): Reflection of climate changes in the structure and morphodynamics of talus slopes (the Tatra Mountains, Poland). Geomorphology 263, 39–49, https://doi.org/10.1016/j.geomorph.2016.03.024.

Guzzetti, F., Peruccacci, S., Rossi, M., Stark, C. P. (2007): Rainfall thresholds for the initiation of landslides in central and southern Europe. Meteorology and Atmospheric Physics 98(3), 239–267, https://doi.org/10.1007/s00703-007-0262-7.

Guzzetti, F., Peruccacci, S., Rossi, M., Stark, C. (2008): The rainfall intensity-duration control of shallow landslides and debris flows: An update. Landslides 5(1), 3–17, https://doi.org/10.1007/s10346-007-0112-1.

Ilinca, V. (2014): Characteristics of debris flows from the lower part of the Lotru River basin (South Carpathians, Romania). Landslides 11(3), 505–512, https://doi.org/10.1007/s10346-014-0489-6.

Ingr, M., Šarík, I. (1970): Suťový prúd v Roháčoch. Mineralia Slovaca 2(8), 309–313.

Innes, J. L. (1983): Debris flows. Progress in Physical Geography 7(4), 469–501, https://doi.org/10.1177/030913338300700401.

Iverson, R. M. (1997): The physics of debris flows. Reviews of Geophysics 35(3), 245–296, https://doi.org/10.1029/97RG00426.

Jakob, M. (2005): A size classification for debris flows. Engineering geology 79(3–4), 151–161, https://doi.org/10.1016/j.enggeo.2005.01.006.

Jakob, M., Hungr, O. (2005): Introduction. In: M. Jakob, O. Hungr (Eds.), Debris-flow hazards and related

phenomena. Springer, Berlin, https://doi.org/10.1007/3-540-27129-5_1.
Jibson, R. W. (1989): Debris flow in southern Porto Rico. Geological Society of America, Special Paper 236, 29–55, https://doi.org/10.1130/SPE236-p29.
Jurczak, P., Migoń, P., Kaczka, R. (2012): Występowanie i wybrane cechy morfometryczne szlaków spływów gruzowych w Tatrach i Karkonoszach. Czasopismo Geograficzne 83(1–2), 29–46.
Kanji, M. A., Massad, F., Cruz, P. T. (2003): Debris flows in areas of residual soils: occurrence and characteristics. Int. Workshop on Occurrence and Mechanisms of Flows in Natural Slopes and Earthfills. Associacione Geotecnica Italiana, Sorrento, 1–11.
Kapusta, J., Stankoviansky, M., Boltižiar, M. (2010): Changes in activity and geomorphic effectiveness of debris flows in the High Tatra Mts. within the last six decades (on the example of the Velická dolina and Dolina Zeleného plesa valleys). Studia Geomorphologica Carpatho-Balcanica 44, 5–34.
Kedzia, S. (2010): The age of debris surfaces on the Żółta Turnia Peak (the Polish Tatra Mts.). Geomorphologia Slovaca et Bohemica 10(2), 29–38.
Kłapyta, P. (2015): Relief of selected parts of the Western Tatra Mountains. In: K. Dabrowska, M. Guzik (Eds.), Atlas of the Tatra Mountains: Abiotic Nature. TPN, Zakopane.
Kotarba, A., Kaszowski, L., Krzemień, K. (1987): High-mountain denudational system of the Polish Tatra Mountains. Ossolineum, Wrocław.
Kotarba, A. (1989): On the age of debris flows in the Tatra Mountains. Studia Geomorphologica Carpatho-Balcanica 23, 139–152.
Kotarba, A. (1991): On the Ages and Magnitude of Debris Flows in the Polish Tatra Mountains. Bulletin of the Polish Academy of Sciences 39(2), 129–135.
Kotarba, A. (1992): High-energy geomorphic events in the Polish Tatra Mountains. Geografiska Annaler 74A(2–3), 123–131, https://doi.org/10.1080/04353676.1992.11880356.
Kotarba, A. (1994): Geomorfologiczne skutki katastrofalnych letnich ulew w Tatrach Wysokich. Acta Universitatis Nicolai Copernici, Geografia 27, 21–34.
Kotarba, A. (1997): Formation of high-mountain talus slopes related to debris-flow activity in the High Tatra Mountains. Permafrost and Periglacial Processes 8(2), 191–204, https://doi.org/10.1002/(SICI)1099-1530(199732)8:2<191::AID-PPP250>3.0.CO;2-H.
Kotarba, A. (1998): Morfogenetyczna rola opadow deszczowych w modelowaniu rzezby Tatr podczas letniej powodzi w roku 1997. Dokumentacja Geograficzna 12, 9–23.
Kotarba, A. (2004): Zdarzenia geomorfologiczne w Tatrach Wysokich podczas małej epoki lodowej. Rola Małej Epoki Lodowej w przekształcaniu środowiska przyrodniczego Tatr. Prace Geograficzne 197, 9–55.
Kotarba, A. (2007): Geomorphic activity of debris flows in the Tatra Mts. and in other European mountains. Geographia Polonica 80(2), 137–150.
Kotarba, A., Rączkowska, Z., Długosz, M., Boltižiar, M. (2013): Recent Debris Flows in the Tatra Mountains. In: D. Lóczy (Ed.), Geomorphological impacts of extreme weather: Case Studies from Central and Eastern Europe. Springer, Dordrecht, https://doi.org/10.1007/978-94-007-6301-2_14.
Králiková, S., Vojtko, R., Sliva, Ľ., Minár, J., Fügenschuh, B., Kováč, M. Hók, J. (2014): Cretaceous-Quaternary tectonic evolution of the Tatra Mts (Western Carpathians): constraints from structural, sedimentary, geomorphological, and fission track data. Geologica Carpathica 65(4), 307–326, https://doi.org/10.2478/geoca-2014-0021.
Krzemień, K. (1988): The dynamics of debris flows in the upper part of the Staroróbocianska valley (Western Tatra Mts). Studia Geomorphologica Carpatho-Balcanica 22, 123–144.
Krzemień, K., Libelt, P., Mączka, T. (1995): Geomorphological conditions of the timberline in the Western Tatra Mountains. Seszyty Naukowe Uniwersytetu Jagiellonskiego, Prace Geograficzne 98, 153–170.
Łajczak, A., Migoń, P. (2007): The 2002 debris flow in the Babia Góra massif–implications for the interpretation of mountainous geomorphic systems. Studia Geomorphologica Carpatho-Balcanica 41, 97–116.
Midriak, R. (1993): Západné Tatry – reliéf, ohrozenosť a deštrukcia ich povrchu. Osveta, Martin, 51–86.
Nemčok, J., Bezák, V., Biely, A., Gorek, A., Gross, P., Halouzka, R., Janák, R., Kahan, M., Mello, Š., Reichwalder, J., Zelman, J. (1994). Geologická mapa Tatier 1 : 50 000 [Geological map of the Tatra Mts. 1 : 50 000]. State Geological Institute of Dionýz Štúr, Bratislava.
Niedźwiedź, T. (1992): Climate of the Tatra Mountains. Mountain Research and Development 12, 131–146, https://doi.org/10.2307/3673787.
Niedźwiedź, T., Łupikasza, E., Pińskwar, I., Kundzewicz, Z. W., Stoffel, M., Małarzewski, Ł. (2015): Variability of high rainfalls and related synoptic situations causing heavy floods at the northern foothills of the Tatra Mountains. Theoretical and Applied Climatology, 119(1), 273-284, https://doi.org/10.1007/s00704-014-1108-0.
Pasuto, A., Silvano, S. (1998): Rainfall as a trigger of shallow mass movements. A case study in the Dolomites, Italy. Environmental Geology 35(2–3), 184–189, https://doi.org/10.1007/s002540050304.
Piotrowska, K. Danel, W., Iwanow, A., Gaździcka, E., Rączkowski, W., Bezák, V., Maglay, J., Polák, M., Kohút, M., Gross, P. (2015): Geology. In: K. Dabrowska, M. Guzik (Eds.), Atlas of the Tatra Mountains: Abiotic Nature. TPN, Zakopane.
Rebetez, M., Lugon, R., Baeriswyl, P. A. (1997): Climatic change and debris flows in high mountain regions: the case study of the Ritigraben torrent (Swiss Alps). Climatic change 36, 371–389, https://doi.org/10.1007/978-94-015-8905-5_8.
Sandersen, F., Bakkehøi, S., Hestnes, E., Lied, K. (1996): The influence of meteorological factors on the initiation of debris flows, rockfalls, rockslides and rockmass stability. In: K. Senneset (Ed.), Landslides. A.A. Balkema, Rotterdam, 97–114.
Smolíková, J., Blahut, J., Vilímek, V. (2016): Analysis of rainfall preceding debris flows on the Smědavská hora Mt., Jizerské hory Mts., Czech Republic. Landslides 13(4), 683–696, https://doi.org/10.1007/s10346-015-0601-6.
Šilhán, K., Pánek, T. (2010): Fossil and recent debris flows in medium–high mountains (Moravskoslezské Beskydy Mts, Czech Republic). Geomorphology, 124(3–4), 238–249, https://doi.org/10.1016/j.geomorph.2010.03.026.

Šilhán, K., Tichavský, R. (2016): Recent increase in debris flow activity in the Tatras Mountains: Results of a regional dendrogeomorphic reconstruction. Catena 143, 221–231, https://doi.org/10.1016/j.catena.2016.04.015.

Šilhán, K., Tichavský, R. (2017): Snow avalanche and debris flow activity in the High Tatras Mountains: New data from using dendrogeomorphic survey. Cold Regions Science and Technology 134, 45–53, https://doi.org/10.1016/j.coldregions.2016.12.002.

Tichavský, R., Šilhán, K., Tolasz, R. (2017): Tree ring-based chronology of hydro-geomorphic processes as a fundament for identification of hydro-meteorological triggers in the Hrubý Jeseník Mountains (Central Europe). Science of the Total Environment, 579, 1904–1917, https://doi.org/10.1016/j.scitotenv.2016.12.073.

Ustrnul, Z., Walawender, E., Czekierda, D., Šťastný, P., Lapin, M., Mikulová, K. (2015): Precipitation and snow cover. In: K. Dabrowska, M. Guzik (Eds.), Atlas of the Tatra Mountains: Abiotic Nature. TPN, Zakopane.

Wieczorek, G. F., Glade, T. (2005): Climatic factors infuencing occurrence of debris flows. In: M. Jakob, O. Hungr (Eds.), Debris flow hazard and related phenomena. Springer, Berlin, 325–362, https://doi.org/10.1007/3-540-27129-5_14.

Wilson, R. C., Torikai, J. D., Ellen, S. D. (1992): Development of rainfall thresholds for debris flows in the Honolulu District, Oahu. US Geological Survey Open-File Report 92–521.

Záruba, Q., Mencl, V. (1969): Landslides and their control. Elsevier, New York.

Zezere, J. L., Rodrigues, M. L. (2002): Rainfall thresholds for landsliding in Lisbon Area (Portugal). In: J. Rybář, J. Stemberk, P. Wagner (Eds.), Landslides. Routledge, London, 333–338, https://doi.org/10.1201/9780203749197.

Żmudzka, E., Nejedlík, P., Mikulová, K. (2015): Temperature, thermal indices. In: K. Dabrowska, M. Guzik (Eds.), Atlas of the Tatra Mountains: Abiotic Nature. TPN, Zakopane.

Kyiv metro and urban imageability: a student youth vision

Oleksiy Gnatiuk*, Olena Kononenko, Kostyantyn Mezentsev

Taras Shevchenko National University of Kyiv, Department of Economic and Social Geography, Ukraine
* Corresponding author: alexgnat22@ukr.net

ABSTRACT

This paper aims to reveal and explain the role of metro stations in a post-socialist metropolis as nodes that determine the perception of the city. By means of Lynch-type mental maps, we sought to find whether metro stations really function as perceptual nodes concentrating urban functions and traffic, and how recent changes of urban built environment and functions induced by neoliberal policy are reflected in the public perception. The results are discussed in relation to transit-oriented development that considers public transport stations and spaces around them as community hubs. The study has confirmed the expectation that the metro system constitutes an important part of the urban image and often functions as a skeleton that is used to arrange and frame the mental map of the city. Most of the metro stations function as perceptual nodes concentrating a particular urban function (monofunctional nodes) or combination of different functions (multifunctional nodes). The current perception of nodal areas around the metro stations reflects the recent transformation of urban built environment and functions, including intense and sometimes aggressive commercialization, as well as deindustrialization, although the role of open green public spaces and waterfronts continues to be important. To promote economic development and produce a more comfortable living environment, the metro-related nodal areas need to balance different functions, resisting abusive commercialization and promoting, keeping, and creating open public spaces, green areas and heritage protections.

KEYWORDS

metro stations; city nodal areas; mental maps; urban structure; Kyiv

Received: 30 August 2022
Accepted: 7 February 2022
Published online: 14 February 2022

Gnatiuk, O., Kononenko, O., Mezentsev, K. (2022): Kyiv metro and urban imageability: a student youth vision.
AUC Geographica 57(1), 16–30
https://doi.org/10.14712/23361980.2022.2

1. Introduction

Whatever the specific concept of urban development is used, the idea of nodes invariably plays an essential role in it. Playing the leading role in the urban planning structure, nodal areas concentrate processes crucial to the life of the city and related city functions (Dronova and Brunn 2018). A system of nodes together with linking paths constitutes a network that unites a city into a single organism and provides access in between its different parts (Cheng et al. 2013). At the same time, they belong to the key elements shaping the urban image and thus largely determine the public perception of the entire city and its individual parts, influencing the behaviour of urban development actors (Cheng et al. 2013). The complex urban forms are stored in our memory in the form of a linked-node configuration, and the process of acquiring spatial knowledge involves continuously adding new nodes to the existing node-link framework (King and Golledge 1978; Yoshimura et al. 2020).

Nowadays, the cities are recognized main foci and drivers of development on different spatial scales, from local to global (Hall 1993; Sassen 2016), and urban nodal areas usually first are facing and mirroring social, economical and cultural challenges, in particular those related to globalization and pervasive neoliberalism. Especially this is true for post-communist cities that during the last decades are being adapted and remodelled to new conditions shaped by the political, economic, and cultural transition to capitalism (Sýkora 2009; Sýkora and Bouzarovski 2012), while neoliberalism is acknowledged as the dominant ideology driving post-communism (Sailer-Fliege 1999; Birch and Mykhnenko 2010; Stenning et al. 2010). Therefore, understanding the processes of functional and morphological transformation of urban nodal areas and their perception gives a clue to understanding the whole transition of the post-communist cities to the market economy.

Among the various types of nodes that may be encountered in the city, specific place belongs to the stations of rapid transit transport, in particular subway/metro stations. In particular, this is true for the largest post-Soviet cities, where the metro was more than just a transport but also an imposing monument to the communist state, a "church of Soviet civilization" (Jenks 2000). Metro stations provide the surroundings with access to places of employment and other social activity, but at the same time they form new points of growth and intense transformation, changing the local built environment, as well as labour and real estate markets (e.g. Cervero and Duncan 2002; Duncan 2011; Roukoni et al. 2012; Forouhar 2016; Li 2019). The role of metro stations as local growth poles is especially important in the framework of transit-oriented development (TOD) and urban polycentricity concepts aimed at urban sustainable development (cf. Bertolini 1999; Dittmar and Ohland 2004). Centralisation of activities and developments around metro station areas is a key TOD policy to encourage more public transport travel through providing maximum access to passengers, thereby enhancing economic efficiency, health, well-being and social inclusion (Zhang et al. 2019).

In this paper, using mental map technique (Lynch 1960), we seek principally to find out to what extent the metro system contributes to the urban imageability (and, consequently, urban identity) of Kyiv, the capital of Ukraine and third of the largest post-Soviet metropolises. In other words, we want to know a role of the metro system in shaping the residents' representations on the city: how significant is its impact on the image of the city in the whole and its individual parts? If this role is significant, which can be supposed from the literature, the individual mental maps of Kyiv should be structured around metro lines and stations, including individual objects and places in the city tied to individual metro stations as urban nodal areas. It can be expected also that some vernacular urban districts will be shaped around metro stations (node-based districts) rather than based on historical urban areas (uniform districts). The question posed is all the more interesting keeping in mind the recent trend of expanding ridesharing taxi services (e.g., Uber, Bolt, Uklon) and the network of bicycle paths. However, it should be mentioned that the bicycle path networks in Kyiv often are starting from the metro stations, and the stop of the metro during the Covid-19 pandemic restrictions in the spring 2020 actually resulted, according to the author's personal experiences, in the collapse of transport communications in the city). On the other hand, if Kyiv metro stations really function as perceptual nodes, it would be yielding to look at their identities in order to access the reflections of recent transformation of urban built environment and functions in the conditions of neoliberal policies.

Thus, starting from the general assessment of the importance of metro system for building the image of the city, we shift to the images (identities) of particular metro stations and access whether they really function as perceptual nodes concentrating urban functions and traffic. After that, the perceptual portraits of the metro stations are examined in order to understand whether and how the recent changes of urban built environment and functions are reflected in the perception of the informants. Finally, we compare our results with the findings of previous study using different methodology (Dronova and Brunn 2018) to evaluate the correspondence between the subjective perceptions and the fact-based evaluation of Kyiv nodal areas.

2. Theoretical background

Kevin Lynch, discussing spatial elements of the mental map of the city in his seminal work (Lynch 1960),

defined a node in two ways. The first types of nodes are junctions of paths, and thus they are points where a decision on the further direction of movement takes place. Lynch argues that "the junction, or place of a break in transportation, has compelling importance for the city observer. Because decisions must be made at junctions, people heighten their attention at such places and perceive nearby elements with more than normal clarity". The second type of nodes includes places of concentration of some special properties (e.g. typical space, planting, activity, etc.). These condensation points can, by radiation, organize large areas around themselves if their presence is somehow signalized in the surroundings. Consequently, some of these concentration nodes are the foci and epitomes of perceptual districts, over which their influence radiates, and of which they stand as symbols. Some nodes may be both junctions and concentrations at the same time. The distinction between these two types of nodes is questioned as it may not be especially informative and somewhat ambiguous (Dalton and Bafna 2003).

Nodes, together with paths and edges, describe the fundamental topological structure of space in relation to movement and visibility; they are "places of heightened awareness and decision-making where people slow down or stop and make choices about what they will do next and where they are going", and thus the functional and aesthetic environments of nodes play a significant role in creating a sense of place (Stevens 2006). They are not merely cognitive, but also behavioural elements, shaping fundamental topological structure of urban space in relation to movement and visibility (Norberg-Schulz 1971, 1980). Urban networks can morphologically be described as major nodes or concentrations of activities and physical and/or functional connections between nodes (Cheng et al. 2012). Like the other elements of a mental map, nodes may have high imageability not only because of their visual stimulus, but due to certain historical or cultural meaning or playing a role of urban spiritual centre (Mumford 1961; Appleyard 1969; Golledge et al. 1978; Hospers 2010; Jiang 2012). Nodes are not only strengthened by the presence of landmarks but provide a setting which almost guarantees attention for any of the latter. At the same time, nodes are more remarkable if provided with one or two objects which are foci of attention. In any event, Lynch argues, the most successful node seemed both to be unique in some way and at the same time to intensify some surrounding characteristic. Also, names and meanings are non-physical characteristics that may enhance the imageability of a node element; names, for example, are important in crystallizing identity (Lynch 1960).

Following Lynch's definition of nodes, Dronova and Brunn (2018) consider them as places or strategic points (foci) of the city that (1) have free access, (2) are mainly located at the crossroads of important transport routes, (3) have a large concentration of urban functions, and (4) are characterized by both centripetal and centrifugal flows. The emergence of these "intersections of processes" leads to a concentration of transport, cultural, economic, social, administrative, communication, and service functions. They implicitly distinguish between a node and a surrounding "nodal area", which is experiencing the influence of the node and is perceived together with it as a single spatial entity.

The original experience of Lynch (1960) showed that subway stations, strung along their invisible path systems, often play the role of strategic junction nodes. In particular, in the case of Boston, some respondents organized the rest of the city around them while making the sketch. Most of the key stations were associated with some key surface feature, had distinct individual characteristics and thus easy to recognize. Simultaneously, some other stations had not so prominent identities, probably due lack of visual interest and the disassociation of the subway node from the street crossing. In view of this, Lynch suggested that a detailed analysis of the imageability of subway systems, as a kind of transit systems in general, would be both useful and fascinating.

More recent analysis of hand-annotated maps showing the locations of prominent places of Boston also suggests that subway stops play an important role in framing a person's mental map (Look and Shrobe 2007). In particular, it was shown that all of the prominent places, marked by the respondents, were extremely close to subway stops (all within 280 meters, with many places located at a subway stop). Conversely, a large majority of the subway stops were within 50 meters of prominent places. It is suggested that, on the one hand, subway stations themselves may be use for structuring mental maps, but on the other, subway stations are often located near important places and these places or features bring to the importance of subway stations.

The role of metro stations as nodes in Moscow, the largest post-socialist metropolis, has been revealed by James Schrader (The Village 2014; Urban Look 2014). Schrader emphasizes the uniqueness of the role of metro in Moscow, opposing the Russian capital to Western metropolises like New York or Los Angeles, where the metro network determines both urban development and the perception of the city to a much lesser extent. He argues that the metro has drastically changed the way people move around the city and thus affected their perception of the city. Metro stations become spatially isolated access points to the surface areas in their immediate vicinity (up to 500 meters). A circle of this diameter is a nodal area shaped around the station. At the same time, it is more difficult for a person to get to the area outside such nodal areas. Furthermore, while travelling, metro passenger usually cannot observe the city space located between the stations. Consequently, the metro turns into something like a horizontal elevator

or a teleportation device that transports people from one point to another through "nowhere" between the beginning and end of the journey. In this way, the city, perceived by a regular metro user, is divided into numerous small nodal areas around the stations, which in turn become a kind of magnet for a variety of functions: residential and commercial real estate, public spaces, and stops for land-based public transport. The adaptation of the urban structure to the configuration of metro stations, turning them into hubs of economic and social activity, has become especially pronounced in the last two decades. The city is being transformed into a set of nodal areas with a metro station in the centre; each of them provides the locals with the entire infrastructure for a comfortable life.

The idea of transforming the city into a set of relatively independent neighbourhoods around metro stations resonates with the concept of transit-oriented development. Among other things, TOD traits include public and civic spaces near public transport stations as community hubs. A multimodal TOD neighbourhood is built around a public transport station or stop, surrounded by relatively high density development with progressively lower-density development spreading outward from the centre. Typical radius of such neighbourhood is 400 to 800 metres – this is considered to be an acceptable walking distance at the start or end of a journey by transit (ITDP 2017). Although it has been shown that the TOD, by improving transportation accessibility, can promote economic development, as well as produce more comfortable living environment (Cervero and Duncan 2002; Gibbons and Machin 2005; Ahlfeldt and Wendland 2009; Duncan 2011; Roukoni et al. 2012), the concept is criticized, as it has raised concerns about gentrification, displacement, re-segregation, and more polarization (Jones and Ley 2016; Renne et al. 2016; Dong 2016, 2017; Derakhti and Baeten 2020). In view of this, the issue of metro stations as foci of urban nodal areas, including their perceptual characteristics, is important not only for urban theory, but for practitioners as well. While cities without a metro usually show a decrease in the density of all functions from the centre to the periphery, with the advent of rapid transit, the density of functions is differentiated based upon the distance from the stations (Osietrin and Omelchuk 2008). Therefore, urban areas around the metro stations possess a high value in terms of urban planning and require a special approach to functional zoning and transport planning solutions aimed at intensifying all urban functions (Osietrin and Omelchuk 2008; Avdiejeva and Bila 2016).

3. Case study area

Kyiv, the capital and largest city of Ukraine, with current registered population of ca. 2,970,000, has experienced intensive socio-economic and spatial transformations in recent decades. New developments typically are associated with deindustrialization, commercialization, especially construction of shopping malls, and housing, which leads to the growing functional diversification of the urban space, its increasing patchiness. Transformation of urban public spaces consists in their commercialization, sacralization (de-sacralization), and domestification; the role of malls as public spaces is increasing with simultaneous significant reduction of the role of squares and parks (Mezentseva and Mezentsev 2017). According to Dronova and Brunn (2018), most of 45 existing and potential nodal areas of Kyiv are experiencing replacement of the cultural, aesthetic, representative, and communication functions by commercial, service, and transport land uses. The development of city and the transformation of urban space largely depend on the private investors, their interests and visions (Mezentseva and Mezentsev 2017). The city gradually loses its original appearance and becomes a cosmopolitan place associated with all kinds of investment projects (Maruniak 2013; Dronova and Maruniak 2019), while modernization, being the positive side of neoliberal development, goes together with replication of monotonous urban landscapes and creation of monstrous forms (Cybrivsky 2014).

The Kyiv Metro is the third among both oldest and largest metro systems in the former Soviet Union, after Moscow and St. Petersburg. It has three lines, having proper names but publicly known by colour designations as "red", "blue" and "green", and 52 stations. In the whole, the red line is the oldest one, while the green line is the newest. In the recent years, the system accounts approximately for a half of Kyiv's public transport load. Three existing lines, intersecting in the city centre, connect the peripheral areas located in opposite directions and basically follow the key surface roads and city-planning axes, serving the areas with high densities of population, jobs and services. However, some vast and densely populated areas of the city are still not covered with the metro network. In particular, this refers to large mass housing neighbourhoods in the north-eastern (Troieshchyna), north-western (Vynohradar) and south-western (Borshchahivka) sectors of the city (Osietrin and Omelchuk 2008). The construction of the fourth "grey" metro line, which is to connect Zhuliany Airport in the southwest of the city and Troieshchyna neighbourhood with more than 400,000 inhabitants in the northeast, was started in 1993 but has been repeatedly postponed and become the subject of jokes (e.g. "man will land on Mars sooner than build a metro to Troieshchyna").

In most cases, metro stations in Kyiv function as urban planning centres (nodal areas). However, there are problematic issues related to the planning and functions of the urban areas around the metro stations. With the transition to a market economy, the territory of high-speed transport has become

attractive for the implementation of various investment projects, including shopping malls and business centres (Osietrin and Omelchuk 2008). Some key nodal areas around the metro stations in the city centre have undergone complex reconstruction, e.g. Maidan Nezalezhnosti, the main square of Kyiv, a venue for political and cultural events of national scale (including construction of underground shopping mall Globus), and Kontraktova Square, the urban public centre of Podil neighbourhood, concentrating business centres and the main offices of the largest banking institutions (Dronova and Polieshko 2017; Bondar 2018).

4. Data and methods

The research is based on the analysis of Lynch-type mental maps (Lynch 1960) drawn by the 2–3 year bachelor geography students in 2018–2019. Each student was asked "to make a sketch map of Kyiv from his/her perspective marking the most prominent and important places, including streets, squares, neighbourhoods, buildings, public places and other landmarks, etc." without receiving additional suggestions from the researchers. This is extremely important because the research is very susceptible to the occurrence of the so-called "interviewer effect", which may influence the resulting sketch substantially (Nawrocki 2017). A total of 31 maps were selected for further processing; the remaining 9 sketches were considered to be unsuitable for analysis (e.g. depicting the contours of the city only). The respondents had approximately one hour to perform a task. Among the students, whose sketches were selected for the research, 25 (80.6%) came from different Ukrainian regions and lived in campus dormitory, while the rest 6 (19.4%) were native Kyivans. Since mental maps were created by geography students, they may be artistically expressive more than it could be expected in case of ordinary people, but this fact is unlikely to affect the list of places and objects depicted on the maps, and therefore cannot have a significant impact on the conclusions.

The first part of the analysis involved general assessment of the importance of metro system for building the image of the city. To perform this task, we (1) classified mental maps according to the role of metro system in the total graphic structure of the individual sketches, (2) examined the spatial distribution of landmarks, marked on the sketches, in relation to the metro lines and individual metro stations, (3) counted the number/percentage of maps on which each metro station was a) denoted and b) labelled, and (4) counted cases when the metro station or other location was marked as a crossroads of transport routes, i.e. as a transport node (including transfer to the other metro line).

The second part of the analysis was focused on the identities of nodal areas shaped around the individual metro stations. For this purpose, we counted associations and mentions of linked landmarks for each station. If a certain landmark is marked on the mental map in the immediate vicinity of the metro station, or otherwise compositionally tied to it by the respondent, such a landmark is defined as an association with the given metro station. Each single recording of an association is considered as a mention. This implies that the number of mentions for each particular metro station can be greater than or equal to the number of associations recorded for this station. Having collected the data on associations and mentions, we characterized the place identity of each metro station in terms of scope, intensity, polarization and semantic content.

The scope of place identity is defined as a number of independent associations to the given metro station. In this way, a large number of associations mean a broad place identity, and vice versa, few associations point at narrow place identity. The intensity of place identity is defined as a frequency of mentions for the most frequently mentioned association (or key association). In other words, this is an imageability of a key association. If a key association is mentioned frequently (i.e. appears on many mental maps), it contributes to the higher intensity of the place identity, and vice versa. The polarization of place identity is an indicator that aims to estimate the balance of representation of associations. It was measured as a coefficient of variation for the numbers of mentions of each association. If mentions are equally distributed between the associations, there is zero polarization. Otherwise, if some associations are more frequent than the others, the coefficient of variation deviates from zero, indicating a certain level of polarization. The polarization is possible to estimate only for places with more than one association. To investigate the semantic content of place identity, we divided associations between semantic categories and then defined the structure of mentions by semantic categories for each metro station.

5. Results and discussion

The analyzed mental maps were divided into 4 categories depending on the role of the metro system in their total graphic structure.

The first category (9 sketches; 29.0%) may be described as totally metro-centric maps. The metro lines play the dominant role and constitute the so called "good figure" of the mental map, structuring the whole image (Figure 1a). The second category (7 sketches; 22.6%) includes maps that are also metro-centric; however, they represent additional paths and nodes beyond the metro system (e.g. rapid tram lines, urban train, some important streets) (Figure 1b). The third category (7 sketches; 22.6%) enclose maps where the metro lines and stations are

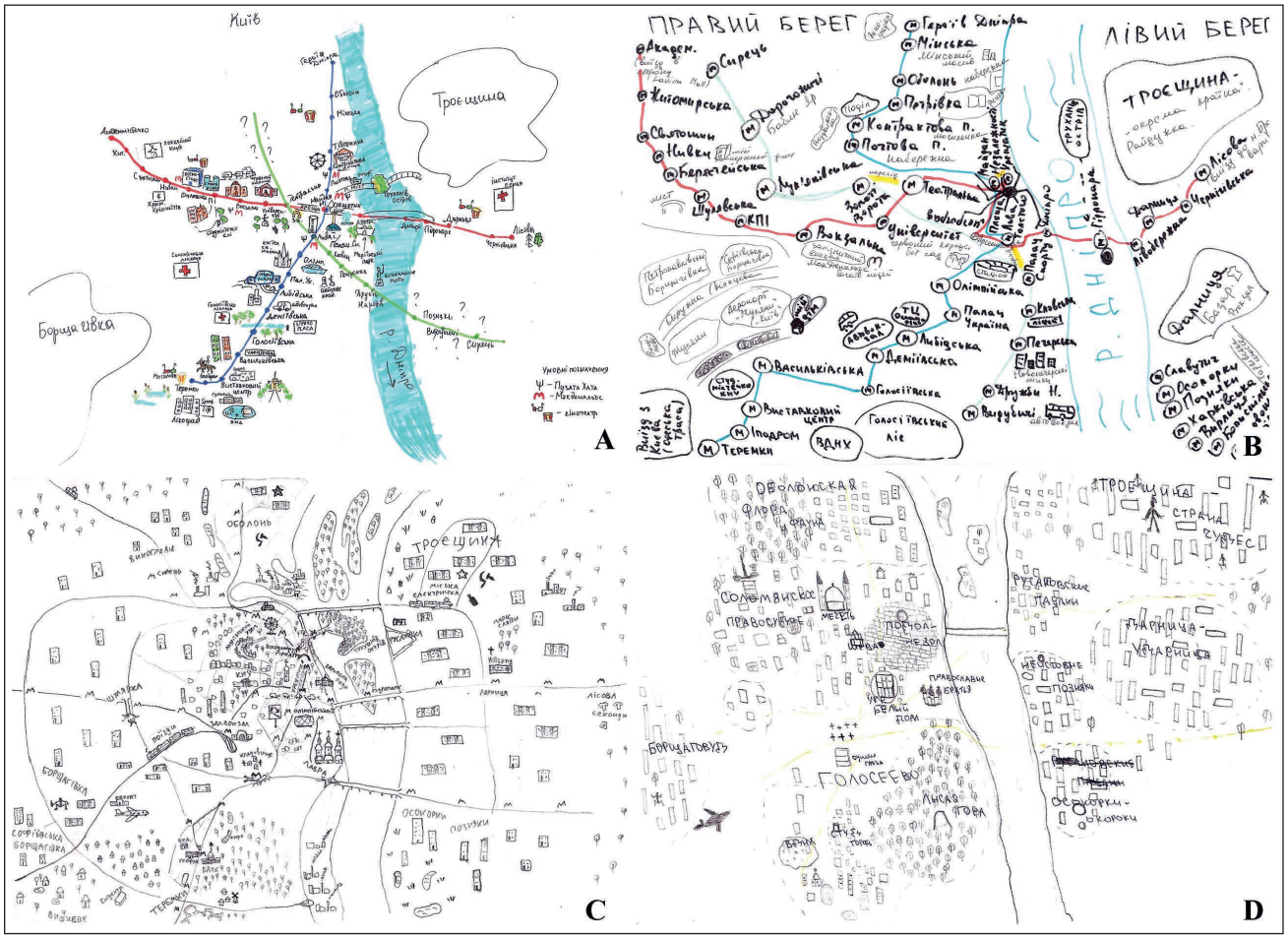

Fig. 1 Examples of mental maps made by participants.
Source: students' work.

marked but they do not dominate the entire mental map. The landmarks on such sketches are more or less evenly filling the urban space and are not strongly linked to the individual metro stations or lines (Figure 1c). The fourth category (8 sketches; 25.8%) represents maps where metro system is almost completely absent. Most commonly such maps represent a system of districts with minimum of paths (Figure 1d).

Although there are certain exceptions, the sketches from first and second categories generally fall into the sequential-type maps dominated by linear elements and the links between them, while the sketches from the third and fourth categories were mostly spatial-type maps with well-elaborated network of districts, according to the typology by Appleyard (1973).

The distribution of the maps between these categories convinces that the metro system constitutes an important part of the image of the city for the absolute majority of the respondents, and for approximately half of them it posturizes a skeleton that is used to arrange and structurize the other elements of the image of the city, and is used to navigate around the city (Kuipers et al. 2003). In this way, the form of transportation around the city has a significant impact on the image of the city, and the mental map of Kyiv is significantly different from the mental maps of cities without subway/metro system like Szczecin, where the most prominent nodes are squares as transport hubs and public spaces (Osóch and Czaplińska 2019), or Konya, where tram stops were marked by the students as nodes (Topcu and Topcu 2021). At the same time, in the case of Kazan, the role of metro system seems to be not so brilliant feature of the mental maps comparing to Kyiv, although some stations do play a role of most prominent nodes (Latypova et al. 2021).

Another observation, pointing out the importance of the Kyiv metro for urban imageability, is the role of metro stations as nodes for urban perceptual districts. In particular, in the part of Kyiv with a dense network of metro stations, most of perceptual districts are shaped around the metro stations, and it is often difficult to determine unambiguously whether an inscription on a map refers to a metro station or the surrounding homonymous district (e.g. metro station Pozniaky and the adjacent residential neighbourhood Pozniaky). The maps of the fourth category, with completely absent metro lines and stations, also often depict perceptual districts with names derived from the names of the metro stations. On the other hand,

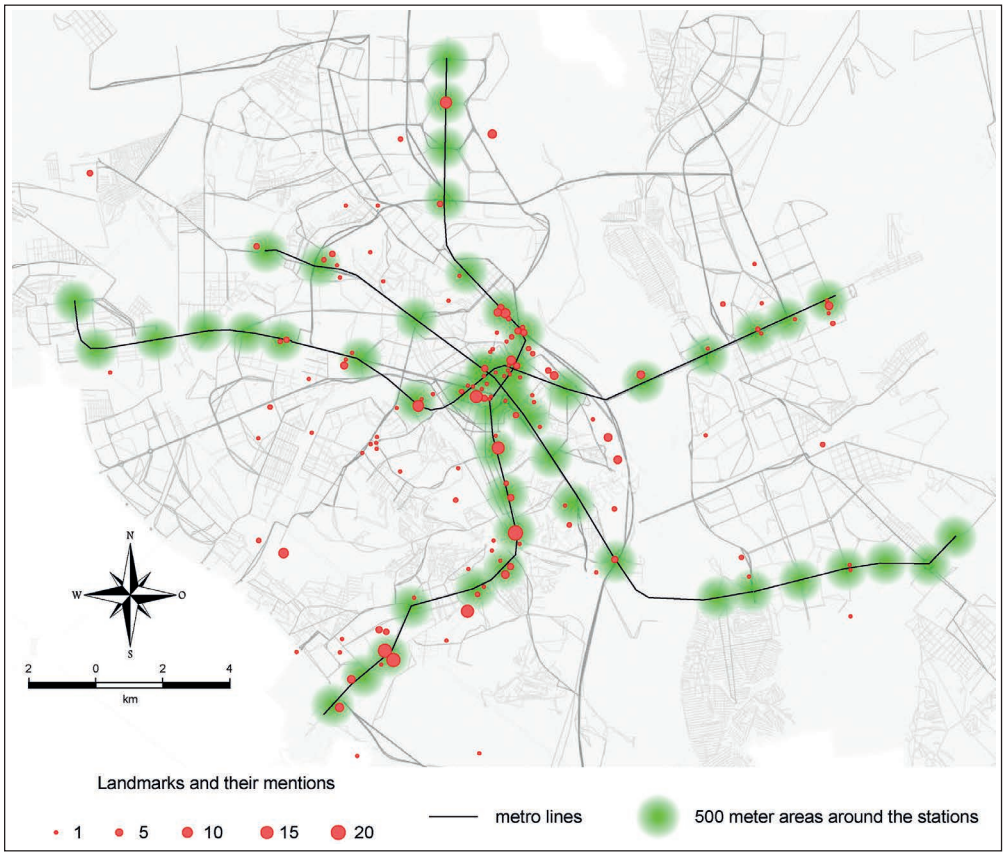

Fig. 2 Distribution of landmarks on mental maps in relation to the metro system.
Source: elaborated by the authors.

the most frequent and clearly represented districts on the mental maps are Troieshchyna and Borshchahivka – exactly those two large neighbourhoods where there is no metro. This means that the rapid transit may significantly restructure traditional perception of urban space, destroying the traditional system of vernacular districts based on historical urban areas and bringing to birth the network system of smaller vernacular districts centred on the stations.

Regarding the differences between the mental maps of Kyiv permanent dwellers and students from outside the capital, the total number of maps is not sufficient for detailed analysis and strong conclusions. However, native Kyivans tend to create more detailed representation of one certain (native and the most familiar) neighbourhood and less rely on the metro scheme when locating other places and objects in the city. In particular, none of the totally metro-centric maps was produced by the permanent dwellers. This means that the importance of the metro for mobility and perception is highest in the early stages of acquaintance with the city. Meanwhile, according to a study by Research & Branding Group (2014), approximately 55% of Kyiv residents were non-natives, and this figure is likely to have just increased, not least due to the inflow of the externally displaced persons from the Eastern Ukraine. Hence, we can assume that nowadays the metro system plays a key role in the urban imageability for most residents of the Ukrainian capital.

The importance of the metro system as a spatial backbone of the city is further strengthened by the spatial distribution of landmarks marked on the sketches. As can be seen from the map (Figure 2), the absolute majority of landmarks are located within the spatial belts along the metro lines. In particular, 59.7% of landmarks and 74.5% of their mentions are concentrated within 500 meters from metro stations. Moreover, practically all frequently mentioned landmarks are located in the vicinity of the metro stations, and vice versa, the landmarks located far from the metro are mentioned rarely. Exceptions are Zhuliany and Boryspil airports, Obolon Embankment, Kyiv-Pechersk Lavra, and the Motherland Monument; the last three objects are stretched along the Dnieper waterfront, and the last two are important landmarks forming the skyline of the right bank Kyiv when seen from the left bank. The only one significant cluster of landmarks beyond the metro line belts is observed around Sevastopolska Ploshcha. On the other hand, among the metro stations, 40 (76.9%) have at least one landmark in the vicinity of 500 meters.

All 52 metro stations have been found on analysed mental maps. They are not only marked but also labelled in the majority of cases. This is another confirmation of the importance of the metro system

as a spatial skeleton of the city. However, some differences in representation are observed for both individual metro stations and entire metro lines: blue line stations are best represented, while green line stations are worst represented, especially this refers to the left bank part of the line (Figure 3). These disparities should be attributed to the specificity of the respondents (university students), whose places of study and residence (university campuses) are mostly located along the blue line course, and thus not surprisingly this line (together with important transport hubs and other places important for the students' life on the other metro lines) is best represented on mental maps. Maidan Nezalezhnosti (located in the city centre on the homonymous square) was the most frequently marked station (27 sketches; 87.1%), while Vyrlytsia (located in the peripheral left-bank residential neighbourhood) was the least mentioned station (2 sketches; 6.5%).

Among all metro stations, 34 (65.4%) have been marked as transport nodes by the respondents. This figure includes six stations used for transfer to another metro line, and they were marked as transport nodes most frequently (38–48% of sketches). The list of the other stations, mentioned as transport nodes by more than 10% of the respondents, includes Teremky, Demiivska, Vydubychi, Darnytsia and Pochaina; all these stations are really located near the important surface crossroads. At the same time, approximately third part of all metro stations have not been marked as transport nodes; in some cases this may be justified, but some of these stations in reality are located near the important transport junctions, e.g. Nyvky or Druzhby Narodiv. Nevertheless, we identified 12 transport nodes different from the metro stations, and all of them were mentioned by less than 10% of the respondents. This means that although not all metro stations are perceived to be important transport nodes, some of them belong to the most recognizable transport nodes in the Ukrainian capital.

Typically the associated landmark is located in the vicinity of metro station. However, in many cases, the distance from the metro station to the associated landmark is large enough, although it is drawn quite near the metro station. Some extreme examples of this kind are the following: Darnytsa railway station is linked to Darnytsia metro station (distance 3.7 km); Lavina Mall is linked to Akademmistechko metro station (distance 3.4 km); Motherland Monument is linked to Druzhby Narodiv metro station (distance 1.8 km); Obolon Embankment is linked to Obolon metro station (distance 1.1 km). This confirms the point that metro stations sometimes may act as nodes not only for the immediate vicinity, but also

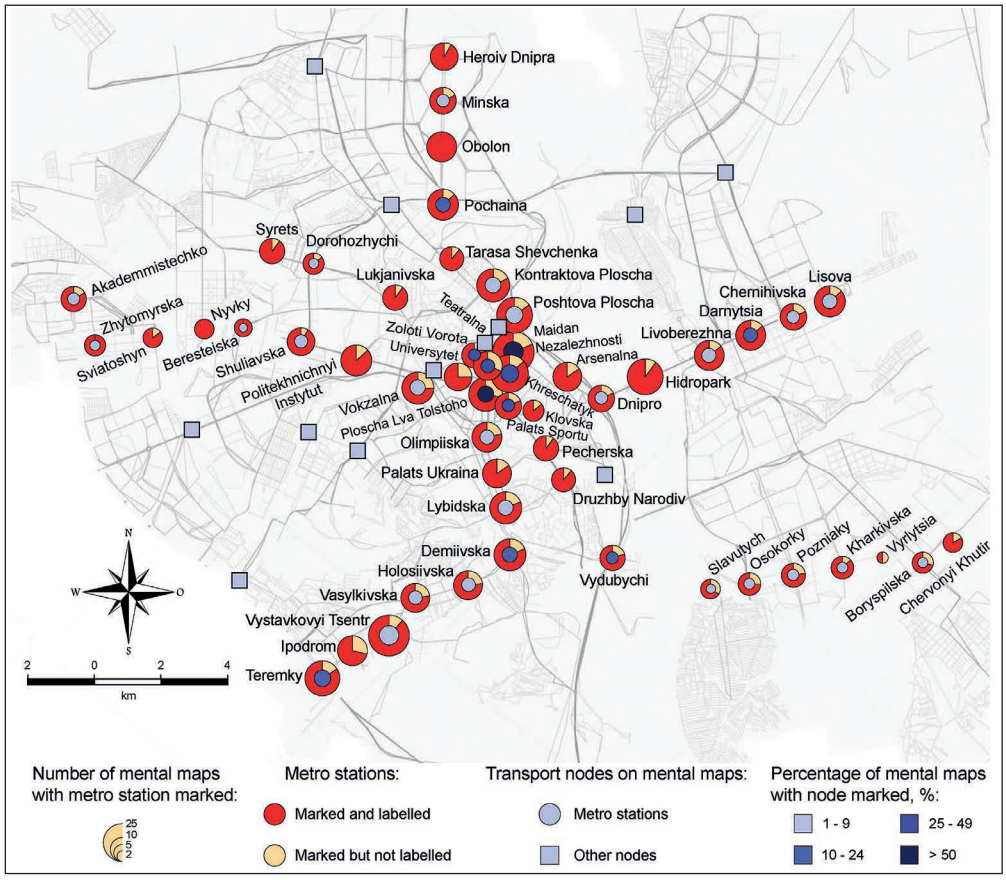

Fig. 3 Metro stations and transport nodes on mental maps.
Source: elaborated by the authors.

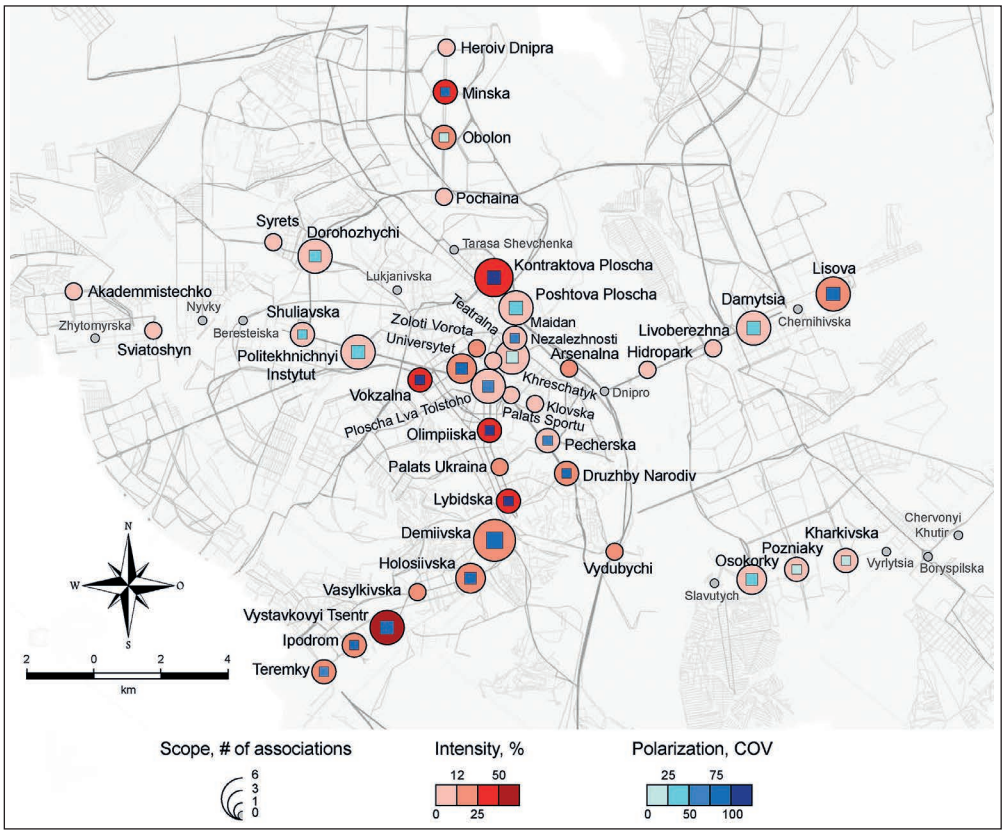

Fig. 4 Metro stations: scope, intensity and polarization of identity.
Source: elaborated by the authors.

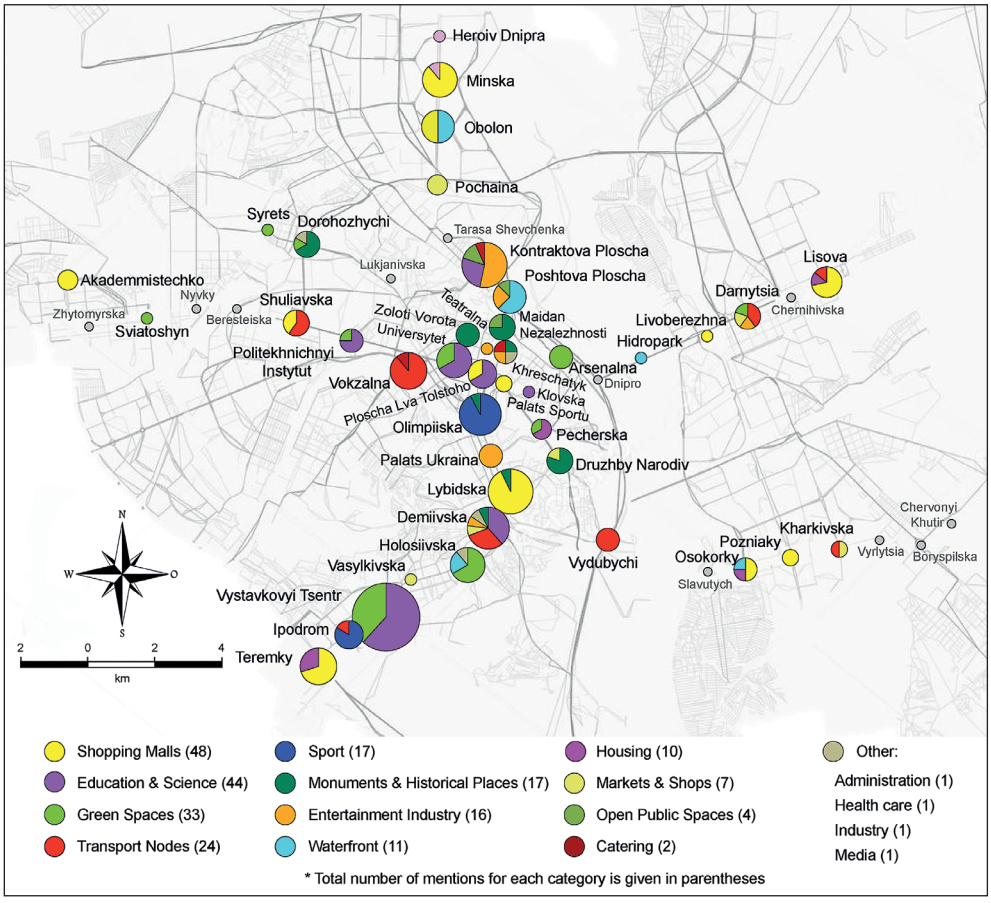

Fig. 5 Metro stations: semantic categories of associations (number of mentions).
Source: elaborated by the authors.

for large areas closest to (or best accessible from) the given station. The toponymic factor may also play a role (e.g. common attributes like Obolon and Darnytsia).

Differences between both the lines and individual stations become more pronounced when focusing on their identities (Figures 4, 5). First of all, the scope of identity varies substantially. There are 11 stations without any association: one on the blue line, five on the red line and another five on the green line. These stations are located mostly in peripheral and semi-peripheral areas of mass housing, industrial development, or green spaces. On the contrary, the broadest identities were recorded for Demiivska (6 landmarks), Kontraktova Ploshcha, Poshtova Ploshcha, Vystavkovyi Tsentr stations of the blue line (4 landmarks per each station), Politechnichnyi Institut, Darnytsia and Lisova stations of the red line (4 landmarks per each station). The green line, joining mass housing areas in the south-east and the north-west of the city, rarely visited by the students, is the worst represented on the mental maps.

The most common semantic categories of associations (and the most common key associations) are the following:

1) Shopping malls (48 mentions; 8 key associations) that have sprouted up on Kyiv streets and squares over the past two decades: Ocean Plaza (Lybidska), Dream Town (Minska and Obolon), Magellan (Teremky), Cosmopolite (Shuliavska), Lavina Mall (Akademistechko), Gulliver (Ploshcha Lva Tolstoho and Palats Sportu), Darynok (Darnytsia), River Mall (Osokorky). It is worth noting that if a shopping mall is located near the metro station, it will most likely be displayed on mental maps.
2) Institutions of education and science (44 mentions; 6 key associations), including three leading universities: Taras Shevchenko National University of Kyiv (Ploshcha Lva Tolstoho, Universytet and Vystavkovyi Tsentr), Kyiv-Mohyla Academy (Kontraktova Ploshcha), Igor Sikorsky Kyiv Polytechnic Institute (Politechnichnyi Instytut).
3) Green spaces (33 mentions; 4 key associations): Holosiiv Park and Forest (Holosiivska), Mariinsky Park (Arsenalna), Syrets Park (Syrets), Sviatoshyn urban forest (Sviatoshyn). Also, important second-order, but extremely frequent association was the Expocentre of Ukraine located on the outskirts of the Holosiiv Forest (Vystavkovyi Tsentr).
4) Transport hubs (24 mentions; 5 key associations): passenger stations like Central Railway Station (Vokzalna), Central Bus Station (Demiivska), Darnytsia Bus Station (Darnytsia and Lisova), Vydubychi Bus Station (Vydubychi), Pivdenna Bus Station (Ipodrom), Kharkivska Bus Station (Kharkivska). All these are important for students arriving to Kyiv and going back to their homes on weekends or vacations. Another key association is Shuliavka Bridge, the infamous "tired bridge" on the transport junction near Shuliavka station that collapsed in February 2017.
5) Monuments and historical places (17 mentions; 4 key associations), including the Golden Gate (Zoloti Vorota), Motherland Monument (Druzhby Narodiv), the Independence Monument and Square (Maidan Nezalezhnosti), Babyn Yar (Dorohozhychi).
6) Sports facilities (17 mentions; 2 key associations): Olimpiiskyi Stadium, the main sports arena of the country (Olimpiiska), and Hippodrome (Ipodrom).

The other semantic categories are much less frequent although may be important for individual stations. For example, entertainment facilities shaped the image of Palats Ukraina station (homonymous concert hall), Soviet mass housing appears to be essential for some peripheral stations like Teremky, Heroiv Dnipra, Minska, Osokorky, Pozniaky, Lisova, while the images of Postova Ploshcha, Obolon, Hidropark, Osokorky and Holosiivska stations benefit from location near waterfronts (embankments and beaches).

Based on the relationship between the scope, intensity and polarization of identity, four groups of stations may be distinguished:

1) Stations with broad and intense identities: Kontraktova Ploshcha, Vystavkovyi Tsentr, Lisova and Demiivska stations. Each of these stations evokes numerous associations, but one of them is stronger than the others and very frequent, causing sufficiently high polarization. Key associations may be different depending on the station and vary from the observation wheel (entertainment industry) to the education and science (Faculty of Geography; National Library) and shopping mall (Darynok). Also, all these stations function as important cross-sections. Such metro stations can be considered well-developed perceptual nodes that not only concentrate some function, but combine various functions in one place and serve different needs of different groups of people at the same time (multifunctional nodes). Thus, we may expand the original description by Lynch (1960) and add a third type of nodes: places where different special properties are in close contact (e.g. the junction of several urban districts or functional zones) may be perceived as nodes as well.
2) Stations with narrow but intense identities: Minska, Vokzalna, Olimpiiska, Druzhby Narodiv, Obolon, Ipodrom, Teremky, Palats Ukraina, Zoloti Vorota, Arsenalna, Vydubychi. Usually there is one strong association, mentioned by the absolute majority of the respondents, and one or two less frequent associations. Common key associations are shopping malls, transport hubs, sports facilities, monuments and historical places; less common are waterfronts and entertainment industry facilities. Polarization is typically extremely high due to the strong dominance of the key association. These stations are places of concentration of some special properties

and functions, and this makes them recognizable perceptual nodes (monofunctional nodes). The only exception with two equivalent associations is Obolon station (Dream Town Mall and Obolon Embankment), which is rather multifunctional node.

3) Stations with broad but subtle identities with polarization from low to moderate: Dorohozhychi, Politechnichnyi Instytut, Poshtova Ploshcha, Darnytsia, Khreshchatyk, Ploshcha Lva Tolstoho. Their identity is not firmly established: most people draw some associations, but they are different and depend on a respondent. Such stations lack a powerful perceptual dominant to be well-imageable. However, they may be considered as potential multifunctional nodes.
4) Stations with narrow and subtle identities. This group includes all other 31 stations, including 11 stations with the absent associations. As for the other stations from this group, typically, there are one or two associations with each station, and each of these associations is mentioned only once. Such associations may be given incidentally, depending on the individual experience of each particular respondent. Given the scarcity of associations, their low frequency and obviously random nature, these stations have no clear and stable identity and cannot be defined as perceptual nodes nowadays. However, they may be considered as potential monofunctional nodes, although some of them, if strengthen the identity through the medium of some (re)construction in the vicinity, may totally change it comparing to the present-day situation.

It should be noted that this classification is reliable only for selected sample of the respondents (students of the Faculty of Geography) and can be extended to the general population of Kyiv only in the part concerning the southern part of the blue metro line and the central part of the city. Metro stations beyond the specified area are less frequently visited by the respondents, and thus they are expected to evoke less variety of associations, and recorded images have less frequency. For example, we may suppose that if our respondents were students of the Institute of International Relations, located near Lukianivska station of the green line, the north-west part of the line would have been much better represented. Nevertheless, even given the limitations of this particular study, it can be concluded that some metro stations definitely play the role of important perceptual nodes. In particular, this refers to all stations that fall into the first and second categories of our classification. With the larger and more representative sample of respondents, we expect many stations from the third and fourth groups to move to the first and second groups. In other words, the results of this study rather underestimate than overestimate the value of a particular metro station as a perceptual node.

The results suggest that some metro stations had to undergo radical changes in their identity over the past decade. In particular, this refers to all metro stations with shopping malls as key associations. Nodal areas, like the other public spaces, seem to actively commercialize, and the role of shopping malls, extending or substituting the existing open public spaces, becomes extremely important (cf. Mezentsev and Mezentseva 2017). Prior to the construction of shopping malls in 2010s, the respective metro stations (or areas where the stations has been constructed) should have had fundamentally different perceptual dominants if any (for example, Soviet mass housing for Minska and Teremky, transport hubs for Lybidska and Lisova, etc). Nowadays, identities of such places often combine old and new associations, reflecting the development of so called hybrid spatialities (Golubchikov et al. 2013), for example, Soviet modernist building known as 'Tarilka' (*The Plate*) and shopping mall 'Ocean Plaza' at Lybidska station. On the one hand, this testifies to the powerful role of shopping malls as perceptual dominants of the modern Ukrainian capital: they produce difference between previously monotonous locations making them recognizable (and attended) places. Therefore, we can only partially agree with the statement that "the main phenomena that are changing urban processes and functions and that are deforming the nodal areas' spatial structures are commercialization (…) spatial unification, and homogenization" (Dronova and Brunn 2018, p. 101). On the other hand, construction of the shopping malls, as well as office centres etc. often leads to the replacement of the other associations with a place (the association with a shopping mall, once emerging, tends to dominate), endangering the authentic image of the city and oversimplifying it (cf. Dronova and Brunn 2018, p. 96).

Dronova and Brunn (2018) distinguished several types of existing and potential nodal areas in Kyiv, assessing them according to the predefined criteria. The comparison of their assessment with the results of this study, performed with completely different methodology, shows strong or partial correspondence for the majority of metro stations covered by the both studies (Table 1). At the same time, we found weak correspondence for some stations, which may indicate that subjective perceptions of respective places are different from those expectations based on the fact-based evaluation.

At the same time, some metro stations were underestimated by Dronova and Brann (2018) and even not included in their list of nodal areas, which is questioned by our results. For example, Holosiivska station, due to vast parks, forests and ponds in the vicinity, seems to be well-shaped nodal area with a function of a green public space used for socializing, recreation and relaxation; Lisova and Teremky stations are nodes of the surrounding mass housing neighbourhoods with prominent commercial and transport function; Dorohozhychi station functions as

Tab. 1 Comparison of the assessment of metro stations as nodal areas in two studies.

Metro station	Assessment by Dronova and Brunn (2018)	Assessment in this study	Correspondence
Arsenalna	Areas in Kyiv's centre (highest score for 'political gatherings', high score for 'parks, squares, elements of unique natural landscapes')	Monofunctional node (key association – Mariinsky Park)	Partial
Demiivska	Reconstructed areas with transport as the predominant function	Multifunctional node (with Central Bus Station among the 2 key associations)	Strong
Khreshatyk	Areas in Kyiv's centre (almost balanced but low scores)	Potential multifunctional node (catering; entertainment industry; monuments and historical places; administrative buildings)	Strong
Kontraktova Ploshcha	Public spaces of special social significance	Multifunctional node (entertainment industry; education and science; public spaces)	Strong
Livoberezhna	Areas with transport function that require reconstruction	Potential monofunctional node (key association – shopping mall 'Komod')	Weak
Lukianivska	Areas with transport function that require reconstruction	No associations	Weak
Lybidska	Areas significantly transformed due to the shopping malls	Monofunctional node (key association – shopping mall 'Ocean Plaza')	Strong
Maidan Nezalezhnosti	Public spaces of special social significance	Multifunctional node (monuments and historical places; public space)	Strong
Minska	Areas significantly transformed due to the shopping malls	Monofunctional node (key association – shopping mall 'Dream Town')	Strong
Obolon	Territories that have potential features of nodal areas	Multifunctional node (shopping malls; waterfronts)	Weak
Palats Sportu	Areas significantly transformed due to the shopping malls	Potential monofunctional node (key association – shopping mall 'Gulliver')	Strong
Pecherska	Areas in Kyiv's centre (all scores equal to zero except for high transport accessibility)	No associations	Partial
Ploshcha Lva Tolstoho & Universytet	Areas in Kyiv's centre; Public spaces of special social significance	Multifunctional node (education and science; green spaces; shopping malls)	Strong
Pochaina	Areas with transport functions, including intercity, national, and international routes	Potential monofunctional node (key association – book market)	Weak
Poshtova Ploshcha	Reconstructed areas with transport as the predominant function (highest score for 'parks, squares, elements of unique natural landscapes')	Potential multifunctional node (waterfronts; entertainment industry; public spaces)	Partial
Shuliavska	Areas with transport function that require reconstruction	Potential multifunctional node (key association – Shuliavka bridge)	Strong
Teatralna	Areas in Kyiv's centre (almost balanced but low scores)	Potential monofunctional node (key association – National Opera House)	Partial
Vasylkivska	Territories that have potential features of nodal areas	Potential monofunctional node (key association – chain store 'Varus')	Strong
Vokzalna	Areas with transport functions, including intercity, national, and international routes	Monofunctional node (key association – Central Railway Station)	Strong
Vydubychi	Areas with transport functions, including intercity, national, and international routes	Monofunctional node (key association – Vydubychi Bus Station)	Strong
Zoloti Vorota	Areas in Kyiv's centre (high score for 'cultural, historical, sacred, or aesthetic monuments and artefacts')	Monofunctional node (key association – historical monument 'Golden Gate')	Strong

a recognizable historical place (with Babi Yar, a site of massacres carried out by Nazis in 1941, as a key association); Olimpiiska station (and the adjacent square) is strongly associated with the Olimpiiskyi Stadium, a place for sports competition, as well as the other festive events, etc. This means that it is advisable to combine quantitative and qualitative methods for in-depth study of urban nodal areas, especially when they are understood as perceptual nodes structuring a mental map of the city.

6. Conclusions

Although the sample of informants imposes some limitations on our research, some conclusions can be drawn:

1. The Kyiv Metro seems to have significant impact on the image of the city. Approximately for the half of the informants, it constitutes a "good figure" of a mental map and a "skeleton" that is used to structure the other paths and landmarks and to navigate

the city. Areas that are not covered by the metro and are not either way involved into the everyday activity of the informants, represent *terrae incognitae* for the most informants. Conversely, metro lines and stations typically are the only details marked in parts of Kyiv not familiar to respondents from personal activity. Having the previous results on Moscow (The Village 2014; Urban Look 2014), these findings can be extended to other large cities in the post-Soviet space. However, the peculiarities of the city-planning structure may make difference in the each individual case.

2. Most of the metro stations do function as perceptual nodes of the image of the city. Some stations are primarily junctions of pathways, but most of them concentrate some urban functions (monofunctional nodes) or even show combination of different functions (multifunctional nodes); the latter are among the nodes with the highest imageability. The most common landmarks associated with metro stations are malls, universities, parks, passenger stations and other kinds of transport hubs, monuments and historical places, stadiums and concert halls.
3. Perception of nodal areas around the metro stations reflects recent transformation of urban built environment and functions under the neoliberal policy regime. Only one recorded association with industrial facility mirrors deindustrialization process. On the contrary, shopping malls, being the most visible product of recent commercialization, are the most frequent associations with metro stations and often tend to replace previously existing associations cardinally changing the place identity. However, the role of open green public spaces, as well as embankments, in shaping the place identities for metro-related nodal areas is also very important. Monuments and historical places keep the role of perceptual dominants but only in the areas not touched by aggressive commercialization, and their imageability seems to be lower comparing with the aforementioned landmarks.
4. The study of nodal areas should combine both quantitative and qualitative approaches to achieve the best results, since the subjective perceptions resulting from the mental maps does not always coincide with the fact-based evaluation.

To summarize, metro system in post-Soviet city, apart from performing basic function of transportation, constitutes an important element of urban identity and imageability, both in the city-wide dimension and the dimension of individual neighbourhoods. In view of this, much attention should be paid by urban planners to the layout of new metro lines and the land use planning in the vicinity of already existing and intended stations. It is recommended to use TOD for development of the nodal areas in order to reduce car use and create multimodal transport opportunities. It is important to mix residential, commercial, retail, office, green zones and public civic spaces within walking distance of metro stations. According to the results of the study, in order to improving urban sustainability, the metro-related nodal areas of Kyiv need to balance functions with an emphasis on their compactness and safety, convenience of public transport use, keeping/creation of the open public spaces and heritage protection.

Acknowledgements

We are thankful to the students for their work on mental maps. Also, we would like to thank two anonymous reviewers for their constructive and helpful comments.

References

Ahlfeldt, G. M., Wendland, N. (2009): Looming stations: valuing transport innovations in historical context. Economics Letters 150, 97–99, https://doi.org/10.1016/j.econlet.2009.06.010.

Appleyard, D. (1969): Why buildings are known. Environment and Behavior 1(2), 131–156, https://doi.org/10.1177/001391656900100202.

Appleyard D. (1973): Notes on urban perception and knowledge. In: Downs, R. M., Stea, D. (eds.). Image and Environment. Chicago, Aldine, 109–114.

Avdiejeva, N., Bila, A. (2016): Orhanizatsija transportno-peresadkovykh vuzliv jak kliuchovykh spoluchnykh elementiv transportnoji systemy mista [Organization of transfer assemblies as key connecting elements of the city transport system]. Problemy Rozvytku Miskoho Seredovyscha 15(1), 68–75.

Birch, K., Mykhnenko, V. (eds.) (2010): The Rise and Fall of Neoliberalism: The Collapse of an Economic Order? London, Zed, https://doi.org/10.5040/9781350223486.

Bondar, V. (2018): Istorychni aspekty formuvannia zahalnomiskoho tsentru stolychnoho metropolisa [Historical aspects of the city centre development in the capital metropolis]. In: Lisovskyi, S., Pidhrushnyi, G., Maruniak, E., and others (eds.). Geographical Science and Education: From Statement to Constructivism (International Conference, 28–29 September, 2018). Kyiv, National Academy of Science of Ukraine, 131–133.

Cervero, R., Duncan, M. (2002): Transit's value-added effects: light and commuter rail services and commercial land values. Transportation Research Record: Journal of the Transportation Research Board 1805, 8–15, https://doi.org/10.3141/1805-02.

Cheng, J., Bertolini, L., Clercq, F., Kapoen, L. (2013): Understanding urban networks: Comparing a node-, a density- and an accessibility-based view. Cities 31, April 2013, 165–176, https://doi.org/10.1016/j.cities.2012.04.005.

Cybriwsky, R. A. (2014): Kyiv, Ukraine. The City of Domes and Demons from the Collapse of Socialism to the Mass Uprising of 2013–2014. Amsterdam University Press, https://doi.org/10.1515/9789048531738.

Dalton, R., Bafna, S. (2003): The syntactical image of the city: A reciprocal definition of spatial elements and spatial syntaxes. In: Proceedings of the 4th International space syntax symposium, 59.1–59.22. London, Space Syntax.

Derakhti, L., Baeten, G. (2020): Contradictions of transit-oriented development in low-income neighborhoods: the case study of Rosengård in Malmö, Sweden. Urban Science 4, 20, https://doi.org/10.3390/urbansci 4020020.

Dong, H. (2016): If you build rail transit in suburbs, will development come? Journal of the American Planning Association 82(4), 316–326, https://doi.org/10.1080 /01944363.2016.1215258.

Dong, H. (2017): Transit induced neighborhood change and the affordability paradox of TOD. Journal of Transport Geography 63, 1–10, https://doi.org/10.1016/j.jtrangeo .2017.07.001.

Dronova, O., Brunn, S. D. (2018). How neoliberal globalization processes are transforming Kyiv's nodal areas. Urbani Izziv 29(2), 96–110, https://doi.org /10.5379/urbani-izziv-en-2018-29-02-003.

Dronova, O., Maruniak, E. (2019): Changing the symbolic language of the urban landscape: post-socialist transformation in Kyiv. In: Brunn, S., Kehrein, R. (eds.). Handbook of the Changing World Language Map. Cham, Springer, 2941–2972, https://doi.org/10.1007 /978-3-030-02438-3_117.

Dronova, O., Polieshko, D. (2017): Funktsionalni ta prostorovi zminy vuzlovykh terytorij Kyjeva [Functional and Spatial Changes of the Nodal Areas in Kyiv]. In: Mezentsev, K., Oliinyk, Y., Mezentseva, N. (eds.). Urbanistychna Ukrajina: v epitsentri prostorovykh zmin [Urban Ukraine: In Epicenter of Spatial Changes]. Kyiv, Fenix, 211–226.

Duncan, M. (2011): The impact of transit-oriented development on housing prices in San Diego, CA. Urban Studies 48(1), 101–127, https://doi.org/10.1177 /0042098009359958.

Forouhar, A. (2016): Estimating the impact of metro rail stations on residential property values: evidence from Tehran. Public Transport 8, 427–451, https://doi.org/10.1007/s12469-016-0144-9.

Gibbons, S., Machin S. (2005): Valuing rail access using transport innovations. Journal of Urban Economics 57, 148–169, https://doi.org/10.1016/j.jue.2004.10.002.

Golledge, R., Spector, A. (1978): Comprehending the urban environment: Theory and practice. Geographical Analysis 10(4), 403–426, https://doi.org/10.1111 /j.1538-4632.1978.tb00667.x.

Golubchikov, O., Badyina, A., Makhrova, A. (2014): The hybrid spatialities of transition: Capitalism, legacy and uneven urban economic restructuring. Urban Studies 51(4), 617–633, https://doi.org/10.1177 /0042098013493022.

Hall, P. (1993): The changing role of capital cities: Six types of capital city. In: Taylor, J. (ed.). Capital cities – International perspective. Ottawa, Carleton University Press, 69–84.

Hospers, G. (2010): Lynch's The image of the city after 50 years: City marketing lessons from an urban planning classic. European Planning Studies 18(12), 2073–2081, https://doi.org/10.1080/09654313.2010.525369.

ITDP (2017): TOD Standard, 3rd ed. New York: Institute for Transportation and Development Policy.

Jenks, A. (2000): A metro on the mount: The underground as a church of Soviet civilization. Technology and Culture 41(4), 697–724, https://doi.org/10.1353/tech .2000.0160.

Jiang, B. (2012). Computing the image of the city. In: Campagna, M., De Montis, A., Isola, F., Pira, C., Zoppi, C. (eds.). Proceedings of the 7th International Conference on Informatics and Urban and Regional Planning. Milan, Franco Angeli, 111–121.

Jones, C. E., Ley, D. (2016): Transit-oriented development and gentrification along Metro Vancouver's low-income SkyTrain corridor. Canadian Geographer / Le Géographe Canadien 60(1), https://doi.org/10.1111/cag.12256.

King, L. J., Golledge, R. G. (1978): Cities, Space, and Behaviour: the Elements of Urban Geography. Englewood Cliffs, NJ, Prentice-Hall.

Kuipers, B., Tecuci, D. G., Stankiewicz, B. J. (2003): The skeleton in the cognitive map. Environment and Behavior 35(1), 81–106, https://doi.org/10.1177 /0013916502238866.

Latypova, M., Mingalimova, E., Rubtsova, A., Tazov, A. (2021): Empirical study of the mental representation of the image of the city (on the example of Kazan and Naberezhnye Chelny). In: 2nd International Scientific Conference on Socio-Technical Construction and Civil Engineering (STCCE – 2021). E3S Web of Conferences 274, 01034 (2021), https://doi.org/10.1051/e3sconf /202127401034.

Li, S., Chen, L., Zhao, P. (2019): The impact of metro services on housing prices: a case study from Beijing. Transportation 46, 1291–1317, https://doi.org /10.1007/s11116-017-9834-7.

Look, G., Shrobe, H. E. (2007): Towards intelligent mapping applications: a study of elements found in cognitive maps. In: Proceedings of the 12th international conference on Intelligent user interfaces, 309–312, https://doi.org/10.1145/1216295.1216354.

Lynch, K. (1960): The image of the city. Cambridge, MA, MIT Press.

Maruniak, (2013): Reaktsija gorodskogo prostranstva na vyzovy globalizatsii [Urban Space Reaction on Globalization Challenges]. In: Rudenko, L. (ed.). Izmenenija gorodskogo prostranstva v Ukraine [Urban Territories Changes in Ukraine]. Kyiv: Referat, 21–34.

Mezentsev, K., Mezentseva N. (2017): Suchasni transformatsiji publichnykh prostoriv Kyjeva: peredumovy, projav ta spetsyfika [Modern transformations of Kyiv public spaces: prerequisites, manifestation and specifications]. Chasopys Sotsialno-Ekonomichnoji Heohrafiji / Human Geography Journal 22(1), 39–46, https://doi.org/10.26565/2076-1333 -2017-22-07.

Mezentseva, N., Mezentsev, K. (2017): Vstup: zminy miskoho prostoru stolytsi [Introduction: Changes of the Urban Space in the Capital]. In: Mezentsev, K., Oliinyk, Y., Mezentseva, N. (eds.). Urbanistychna Ukrajina: v epitsentri prostorovykh zmin [Urban Ukraine: In Epicenter of Spatial Changes]. Kyiv. Fenix, 181–184.

Mumford, L. (1961): The City in History: Its Origins, its Transformations, and its Prospects. New York, Harcourt, Brace & World.

Nawrocki, T. (2017): The usefulness of mental maps for sociological research of the city. Architecture, Civil Engineering, Environment 10(3), 19–31, https://doi.org/10.21307/acee-2017-032.

Norberg-Schulz, C. (1971): Existence, Space and Architecture. New York, Praeger.

Norberg-Schulz, C. (1980): Genius Loci: Towards a Phenomenology of Architecture. London, Academy Editions.

Osietrin, M., Omelchuk, M. (2008): Problemy mista, jaki povjazani z rozvytkom merezhi metropolitenu (na prykladi Kyjeva) [Urban isuues related to the metro development (the case of Kyiv)]. Suchasni Problemy Arkhitektury ta Mistobuduvannia 20, 203–210.

Osóch, B., Czaplińska, A. (2019): City image based on mental maps – the case study of Szczecin (Poland). Miscellanea Geographica 23(2), 111–119, https://doi.org/10.2478/mgrsd-2019-0016.

Renne, J. L., Tolford, T., Hamidi, S., Ewing, R. (2016): The cost and affordability paradox of transit-oriented development: a comparison of housing and transportation costs across transit oriented development, hybrid and transit-adjacent development station typologies. Housing Policy Debate 26(4–5), 819–834, https://doi.org/10.1080/10511482.2016.1193038.

Roukouni, A., Basbas, S., Kokkalis, A. (2012): Impacts of a metro station to the land use and transport system: the Thessaloniki Metro case. Procedia – Social and Behavioral Sciences 48, 1155–1163, https://doi.org/10.1016/j.sbspro.2012.06.1091.

Sailer-Fliege, U. (1999): Characteristics of post-socialist urban transformation in East Central Europe. GeoJournal 49(1), 7–16, https://doi.org/10.1023/A:1006905405818.

Sassen, S. (2016): The global city: Strategic site, new frontier. In: Keiner, M., Koll-Schretzenmayr, M., Schmid, W. A. (eds.). Managing Urban Futures: Sustainability and Urban Growth in Developing Countries. London, Routledge, 89–104, https://doi.org/10.4324/9781315249827-16.

Stenning, A., Smith, A., Rochovska, A., Swiatek, D. (2010): Domesticating neo-liberalism: Spaces of economic practice and social reproduction in post-socialist cities. Oxford, Wiley-Blackwell, https://doi.org/10.1002/9781444325409.

Stevens, Q. (2006): The shape of urban experience: A reevaluation of Lynch's five elements. Environment and Planning B: Planning and Design 33(6), 803–823, https://doi.org/10.1068/b32043.

Sýkora, L. (2009): Post-socialist cities. In: Kitchin, R., Thrift, N. (eds.). International Encyclopedia of Human Geography 8, 387–395, https://doi.org/10.1016/B978-008044910-4.01072-5.

Sýkora, L., Bouzarovski, S. (2012): Multiple transformations: Conceptualising the post-communist urban transition. Urban Studies 49(1), 43–60, https://doi.org/10.1177/0042098010397402.

Topcu, K. D., Topcu, M. (2012): Visual presentation of mental images in urban design education: cognitive maps. Procedia – Social and Behavioral Sciences 51, 573–582, https://doi.org/10.1016/j.sbspro.2012.08.208.

The Village (2014): Big Bang Data: Kak student "Strelki" dokazal, chto Moskva – vsio escho feodalnyj gorod [Big Bang Data: How a Strelka student proved that Moscow is still a "feudal" city], https://www.the-village.ru/village/city/big-data/171117-schrader (accessed June 24, 2021).

Urban Look (2014): Stantsii moskovskogo metro: tsentry pritiazhenija dlia "uzlovogo" goroda [Moscow metro stations: centres of gravity for the "nodal" city]. Access mode: https://urbanlook.ru/stancii-moskovskogo-metro-centry-prityazheniya-dlya-uzlovogo-goroda (accessed June 24, 2021).

Yoshimura, Y., He, S., Hack, G., Nagakura, T., Ratti, C. (2020): Quantifying memories: mapping urban perception. Mobile Networks and Applications 25, 1275–1286, https://doi.org/10.1007/s11036-020-01536-0.

Zhang, Y., Marshall, S., Manley, E. (2019): Network criticality and the node-place-design model: Classifying metro station areas in Greater London. Journal of Transport Geography 79, 102485, https://doi.org/10.1016/j.jtrangeo.2019.102485.

Expression of regional identity in urban toponomy of major Kosovar cities

Arsim Ejupi*

University of Prishtina, Faculty of Mathematical and Natural Sciences, Department of Geography, Kosovo
* Corresponding author: arsim.ejupi@uni-pr.edu

ABSTRACT
This paper presents the model of identity research using the street names from five major Kosovar cities. The purpose of this research is to demonstrate the fact that identity in the urban environment can be determined through the analysis of street names, to uncover the difference in the presence of hodonyms that express regional identity from those that express national identity, and to investigate the presence of urban toponyms of international importance. This paper also aims to examine the relationship between regional identity and ethnic and religious structure, as well as to identify the role of historical-political circumstances at the level of the manifestation of regional identity. We found that the regional identity has been expressed more deeply compared to the national and international hodonyms, which have a lower representation. Although regional hodonyms dominated in all cities that were analyzed, there were differences in the representation of regional hodonyms which were related to personalities, events, or geographical objects that belong to the respective city or surroundings.

KEYWORDS
identity; region; names; streets; geography

Received: 1 October 2021
Accepted: 20 February 2022
Published: 4 March 2022

Ejupi, A. (2022): Expression of regional identity in urban toponomy of major Kosovar cities. AUC Geographica 57(1), 31–38
https://doi.org/10.14712/23361980.2022.3

1. Introduction

Identity is a set of characteristics that determine the particularity of an individual or group, especially in relation to similarities or differences with other individuals or groups. The sense of belonging to a society within a region is formed when a significant portion of inhabitants share symbols, values, and aspirations and create a regional identity and cultural system (Giménez 2005). Individual and group identification has always preoccupied both individuals and small groups, as well as society as a whole. The reason is not just the desire to prove the identity and the community to which they belong. But also because of the series of the consequences that such identification can cause, and which is directly or indirectly, expressed in certain geographical space.

The purpose of this research is to contribute to the geographical understanding of spatial identity through the reading of symbolism in the toponymy of five major Kosovar cities. What role will personalities have on the naming of the streets? What meaning do geographical toponyms have in the hierarchy of the cities' urban toponomy? Which identity will dominate? These are research questions addressed in this article.

In the case of Kosovo, regional identity is a lower scale identity than the Albanian identity. Although Kosovo is a small territory, it has very diverse natural conditions which are reflected in regional differences. The Dukagjini plain, Kosovo plain, Rugova, Anamorava, and Drenica are some of the regions that are distinguished not just by natural conditions, but also according to social, demographic, and economic features. The expression of identity in the toponymy of Kosovar cities can be examined through quantitative and qualitative analysis of street names. In the next phase are determined the differences in the participation of hodonyms (names of streets) that express regional identity from those, that express national and international identity. The analysis includes five major cities in Kosovo which are the largest in terms of demographic size, functions and gravitational area. These are Prishtina, which has the status of the capital city; Prizren, which is the second largest city in terms of population; Gjilan, which is the largest city in eastern Kosovo; Peja, which is the largest urban center in western Kosovo; and Gjakova, another large urban center in western Kosovo.

2. Theoretical background

Identity can be divided into individual and group identity. Group or social identity can be shaped by gender, age, sexual orientation, religious beliefs, nation, and region, among others. Most people contain multiple identities stemming from their simultaneous belonging to different groups, such as linguistic, professional, and regional groups (for example: Dukagjinas, Kosovar, European).

Besides the development of theoretical and geographical knowledge on identities, an important part of research in cultural geography is a perceptive understanding of the region based on research of the various forms of identities that have formed or are forming certain regions (Leighly 1978; Raitz 1973; Zelinsky 1988).

The individuality of each region, except natural, social and economic factors, is influenced by the behavior and attitude of each individual towards the region, or recognition of the environment as their own (local environment), the role and position of the individual in society, etc. This is studied as the affiliation (individual perception of geographical space) that any individual or even wider social groups (collective consciousness of regional affiliation) can have (Šabić and Pavlović 2007). In this way, by adding socio psychological attitudes of the population towards regional identity to the geographical criteria, the individuality of the geographical region is pointed out even more.

The sense of belonging to a society within a region, formed when a significant part of inhabitants shares symbols, values and aspirations creates regional identity and an own cultural system (Giménez 2005). Since the region is principally the study object for geographers, it is not surprising that there have been a large number of contributions to the geographical scientific literature that deal with regional identities and their spatial expression.

At the same time, the region is defined as a complex set of relations between population groups and certain territories (Crljenko 2008). These reports are based on the awareness of members of the regions about the common culture and diversity vis-a-vis other groups. The region is therefore symbolically defined as being part of such a unit (Vresk 1997). Anssi Paasi (2002) emphasizes that regional identity is the main factor affecting the process of institutionalization of regions. The boundaries of their extent may or may not necessarily coincide with territorial administrative units within a given space (as in the case of national identity). In the absence of such an agreement, regional identity can become a constitutive element of regional resistance and can lead to extreme regionalism, which can later be used for political purposes and even for attempts to redefine national borders, potentially causing conflicts.

Regional identity is approached from two aspects. One is the identity of the region based on the many elements that make it up, such as nature, landscape, built environment, culture, ethnicity, dialect, economic success, center-periphery relations, marginalization, stereotypes about people and community (Paasi 2003). The identity of a region is represented by the characteristics of nature and culture, but also by the people who use them in discourses and classifications of science, politics, cultural activism, regional

marketing, administration and political or religious regionalization to distinguish one region from another (Paasi 2003).

Regional identity has been recognized as a key element in the making of regions as social and political spaces, but it is difficult to elucidate what this identity consists of and how it affects collective action and politics (Keating 1998). The crucial question is how political passions are regionalized, and here institutions constitutive of region-building (economy, governance, language, media, and literature) and inherent power relations are significant (Passi 2003). In the case of Kosovo, historical and political circumstances had a significant impact in the formation of a new identity.

According to Crang (1998), identity can be expressed through the system of symbols through which values, beliefs, and ideologies of the population are displayed. These symbols can be a state, region, or city flag, or dialectical linguistic features (local and regional identities), as well as visible elements of the landscape such as monumental heritage, architectural style, graffiti, and urban toponymy (Sakaja 2003).

Site names have special importance in shaping territories and territorial identities (Azaryahu 2001). The same applies to the names of streets, squares, and crossings which reference the territory and symbolically indicate the ownership and importance of the territory (Culcasi 2011). Naming the streets is of crucial importance in manipulating and managing the social construction of identity (Wanjiru and Kosuke 2014). Streets, squares, and buildings can be named after personalities of national importance, commemorate important events, or serve as reminders of some traditional customs (Drozdzewski 2014). Some authors define the city as text (also known as a city-text) as a conglomeration of signs that are written, deleted, and reinstalled, consisting of existing markers that are visible in space, as well as in memory and photographs from the past. Azaryah (1986) sees city-text as a system of symbols that transfer official history and identity to the urban semiosphere – a system which primarily consists of street names and other names in public spaces that reveal the past and the dominant value system in the society. Recent work that deals with the study of toponyms emphasizes the need for attention to the process of forming names of streets, i.e. determining the cultural and political events and institutions that participated in their establishment (Bucher et al. 2013).

In terms of identity, after the war and especially after the declaration of independence, according to Albertini (2012), Kosovo is perceived as the place where two main discursive forms clash. The first one concerns the historical struggle for defending a national and Albanian identity during the long age of Serbian sovereignty over this province – a discourse which pivots on a narrative of a century-long conflict between the Serbian and Albanian ethnic groups, overstuffed by examples, memories, and practices confirming their impossibility to live together in the same state. The second discourse is much wider than the first. It portrays the often conniving international interests and the profitable power relations established in Kosovo following the NATO bombing of Yugoslavia, and United Nations' administration of the province. The only way to understand what kind of identity is going to be forged in Kosovo, then, is to track and identify these global–local relations that emerge through the different scapes that shape culture and society. The relationship between these discourses defines the consequences on the people, at the same time actor and target of the new identities and lifestyles (Albertini 2012).

3. Research methods and study area

In this paper street names were analyzed using statistical methods for the quantitative portion of the analysis and the meanings of street names were analyzed using interpretive methods for the qualitative portion. It was used Location Quotient (LQ) which is often an applicable indicator in geographical analyzes because it defines precisely enough the relation of smaller and larger unit. In order to obtain sustainable results, in addition to regional and national hodonyms, whether they are double or not, were taken also hodonyms that express exclusively a unique identity (regional or national). In addition, a comparative method has been used to determine the differences in the expression of different levels of spatial identity, from regional to international. The main source of data is the city plans from which a total of 539 hodonyms were analyzed, and the population data for the cities was obtained from the Kosovo Agency of Statistics. For the purposes

Fig. 1 Kosovo with its five major cities.

of this paper, street names were analyzed from five major Kosovar cities.

After identification of the toponyms, we have divide them by scale into the different groups. Regional identity is associated with the wider region of studying city. To this category belong historical dates, geographical names and personalities. The last ones by their activity helped in the development of culture, art, political self-determination or they helped economic development of the region. For example, the city of Gjakova in the Dukagjini region has many street names of regional importance such as Besim Bokshi, Ganimete Terbeshi, Emin Duraku etc.

National identity is bound to a state. This group of toponyms should reflect the names of streets and squares that have national meaning. For example, Mother Teresa, Beselidhja, Gjeravica, Berlin Congress etc. International hodonyms that are connected with the people and events or concepts outside of Kosovo and have international importance (e.g. Justinian Emperor, Constantine The Great, Bill Clinton, Johan V. Hahn, etc.).

Among cities that were chosen to be analyzed are Prishtina as a capital city which is relatively new settlement, but due to the decision to be declared the capital, has faced a rapid urban, demographic and territorial development. Now it has a population of more than 350,000 inhabitants (Settlements of Kosova 2018). Prizren is the largest city in the entire Dukagjini region with more than 100,000 thousands inhabitants. It has played an important role in the history of the Albanian people. In Prizren in 1878, the political organization named the League of Prizren was founded (Kosova, a monographic survey 2011). Prizren is the center of Turkophone Albanians (Guy 2008), that's why we'll make attempts to throw light on how much this fact determines the emergence of regional identity. On the other hand, the city of Gjakova in western Kosovo is surrounded by a religious minority of Catholic Albanians. After the Second World War, the massification of education in Kosovo began, which led to the reduction of illiteracy rates and cultural emancipation in general. The population began to attend secondary and higher education, primarily in cities. Among them, it is important to mention especially Gjakova, where many young people begin to attend higher education in university centers of the former Yugoslavia, such as Belgrade, Zagreb, Ljubljana, Sarajevo and in other European countries. After graduation, they returned to Kosovo and were positioned as the leaders of the main leading political and academic institutions.

The fourth city being analyzed is Peja, the largest city in western Kosovo. It is located at the exit of the Rugova Gorge in the Dukagjini Plain. It is known for its long craft and trade tradition as well as many years of resistance and efforts for the freedom of the Albanian people in Kosovo. Gjilan, the final city, is the largest city in eastern Kosovo. Compared to other cities, it is newer and has a more diverse ethnic structure, especially in its surroundings, where a community of ethnic Serbs lives.

4. Results and discussion

4.1 Hodonymes according to spatial identity

Through the quantitative analysis of urban toponymy in all selected cities, it is clear that all three levels of spatial identity (regional, national, and international) have been expressed, but regional hodonyms are most present, and only a few have international importance. The high share of regional and local hodonyms, which make up more than half of all hodonyms, is understandable. As a matter of fact, these hodonyms, in the best way, show the desire of the inhabitants to preserve the local names which bring attention to the importance of a person, historical event, meaning, or locality which has significantly affected the development of the city or the surrounding area.

Similar results emerge through the analysis of the distribution of hodonyms by city. From the beginning, it is noticeable that the participation of some hodonyms differs from one city to another. This is a result of the specific historical, geographical and political development of certain cities, their functional importance, and political status. However, the consistency can be detected by dominance of regional hodonyms compared to national or international ones.

To determine whether there is a difference in the representation of regional and national toponyms in the analyzed cities we have used location quotient which determined the degree of regional and national toponyms representation. From table 1 we can see that the location quotient is changing significantly from one city to another. In Prizren, Prishtina and Gjilan it is seen that national and international toponyms are more represented compared to regional toponyms while in Gjakova and Peja regional identity is more represented than national identity.

Deviating cases are the result of specific conditions of development of an individual city. For example, in the analysis of all toponyms that express spatial

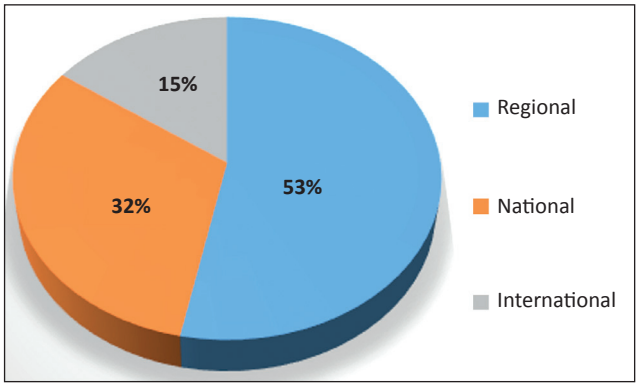

Fig. 2 Expression of identity in the urban toponomy of all cities.

Tab. 1 Location quotient of expression of regional and national identity in urban toponomy.

City	All toponyms that express		Toponyms that express exclusively	
	regional identity	national identity	regional identity	national identity
Prishtina	0.92	1.18	0.86	2.15
Prizreni	0.79	1.22	0.81	2.28
Peja	1.38	0.71	1.18	0.47
Gjakova	1.45	0.63	1.22	0.39
Gjilani	0.85	1.21	0.59	0.91
Total	1.08	0.99	0.93	1.24

identity (regional or national) the largest representation of regional hodonyms in Gjakova is explained by the multitude of doubled regional-national hodonyms. Most of streets and squares are named after people from Gjakova such as Pajazit Nushi, Emin Duraku, Esat Stavileci that has both regional and national importance. Analysis of street toponyms that express a unique regional identity highlight other specific issues. The largest deviation of regional hodonyms was recorded in Gjilan. Lower representation of regional toponyms in Gjilan compared to other Kosovar cities is partly the result of the greater presence of local hodonyms because of more diversified ethnic structure. These statistical indicators actually point out that the assumption of a more pronounced regional identity in Gjakova and Peja is the result of the presence of street nomenclature which is linked with names of personalities, those of geographical character and important historical dates that in one or another way are linked with the above mentioned cities and their surroundings.

After the disintegration of Yugoslavia, each of the newly formed states began to build new state identity, reinterpret and revise history, and establish new national symbols. The same happened after the change of political regime in 1989 in Czechoslovakia, where is evident the revision of historic facts, mostly those that formed part of modern history (Bucher et al. 2013). Changing the names of institutions, streets, and squares and erecting monuments to previously neglected personalities from national history is one of the results of this process. Today's Kosovo makes no exception from the rest of the former Yugoslavia. From 1999 onwards, in Kosovo, there have been many attempts to establish a new Kosovo identity. After the end of the war, and especially after the declaration of independence in 2008, through political decisions of municipal bodies, many streets of Kosovar cities have been renamed to be connected to the recent history of Kosovo and its efforts for independence. It was done by replacing the street names bearing the names of the fighters of the national liberation war. During this time were also renamed those streets dating from the period when the municipal leadership was controlled by Serbs, bearing the names of various Serbian historical personalities that reflects ethnically diversified structure of cities in Kosovo. In Pristina, for example, the street that once held the name of the Yugoslav communist Djuro Djakovic has been renamed Justinian Street. The street that once was named after Miladin Popovic, a Yugoslav partisan and the organizer of the partisan fighting in Kosovo, is now named after Ganimete Tërbeshi, a Kosovar fighter of the national liberation war. The street in Pristina that today bears the name of Agim Ramadani, one of the most prominent fighters of the Kosovo Liberation Army was originally named after the Serbian emperor, Tsar Dushani. At the same time, the municipal leadership of Pristina (which consisted of Serbs since the Albanians were at that time expelled from state institutions) had given way to the name of Sejdo Bajramovic, who was appointed as a representative of Kosovo in the presidency of the Yugoslav federation.

Prishtina, as a capital city, has the largest percentage of hodonyms of international character. Within the analyzed urban space of Prishtina, eighteen names express international identity. Some of the streets in Pristina that reference international figures hold the names of Johann Georg Von Han, the Austrian diplomat, philologist, and albanologist; Byzantine emperor Justinian, who was born in the vicinity of Lebane, part of dardanian empire; Garibaldi, the famous Italian military official, who is given credit for the unification of Italy; Gustav Meyer, the German writer and albanologist; Lord Byron, the English guide and writer who visited Albania; Dimitrije Tucovic, the Serbian politician; and Henri Dunant, the humanist and Swiss businessman. In other cities, although less prevalent, there are a few toponyms that express international identity. In Prizren, a street holds the name of the Scottish microbiologist and physicist Alexander Fleming; in Gjilan, a street has the name of one of the most famous victims of the Holocaust, Anne Frank; and another humanist and human rights activist Eva Brandly that was expelled from Kosovo by Milosevic regime, etc.

As a sign of salutation and honour for the help that the international community has given for the liberation of the country, several streets have been named after politicians, primarily American ones. This the case of Bill Clinton Square, named after the US President who ordered the bombing campaign angainst Serbian military and police targets in Kosovo and Serbia; George W. Bush, former US President; and Robert Doll, US Republican congressman. In Gjilan, a street is named after Madeleine Albright, former Secretary of State in the administration of President Bill Clinton. In Peja, one street is named after US Army General Wesley Clark, and another is named after William Walker, the American diplomat who incited the NATO bombing. In Prizren, a street is named Rambouillet after the small town on the periphery of Paris, where an

international peace conference was held, prior to the NATO bombing campaign against Serbia.

In 1947, Prishtina was declared a capital city, and it began to expand territorially while taking on various functions. In addition to these processes, Prishtina had a rapid increase of population, from 19,000 inhabitants in the 1948 census to 108,000 inhabitants in 1981, and today it has around 300,000 inhabitants. Prior to the entry of NATO troops, there were about 30,000 Serbs and Montenegrins in Pristina who made up about 18% of the city's population. This was also evident in urban toponymy where many streets held the names of Serbs and other non-Albanians. Immediately after the war, the streets that held these names were renamed. However, even today, some streets have the names of Serbs and non-Albanians. Some examples of non-Albanians who are namesakes for streets in Kosovo include the founder of the Social Democratic movement in Serbia, Dimitrije Tucovic; the Serbian physicist and philanthropist who lived and worked in the US, Mihajlo Pupin; Serbian journalist, politician, and professor, Kosta Novakovic; Serbian poet from Kosovo, Lazar Vuckovic; Croatian linguist, Henrik Baric, known as a founder of Department of Albanian Language in the University of Belgrade in 1921; Serbian academician Vojislav Dancetovic, who was one of the first professors of this chair; and the Montenegrin writer Radovan Zogovic, among others.

Prizren has the highest participation of national hodonyms, due to the fact that it has been an important political and administrative center since the time of the Ottoman Empire. The headquarters of the League of Prizren was there, which represented the most important political and military organization of Albanians at the end of the 19th century.

On the eve of the Congress of Berlin and the Treaty of St. Stephen, representatives of all regions of Albania met in Prizren. In this assembly, 300 delegates from all different Albanian lands established the Albanian Assembly known as the League of Prizren. One of the approved documents that derived from this meeting was the Memorandum of Independence of Albania which would include the territories of the Vilayet of Kosovo, Bitola, Shkodra, and Ioannina. Today, Prizren is the most famous tourist center of Kosovo. The main monuments of cultural heritage are the League of Prizren Complex, the Mosque of Sinan Pasha, the Hammam of Gazi Mehmet Pasha, and the church of Levishka from the Orthodox religious heritage, which is on the list of protected monuments by UNESCO.

National hodonyms are mostly dominated by the names of personalities including writers, patriots, scientists, academics, and others. Some of them were founders of the League of Prizren, as in the case of Sami Frashëri, while others were the most prominent representatives of the national renaissance such as Gjergj Fishta, Ndre Mjeda, and Selman Riza. National hodonyms of a geographical character are less common This includes Gjeravica, which is the highest mountain peak in Kosovo at 2,656 m; Ulqini and Ohri, cities within the Albanian geospace; and Bojnik, a settlement in the Toplica area, which before the Berlin Congress, was inhabited by a significant number of Albanians.

The expression of regional identity is related to the ethnic, but also religious, structure of the population. Before the last war, Prizren was known for its ethnic structure, where in addition to Albanians as the largest ethnic community, lived Serbs, Turks, Roma, and others. According to the 1981 census in Prizren, there were 63.7% Albanians, 12.4% Serbs, and 9.2% Turks. During the withdrawal of Yugoslav army and police troops, most Serb residents also left Prizren.

Because of this, in Prizren there are some streets that are named after different Turkish personalities, such as Emin Pasha Street, after an Ottoman scientist of Jewish origin; Evlia Çelebi, Suzi Çelebi and Ynus Emre, Ottoman writers; and Nysret Seharsaroj, Turkish writer.

4.2 Structure of regional hodonymes

From the analysis of the distribution of hodonyms according to the spatial level in observed cities, there is the largest presence of regional hodonyms. In this regard, their structure was analyzed in order to see how they are named. The table shows that in most cases, the names belong to persons who have played an important role in the development of the city or region. Out of a total of 539 hodonyms, 387 of them (or 71.8%) are named after personalities. Since Kosovo emerged from an armed war only two decades ago, this is consequently expressed by the large number of urban toponyms devoted to regional warriors of the recent war. This happened especially after the end of the war, when by municipal decision, the streets were renamed which had been previously named after warriors of World War Two. The exception is the city of Gjakova where even today, thirteen streets are named after warriors of World War Two, born mainly in the city of Gjakova (Tefik Çanga, Ganimete Tërbeshi, and Emin Duraku, for example).

Out of all cities that are part of the research, the regional identity is most expressed in the city of Gjakova, where out of 105 streets, 82 of them are named after personalities, while only 38 streets hold the names of personalities that are from Gjakova. The important fact is that among the personalities, apart from the warriors of the last war and the Second World War, many streets are named after academics, including scientists and university professors such as Fehmi Agani, Besim Bokshi, Pajazit Nushi, and Esat Stavileci.

Regional identity, while less than in other cities, is still expressed in the city of Gjilan, where from the total of 105 hodonyms, 48 of them are regional, and only 8 of them are named after individuals who were born in Gjilan. One street is named after Halim Orana,

Tab. 2 Structure of hodonymes of all spatial levels.

City	Personality		Geography		Event		Other	
	Number	%	Number	%	Number	%	Number	%
Prishtina	76	67.8	23	20.1	10	8.9	3	2.3
Gjakova	82	78.1	5	4.8	13	12.4	5	4.7
Prizreni	69	61.6	22	19.6	17	15.2	4	3.6
Peja	81	77.1	8	7.6	13	12.4	3	2.9
Gjilani	79	75.2	9	8.6	12	11.4	5	4.8
Total	387		67		65		20	

a patriot from Gjilan, another has the name of university professor Sadulla Brestovci, and another holds the name of the last warrior, Shaban Ukshini. Other hodonyms that express regional identity but are related to events or geographical objects have been also identified. These include the streets: Gjilan War, June 15, which is marked as the day of the liberation of the city, "Besëlidhja", "Gjinollët", a rich family of Gjilan. Regional hodonyms are also those that have geographical character as in the case of a street named Preveza, a city in the Albanian territory of Chameria which is now inside political borders of Greece; Tivari, a city in Montenegro that was previously inhabited by Albanians; Pashtriku, some mountains in Kosovo; and Butrint, a settlement and archeological site in southern Albania.

Out of 105 streets in the city of Peja, 81 of them express regional identity, and over half of them are named after personalities. Among them are warriors of the last war, such as Gazmend Berisha, Remzi Husaj, Mikel Marku, and Mustafë Kelmendi. Regional hodonyms of a geographical character appear nine times, mostly on roads, such as Dukagjini, Presheva, Tepelena, and Lezha. In the city of Peja, national identity is expressed in 18 different hodonyms. This includes the streets Mother Teresa, Mbreti Zog, Naim Frashëri, Çajupi, Hasan Prishtina, and Adem Jashari. International identity is expressed in the names of the streets named after Bucharest, Eliot Engell, Constantine the Great, Emperor Justinian, and American General Wesley Clark.

5. Conclusion

Symbolism satisfies a number of functions during the process of regional formation. It contributes to shaping the image, highlighting the values, and building the relationships of the inhabitants with the region in which they live. The collective identity of the urban population can be understood by observing street names which can be analyzed by statistical (quantitative) and interpretation (qualitative) methods. From the analysis of the expression of identity in the hodonyms of the five major Kosovar cities, the regional identity is much more widely expressed, compared to the national and international hodonyms, which have a smaller representation. Although regional hodonyms dominate in all cities that were analyzed, there are differences in the representation of regional hodonyms which are related to personalities, events, or geographical objects related to the respective city or surroundings. In this sense, regional identity is more evident in Gjakova and less in Gjilan. The functional status of the city, the historical-political processes, as well as the ethnic and religious structure influence of the hodonyms. Consequently, in Prishtina, in addition to regional hodonyms, there is a higher participation of national and international hodonyms. In contrast Prizren, due to its role in numerous historical-political developments, there is a slightly higher representation of hodonyms that express national identity, while regional hodonyms also express a heterogeneous ethnic structure with some toponyms named after Turkish personalities. In all cities the most common hodonyms are named after individuals, mainly after warriors of the last war, then scientists, artists, religious leaders, and others.

Regional identity is also conditioned by ethnic and religious structure. Thus, for example, in cities with a more heterogeneous ethnic structure, such as Prizren, in addition to streets that are named after historical Albanian figures, there are also streets bearing the names of Turks, or as in Prishtina, Serbs. After the disintegration of Yugoslavia, began to build new state identities, by reinterpreting and revising history, and establishing new national symbols. Changing the names of institutions, streets, and squares and erecting monuments to previously neglected personalities from national history is one of the results of this process. From 1999 onwards, in Kosovo, there is attempts of establishing a new Kosovo identity. After the end of the war and especially after the declaration of independence in 2008 through political decisions of municipal bodies many streets of Kosovar cities have been renamed by naming them connected to the recent history of Kosovo and its efforts for independence. This has been made clear while highlighting the regional differences in the use of street names in major Kosovar cities.

References

Albertini, M. (2012): Kosovo: An Identity between Local and Global. Ethnopolitics Papers no. 15, https://www.psa.ac.uk/sites/default/files/page-files/EPP015_0.pdf.

Azaryahu, M. (1997): German reunification and the politics of street names: the case of East Berlin. Political Geography 16(6), 479–493, https://doi.org/10.1016/S0962-6298(96)00053-4.

Azaryahu, M. (1986): Street names and political identity: The case of East Berlin. Journal of Contemporary History 21(4), 581–604, https://doi.org/10.1177/002200948602100405.

Bucher, S. Matlovič, R. Lukáčová, A. Harizal, B. Matlovičová, K. Kolesárová, J. Čermáková, L. Michalko, M. (2013): The perception of identity through urban toponyms in the regional cities of Slovakia. Anthropological Notebooks 19(3), 23–40, http://www.drustvo-antropologov.si/AN/PDF/2013_3/Anthropological_Notebooks_XIX_3_Bucher.pdf.

Crang, M. (1998): Cultural Geography. London and New York: Routledge, https://doi.org/10.4324/9780203714362.

Crljenko, I. (2008): Expression of Identity in Urban Toponymy of the Towns in Kvarner and Istria. Croatian Geographical Bulletin 70(1), 67–89, https://doi.org/10.21861/hgg.2008.70.01.04.

Culcasi, K. (2011): Cartographies of supranationalism: Creating and silencing territories in the "Arab Homeland". Political Geography 30(8), 417–428, https://doi.org/10.1016/j.polgeo.2011.08.003.

Drozdzewski, D. (2014): Using history in the streetscape to affirm geopolitics of memory. Political Geography 42, 66–78. https://doi.org/10.1016/j.polgeo.2014.06.004.

Leighly, J. (1978): Town names of colonial New England in the West. Annals of the Association of American Geographers 68(2), 233–248, https://doi.org/10.1111/j.1467-8306.1978.tb01193.x.

Giménez, G. (2005): Territorio e identidad. Breve introducción a la geografía cultural. Trayectorias 7(17), 8–24, https://www.redalyc.org/pdf/607/60722197004.pdf.

Guy, N. C. (2008): Linguistic boundaries and geopolitical interests: the Albanian boundary commissions, 1878–1926. Journal of Historical Geography 34(3), 448–470, https://doi.org/10.1016/j.jhg.2007.12.002.

Jukopila, D. (2017). Medjimurje – razine prostornog identiteta pogranicne tradicijske regije, (PhD Thesis), University of Zagreb, 221.

Keating, M. (1988). State and Regional Nationalism: Territorial Politics and the European State. London: Harvester Wheatsheaf.

Kosova, monographic survey (2011): Kosovar Academy of Sciences and Arts, 2011.

Paasi, A. (2002). Place and region: regional worlds and words. Progress in Human Geography 26(6), 802–811, https://doi.org/10.1191/0309132502ph404pr.

Paasi, A. (2003): Region and place: regional identity in question. Progress in Human Geography 27(4), 475–485, https://doi.org/10.1191/0309132503ph439pr.

Raitz, K. (1973): Ethnic settlements on topographic maps. Journal of Geography 72(8), 29–40, https://doi.org/10.1080/00221347308981340.

Rose-Redwood, R., Alderman, D., Azaryahu, M. (2010): Geographies of toponymic inscription: new directions in critical place-name studies. Progress in Human Geography 34(4), 453–470, https://doi.org/10.1177/0309132509351042.

Settlements of Kosova: Lexicon (2018): Kosovar Academy of Sciences and Arts, 2018.

Šabić, D., Pavlović, M. (2007): Regionalna svest i regionalni identitet. Zbornik Radova 55, 151–158.

Šakaja, L. (2003): Imaginativna geografija u hrvatskim ergonimima. Hrvatski geografski glasnik 65(1), 25–43, https://doi.org/10.21861/HGG.2003.65.01.02.

Vresk, M. (1997). Uvod u geografiju: razvoj, struktura, metodologija. Udžbenici Sveučilišta u Zagrebu: Školska knjiga.

Zelinski, W. (1988): Nation into State: The Shifting Symbolic Foundations of American Nationalism. Chapel Hill, NC: University of North Carolina Press.

The sequentially divergent-convergent development of mortality

Adéla Pola*

Charles University, Faculty of Science, Department of Demography and Geodemography, Czechia
* Corresponding author: adela.jodlova@natur.cuni.cz

ABSTRACT
This article aims to explore the convergence and divergence of mortality in different world regions along with factors influencing these developments. It identifies the most important deviations from global trends, explains their causes, and distinguishes world regions at risk of unfavorable demographic development resulting, for example, from excess male mortality or the failure to combat cardiovascular diseases. Finally, the article analyzes the divergent trends of mortality in the European post-socialist countries. The divergent-convergent development of mortality is understood as a sequential development, in contrast to traditional approaches, which study overall convergence and divergence trends, not their sequential course. Using the example of the development of the life expectancy at birth, the article shows that the phases of divergence and convergence are repeated.

KEYWORDS
mortality; sequentially divergent-convergent development; life expectancy at birth; post-socialist area

Received: 3 December 2021
Accepted: 26 April 2022
Published online: 2 June 2022

Pola, A. (2022): The sequentially divergent-convergent development of mortality. AUC Geographica 57(1), 39–47
https://doi.org/10.14712/23361980.2022.4

1. Introduction

Convergence and divergence can be understood as processes in which certain trends come together or delay, whether it is in demography, economy, or sociology. The study of convergent and divergent tendencies of demographic behavior is still a current and relevant topic, which records the development both in terms of content depth and scope and in terms of methodology. This article is mainly of a theoretical nature and therefore focuses on selected theoretical concepts that are within the core of the field of demography and population development, and their relationship to convergent or divergent mortality trends. The aim is to map the origin of the approximation and delay of mortality rates and to illustrate the relationship between convergence/divergence and stages of population development, as it is summarized in the theory of demographic revolution and health transition. The relationship between these processes may seem one-time causal when we consider the demographic revolution and the health transition as the causes of convergence or divergence of mortality. However, this relationship is in fact sequentially divergent-convergent. In general, when there are certain changes in the population, such as improved hygiene conditions or a reduction in infant mortality, they spread gradually and manifest themselves in different parts of the globe at various intervals, which leads to a divergence in mortality. Eventually, these changes will be reflected in the rest of the world, leading to convergence (Vallin and Meslé 2004). However, over time, technological innovations and advances in health care will trigger a new divergence, and therefore there is a constant alternation of phases of divergence and convergence. This sequential approach to the study of convergence and divergence of mortality is still not quite common in the literature.

The analysis of convergent and divergent tendencies has yet another benefit. It offers the possibility to identify regions or countries that differ from general development, thus opening the door to further examination of the causes and consequences of these deviations. Usually, demographic development, at least since the beginning of the demographic revolution, is divergent-convergent, as discussed above. However, several times in history, we have seen that there are periods or regions in general convergence trends that show signs of growing diversity or internal heterogeneity due to uneven development. Some of these specific developments are also mentioned in the literature, such as the regions of Africa where divergent-convergent development has been disrupted by the HIV/AIDS epidemic, or the post-socialist area where it has been suspended by political and economic reforms (Horiuchi 1999).

It was in the latter area that demographic development was specific in many respects in the 20th century. Firstly, mortality in the post-socialist region declined at the beginning of the century, following the example of developed countries, but increased in the 1960s, which is not expected according to the classical theory of the demographic revolution. Second, the development was also unique in terms of birth rates because the level of this process in the second half of the 20th century dropped sharply to much lower values than the theory of the demographic revolution assumed. Last but not least, the post-socialist region deserves a more detailed analysis in terms of demographic behavior, also because development in individual countries is very heterogeneous and it is questionable whether convergence will eventually be achieved here as well.

The relevance of the topic is also clear in our current global situation with the COVID-19 pandemic, as the long-term observed and still-expected development of mortality was disrupted. However, we cannot claim that the current development contradicts the sequentially divergent-convergent development of this process, on the contrary. After all, the last stages of the epidemiological transition, which is presented in the theoretical chapter, presuppose the return or occurrence of new infectious diseases (Caselli et al. 2002). Therefore, it can be concluded that the processes of convergence and divergence of mortality are still not completed because there is a constant alternation of these phases.

This paper opens a discussion on the analysis of sequentially divergent-convergent development, in this case in the area of mortality, which will allow a more relevant assessment of the impacts of such phenomena or events. The aim of this article is not to study these specific events and their impacts, but to define a sequential approach in the context of key theoretical concepts describing general trends in demographic development and reproductive behavior. The partial goals and contributions of this article can be summarized in three points. First, putting the sequential development of mortality in the context of demographic theories and proving it by linking the theory of demographic revolution and health transition with the timing of divergent and convergent phases of mortality. Second, an illustration of the possible perception of sequential demographic development from a practical point of view, which means to be able to find deviations not from the assumption of linear and uniform convergence development, but from that sequential one. Third, the identification of key areas or regions that may be affected by this specific development and deviations from the sequentially divergent-convergent development of mortality. It is highly desirable to study these regions in detail, as their divergent development can have huge impacts, not only demographic but also social or economic.

As previously mentioned, there are several goals and questions worthy of analysis, which this article examines: What do convergence and divergence of mortality stem from? What are the exceptions to the

sequentially divergent-convergent development of mortality? What are the specifics of the post-socialist region in the period from the 19th century to the present?

The theoretical background of convergence and divergence of mortality is dealt with in the second chapter describing the basic principles of selected theoretical concepts. This is followed by a third chapter on the data, methods and selection of countries to be analyzed. The subsequent practical section then examines sequentially divergent-convergent development of mortality and shows that demographic theories naturally carry the assumption of convergent and divergent tendencies. The analysis also makes it possible to identify deviations and specifics of selected areas.

2. Theoretical background

2.1 Demographic revolution

The beginnings of demographic convergence and divergence are usually associated with demographic revolution (Chesnais 1986). In reality, they go much deeper into the past, and signs of converging and delaying demographic development can be seen, for example, in plague epidemics. These did not appear all over the world at the same time, but quite differently. Mortality increased in the areas affected, leading to global divergence. Subsequently, the plague spread to other areas, resulting in global convergence (Bergdolt 2002). However, due to the absence of data, it is very difficult to carry out a demographic analysis of these events. Such analysis is worthy of exploration, but is beyond the scope of this article and belongs more to the field of historical demographers or epidemiologists.

In the 20th century, demographic revolution ended in many countries, which can be considered one of the most important changes in modern history. "The demographic revolution could be described briefly as a revolutionary and in the entire history of mankind unique quantitative-qualitative transformation of the nature of the demographic pattern, which in its outcome is most marked in changes in the levels of fertility, mortality and the age structure of individual populations" (Pavlík 1980: 135). The primary feature of this transformation is the change in the demographic regime from a high level of mortality and fertility to relatively low values, which we distinguish in three basic phases. The first is characterized by a high mortality rate, about three to four times higher than in Europe today. Fertility also reaches high values, which at this stage range from 4.5 to 7.5 live births per woman (Coale 1974). The levels of both processes are almost balanced and, as a result, there is minimal population growth. During the second phase, there is first a reduction in mortality and then in fertility. The transformation of mortality is usually more significant and the result is considerable population growth. The third phase is characterized by low and stable mortality rates, which are being approached by the birth rates, and in response, the rate of population growth decreases (Rabušic 2001).

However, the course, pace, and intensity of this transformation vary from country to country. Similar to plague epidemics, demographic revolution around the world manifested itself at different times. The beginning dates back to the second half of the 18th century and among the pioneers are the countries of Europe. Here, the demographic revolution took place circa in 1750–1930 and began in France and England, then manifested in northern, southern, and eastern Europe, and later progressed through the United States and Australia to Japan. In developing countries, it began to take place much later – in the 20th century. First in Latin America, then in Asia, and finally in Africa, and in many countries it is still unfinished (Pavlík 2004). We can therefore say that demographic revolution is a universal process that is taking place gradually in all countries of the world. Initially, it is characterized by relatively homogeneous levels of both key processes. During the transition, heterogeneity then increases as individual states gradually go through the various stages of the demographic revolution, and therefore divergence occurs. At the end, both processes reach a low level and again there is a tendency for convergence between states and populations.

2.2 Health transition

One concept close to the demographic revolution is the health transition, which explains the development of mortality and morbidity and closely touches the topic of demographic convergence and divergence. In 1971, Abdel Omran (1971) defined an epidemiological transition that describes the development of health in developed countries in three phases from the 18th century to the 1960s. The first phase is called the age of pestilence and famine, during which the mortality rate is high and fluctuates. Infectious diseases are among the leading causes of death, and mortality crises caused by epidemics and famines emerge. Life expectancy at birth does not exceed 30 years, on average. The second phase is the age of receding pandemics, when there is a significant increase in life expectancy at birth to 50 years, mainly due to the remission of infectious diseases. The third phase corresponds to the age of degenerative and man-made diseases which are characterized by a slowdown in the decline in mortality, as the suppression of infectious diseases makes degenerative and civilizational diseases more visible (Vallin and Meslé 2004).

At the time when Omran was developing his theory, a convergence within developed countries did occur, as the incidence of infectious diseases had already been greatly reduced there. Even less-developed countries made significant progress and were

gradually gaining control of infectious diseases. In the 1960s, however, the increase in life expectancy at birth slowed down and in some countries even stagnated, especially due to the growing impact of man-made diseases caused by smoking or traffic accidents. Progress was also not expected in the causes of death, which at the time were thought to be chiefly associated with the inevitable degeneration in old age, such as cancer or cardiovascular diseases. However, the increase in mortality from man-made diseases has been suppressed by effective policies and, in particular, by the revolution in the treatment of cardiovascular diseases. In the 1970s, a new period of progress began due to the cardiovascular revolution, which quickly appeared in developed countries. In response, mortality in adult and older ages began to decline again, especially from diseases of the circulatory system (Caselli et al. 2002). However, Omran could not have expected this development, as he based the formulation of the epidemiological transition only on the knowledge acquired before the 1960s, and therefore considered the third phase of the transition to be the last. Thus, Omran's theory soon became unsustainable, and considerations about the next stages of the epidemiological transition began to emerge gradually in connection with the cardiovascular revolution and the spread of HIV/AIDS. Finally, in 1991, Frenk et al. (1991) proposed to replace the epidemiological transition with a broader concept of health transition, which includes not only the development of epidemiological characteristics but also the policies and strategies of individual societies (Caselli 1995; Meslé and Vallin 2000). The first stage of this health transition is usually identified with the entire epidemiological transition and is generally considered to last until the end of the 1960s. The second phase then begins with the cardiovascular revolution, and the beginning of the third phase dates to the 1990s and is associated with successes in reducing the diseases of old age (Vallin and Meslé 2004).

Similar to the demographic revolution, the health transition did not take place simultaneously around the globe. For example, the second stage of the epidemiological transition began in the 18th century in northwestern Europe and gradually spread through southern and eastern Europe, where it was seen in the 20th century. In the case of the health transition, we can observe recurring divergent-convergent tendencies, because each significant improvement in mortality first leads to a divergence of populations, but after a certain time, there is a re-convergence. Until the 1960s, indeed, there was largely global convergence. Subsequently, however, dramatic exceptions to the general trend of increasing life expectancy at birth began to emerge. On the one hand, there were nations and regions, especially in Eastern Europe, that did not have enough resources to start a cardiovascular revolution. On the other hand, some countries still did not complete the second period of epidemiological transition, and in this situation, they were severely affected by epidemics such as AIDS (Caselli et al. 2002). Since the turn of the millennium, we can observe a new convergence, as lagging countries gradually catch up with pioneering states.

3. Data and methods

Long-term data are needed to capture the relationship between demographic theories related to the study of divergence and convergence of mortality and the stages of population development. In addition, in order to identify regions or countries that diverge or show a specific course, it is necessary to compare the situation on a global scale. For this reason, Gapminder is used as a main source of data for initial comparison as it provides data and estimates on life expectancy at birth for 197 countries in the period 1800–2100. This huge database is based on multiple sources, mainly data from the Institute of Health Metrics and Evaluation in their Global Burden Disease Studies (GBD 2019), World Population Prospects 2019, and Gapminder-Life expectancy v. 7 which is based on 100 sources (Gapminder). The second source of data used in this paper is the World Population Prospects 2019 (United Nations 2019), specifically the Life expectancy at birth for both sexes combined for the countries of the post-socialist region.

In terms of country selection, several representatives were chosen for each region of the world to represent area-specific development. The length of the time series for which data is available for a given country was also taken into account. Therefore, in Figure 1 we can see representatives of Western, Northern and Southern Europe (United Kingdom, France, the Netherlands, Sweden, Italy), Central Europe (Czechia and Hungary), Eastern Europe (Russia), developed non-European economies (Japan, United States, Australia), Latin America (Mexico), Asia (China and India) and Africa (Nigeria). Given the specific development of the post-socialist region, Figure 3 then shows selected countries in this area.

To analyze the pace and timing of the demographic revolution and the health transition, the basic indicator of mortality, life expectancy at birth, is used. Its advantage is that it makes it possible to easily and comprehensibly compare the development of mortality in the world and identify divergent and convergent tendencies. On the other hand, this indicator needs to be seen as a limit of research as well because it is a comprehensive indicator that hides specific mortality patterns (Borges 2018). Although, it does not allow a more detailed analysis, for example in terms of age or causes of death, it can be considered as a good indicator for creating an overall view, for basic international comparisons and also for finding specifics requiring a more detailed analysis, which is also one of the aims of the text.

The divergent-convergent development of mortality can also be indicated by the variation range, in this case the variation range of life expectancy at birth, which is calculated as the difference between the maximum and minimum value of the indicator.

4. Sequentially divergent-convergent development of mortality

In the light of the previous theoretical introduction, we can describe the development of mortality in the modern era as sequentially divergent-convergent since divergent-convergent cycles are still alternating. The following graph (Fig. 1) shows the development of life expectancy at birth in selected countries of the world, which represent geographical regions and the course typical for them. Due to the insufficient database for the older period, we can observe the development from the beginning of the 19th century to 2015 in the graph, with the number of analyzed countries increasing over time due to better data collection. At the beginning of the observed interval, we can compare only countries where statistics were already advanced in 1800. Not coincidentally, these are the pioneers where the demographic revolution first manifested itself.

Looking at life expectancy at birth in the countries shown in 1800 (United Kingdom, France, and Sweden), it is clear that the values of the indicator are in the range of 30–40 years (Fig. 1). This means that the demographic revolution was already in the process here, as before its start, life expectancy at birth ranges on average between 25–30 years. At the beginning of the reporting period, the level of the indicator was highest in the United Kingdom, where mortality conditions were better than in France, even though the demographic revolution began in the latter country. In the countries of southern and eastern Europe, we can see progress in mortality much later. For example, in Italy, a steady increase in life expectancy at birth began only around the 1870s, and in Hungary or Czechia (i.e. in Eastern European countries) only at the end of the 19th century. The beginning of the improvement in mortality was even later in Russia, where, in addition, there were significant fluctuations in life expectancy at birth. As for non-European developed countries, the demographic revolution spread here since the end of the 19th century. Data for Australia and the United States are available only from the 1870s and 1880s, respectively, but in both cases, we can observe a sharp and linear upward trend. It can therefore be assumed that these countries are among the pioneers, as the data show that both countries were far ahead of others and enjoyed a high life expectancy at birth for a long time (Oeppen and Vaupel 2002). A special case is Japan, which today is one of the most developed countries in the world, but it experienced a steady and significant increase in life expectancy at birth only at the end of the 19th century, much later than other industrialized countries.

In general, we can say that in developed countries the improvement in mortality began at different times

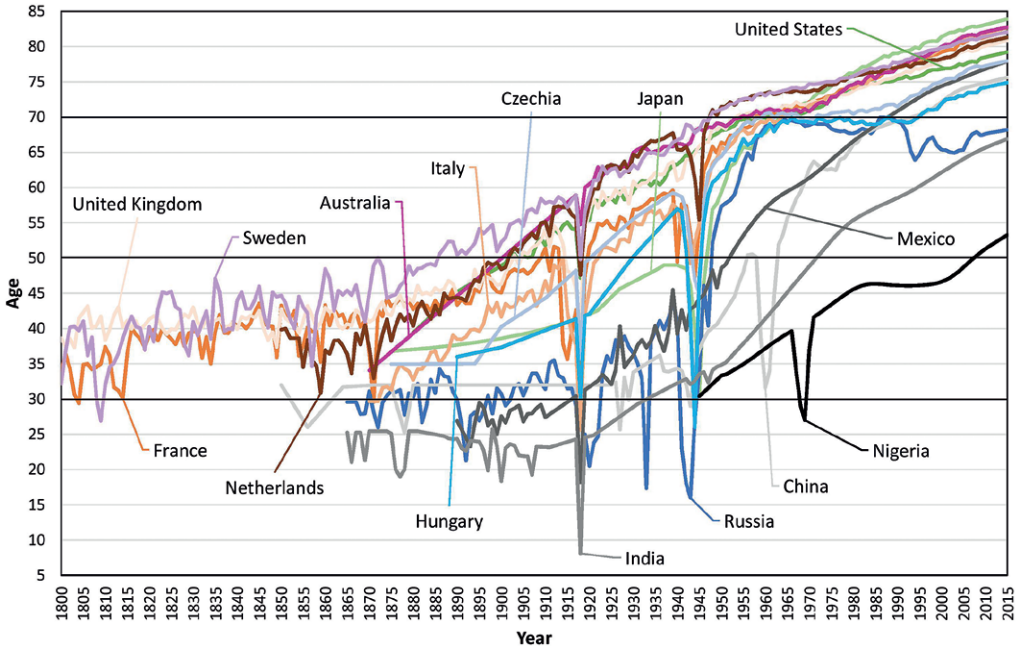

Fig. 1 Life expectancy at birth, both sexes, selected countries of the world, 1800–2015.
Source: Gapminder
Comment: The lower line at the age of 30 roughly defines the beginning of the demographic revolution and at the same time the transition between the first and second phases of the epidemiological transition. The middle line at the age of 50 indicates the break between the second and third phases. The upper line at the age of 70 marks the end of the demographic revolution.

between the end of the 18th century and the beginning of the 20th century, depending on the economic, social, and political context (Vallin and Meslé 2004). It is also important to note that in countries that began a steady increase in life expectancy at birth later, the pace of progress was faster than in pioneering countries. For this reason, we can first observe (Fig. 1) a divergent tendency, which was replaced in the second half of the 20th century by convergence, when all analyzed countries approached life expectancy at birth at the level of 70 years. In developed countries, maximum convergence was achieved in the 1960s. The divergent-convergent development is also indicated by the variation range of values of life expectancy at birth (Fig. 2). At the beginning of the observed period (1800), the indicator in developed countries[1] reached the value of 6.49, but due to the absence of data for most countries, this level cannot be reliably compared with other years. In 1890, we can already calculate the range from all industrialized countries, reaching the value of 20.55. The increase in the indicator is even more noticeable in the following years and the maximum of 50.97 was reached in 1942. Subsequently, the range began to decrease and reached its local minimum of 4.25 in 1964.

The first graph also shows that the development was very different in developing countries. Although data are available only for a later period, it is nevertheless clear that a permanent increase in life expectancy at birth did not occur in these regions until the 20th century: first around 1915 in Mexico, then approximately 1920 in India, 1925 in China, and finally around 1940 in Nigeria. Thus, the demographic revolution had really spread in developing countries from Latin America through Asia to Africa. These countries exceeded the aforementioned limit of life expectancy at birth of 30 years during the first half of the 20th century. However, many countries, especially in Asia and Africa, even today have not yet reached the level of 70 years associated with the end of the demographic revolution.

When we look at the development of life expectancy at birth from the point of view of the health transition (Fig. 1), we can see when countries, and therefore regions of the world, moved from one stage to another. When analyzing the health transition, the diversification of causes of death is crucial, however, the levels of life expectancy at birth, which were defined by Omran, can also be used for the basic definition of stages. In the first phase of the epidemiological transition, the average life expectancy at birth is less than 30 years, and in the second period, there is a significant increase of the indicator to 50 years. Subsequently, countries enter the third phase, when the rate of increase in life expectancy at birth slows down (Vallin and Meslé 2004).

At the beginning of the reporting period, this indicator of mortality level exceeded 30 years in France, England, and Sweden, which means that these countries have already entered the second phase of the epidemiological transition. In the second half of the 19th century, this limit was exceeded in Italy and at the end of the century in Russia. We can therefore say that developed countries entered the second phase of the epidemiological transition, with different timing, during the 18th and 19th centuries. On the contrary, developing countries did not end the first period until the first half of the 20th century. As for the transition from the second phase to the third, this occurred in northern Europe (represented here by Sweden) first, during the 1880s. Then it occurred at the turn of the century in Western Europe (the Netherlands, the United Kingdom, and France), in the 1920s in southern (Italy) and central (Czechia and Hungary) Europe, and finally prior to 1950 in Russia. As for non-European countries, the limit of life expectancy at birth of 50 years was exceeded in the United States and Australia, as in Western Europe, at the turn of the 19th and 20th centuries, while in Japan the third phase of the epidemiological transition began only after World War II. In Latin America (Mexico), the second period ended in the early second half of the 20th century, in Asia (China and India) in the 1960s and 1970s, and in Africa (Nigeria) not until the 21st century.

As mentioned above, the three stages of the epidemiological transition can be included in the first phase of the health transition, which in developed countries ended around the 1960s. At that time, the increase in life expectancy at birth slowed down significantly and often even stopped, and at the same time, the maximum convergence of life expectancy occurred in this decade. The cardiovascular revolution then started a new phase of the improvement of mortality conditions and the second phase of the health transition, simultaneously. However, it did not occur around the world all at once, which led to a divergent development of the indicator. The cardiovascular revolution first manifested itself in the 1970s in developed countries, except for Eastern Europe where it began late in the 1990s. This differing development is also evident in the first graph, where we can observe a renewed increase in life expectancy in Northern, Western, and Southern Europe since the 1970s, as well as in Australia, the United States, and Japan. By contrast, in Eastern Europe, mortality rates began to stagnate or even decline in the late 1960s. In Central Europe (Czechia and Hungary), the rise was resumed in the 1980s and 1990s, respectively, while in Russia mortality rates began to improve steadily only at the beginning of the 21st century. For this reason, we can observe a divergent development in Europe since the 1970s, which was replaced by convergence at the beginning of the 21st century.

1 Among the developed countries are the United States, Japan, France, Russia, the United Kingdom, Italy, Australia, the Netherlands, Sweden, Czechia, and Hungary.

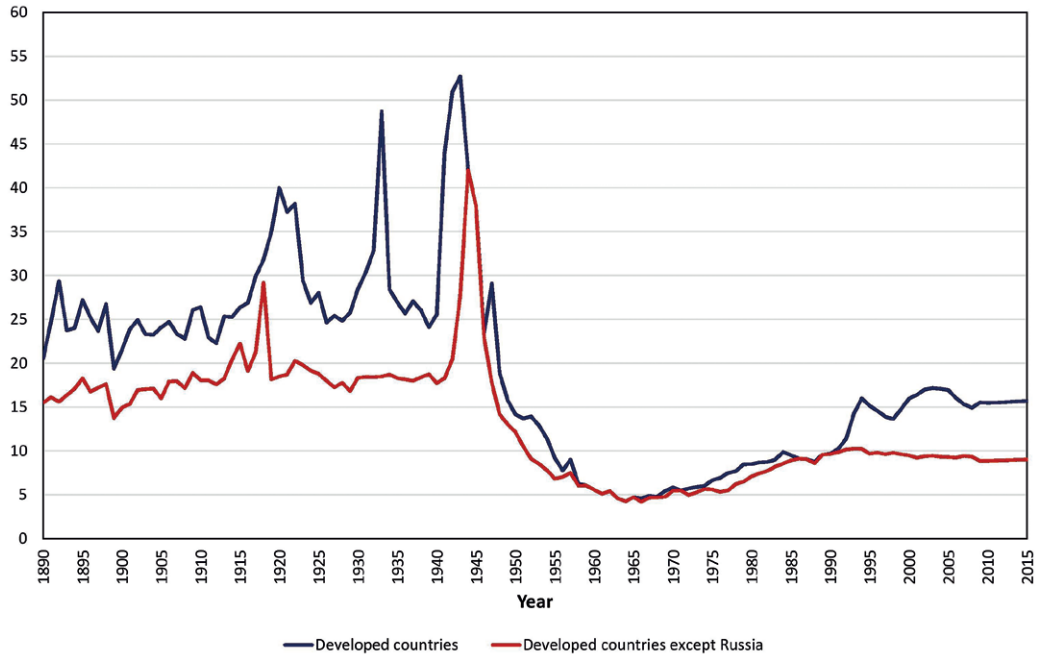

Fig. 2 Variation range of life expectancy at birth, developed countries, 1890–2015.
Source: Gapminder
Comment: The group of developed countries includes the United States, Japan, France, Russia, the United Kingdom, Italy, Australia, the Netherlands, Sweden, Czechia, and Hungary.

However, it is clear that in 2015 the variation range was much larger than in the 1960s, when the local minimum of 4.25 was reached in developed countries (Fig. 2). Subsequently, the value of the indicator increased until 2003, when the local maximum of 17.15 was reached. Since then, the range has decreased until 2010, when it was 15.47 and then increased slightly. The first graph shows that Russia differs significantly from other developed countries in its development and demonstrates a wider range. If we exclude this outlier from the calculation, the indicator reaches much lower values. Nevertheless, we can observe a similar development since 1964 when excluding Russia – the difference in life expectancy at birth grew until 1993 when it was 10.25 years. It then decreased until 2009, when it reached a local minimum of 8.85 and has been rising slightly since then (see Fig. 2). On that basis, we can conclude that some developed countries, especially in Eastern Europe, are lagging in increasing life expectancy at birth.

Turning our attention to developing countries (Fig. 1), we can see that in 2015 Mexico and China achieved similar levels of life expectancy at birth as Central European countries. This means that they have entered the second phase of the health transition, and in this case, we can talk about a convergence of mortality. However, other developing countries have not yet completed the first phase of the health transition, although India is gradually approaching the pace of developed countries. In Africa, the development of mortality is significantly delayed, because the African continent, especially the countries of sub-Saharan Africa, was affected by the HIV/AIDS epidemic just as it entered the second phase of the epidemiological transition. At that time, there should be a significant increase in life expectancy at birth, and this positive development was interrupted by the epidemic. The increase in life expectancy at birth was resumed here at the turn of the millennium, but the level of the indicator still remains very low (in 2015, the average life expectancy at birth in Nigeria was 53.3 years). Therefore, it cannot be said that developing countries are significantly getting closer to developed countries.

Based on the above-mentioned facts and analysis, we can indeed call the development of morality sequentially divergent-convergent. Furthermore, we can identify three groups of countries. The first one consists of developed countries, where divergence took place, especially at the beginning of the 20th century, and was replaced in the 1960s by convergence, which continues with some minor variation today. The second group includes developing countries, where the variation range began to increase from the 1930s, and only from the beginning of the 21st century can we observe a slight decrease in the indicator. This means that divergence dominated in this region during the analyzed period and there is no significant convergence even today. The third group is made up of Eastern European countries, which show a specific course that differs from the traditional development of mortality. Life expectancy at birth has been increasing rapidly since the beginning of the 20th century, as

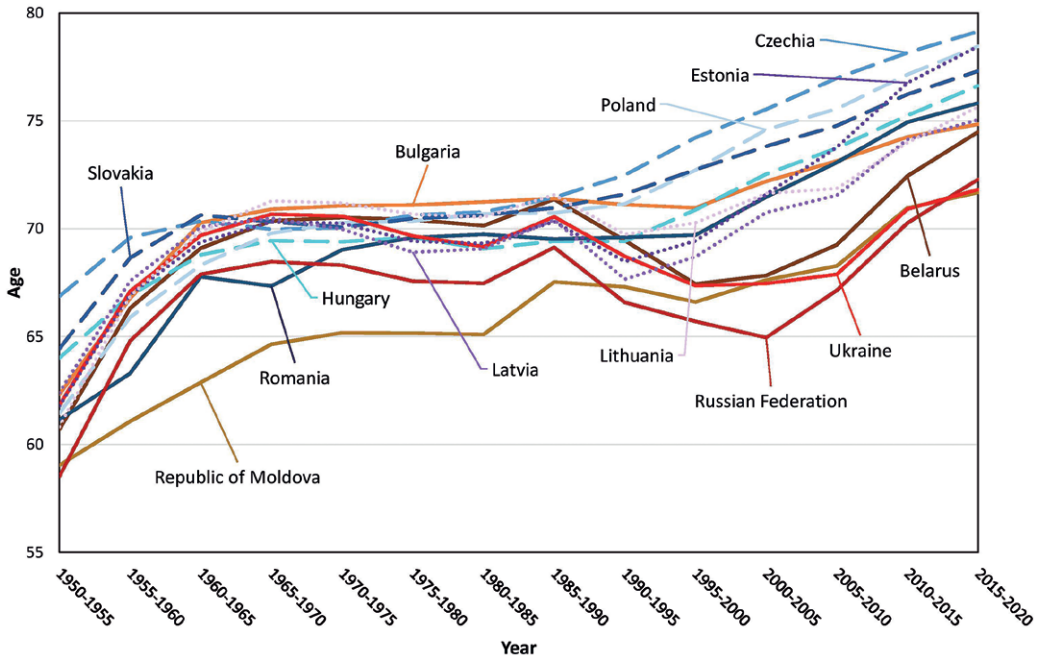

Fig. 3 Life expectancy at birth, both sexes, selected countries of post-socialist region, 1950–2020.
Source: United Nations, 2019

in other countries. At the end of the 1960s, however, growth stopped and even mortality rates dropped, not in response to political unrest or an epidemic, as is the case of Africa.

The post-socialist region, therefore, deserves more detailed analysis, mainly for two reasons. First, it deviates significantly from the development in developed countries, and second, we can observe heterogeneous development within the region. Based on the following graph (Fig. 3), it can be stated that from the middle of the 20th century, life expectancy at birth in the post-socialist area converged until about 1985, when the variation range reached the lowest value of 4.04. Maximum convergence compared to developed countries occurred later, due to the delayed cardiovascular revolution, as mentioned above. Subsequently, however, the indicator showed a markedly divergent trend, as mortality rates developed differently in subregions. The most significant improvement occurred in Central Europe (dashed curve in Fig. 3), with progress first seen in Czechia, then in Slovakia, Poland, and finally in Hungary. In the Baltic States (dotted curve in Fig. 3), life expectancy at birth first decreased and began to increase again from the 1990s, especially in Estonia. In Eastern Europe (the continuous curve in Fig. 3), the decline of the indicator was greater and the reverse did not occur until the turn of the millennium when the variation range in post-socialist region reached a maximum of 10.58 (see Fig. 3). Since then, we can observe a new phase of convergence here, and it can be assumed that the heterogeneous trend of the second half of the 20th century will be replaced by convergence.

5. Conclusion

The analysis of mortality using the development of life expectancy at birth confirms theoretical concepts according to which demographic development is sequentially divergent-convergent. Changes in health, economics, or politics are reflected individually in regions or states in terms of pace and intensity. For this reason, global divergence always occurs first, which is then replaced by convergence. Since new technologies and improvement of health care supervene at different time intervals, new phases of divergence and convergence of mortality are constantly emerging.

Sequentially divergent-convergent development of mortality is evident from the development of life expectancy at birth and variation range – indeed we can first observe global divergence, which was replaced by global convergence after World War II. After 1965, divergent tendencies reappeared, as regions of the world experienced different developments, not only demographic but also economic or political. After a short period of stagnation, developed countries have re-entered the path of progress, while the post-socialist area has faced an economic and social crisis, which has halted the improvement in mortality rates. In developing countries, life expectancy at birth was much lower due to delayed epidemiological transition and the HIV/AIDS epidemic. However, since the turn of the millennium, we can again speak of global convergence, as life expectancy at birth is increasing in all regions and levels are slowly converging. In general, therefore, we can say

that demographic development is sequentially divergent-convergent, where the phases of divergence and convergence gradually alternate and this process is still not complete.

The COVID-19 pandemic, which can be understood as the beginning of another divergence, also fits into this scenario. It began to appear gradually in regions of the world, with some affected more severely, others less so. Likewise, medical knowledge and measures have succeeded in reducing the incidence and mortality with COVID-19 over time, and we can hope for early convergence at a low mortality rate.

References

Bergdolt, K. (2002): Černá smrt v Evropě: velký mor a konec středověku. Praha: Vyšehrad.

Borges, G. M. (2018): Theories and measures of demographic convergence: an application to subnational levels in Latin America. In: Simpson L., González L. M. (eds.). ¿Convergencia demográfca? Análisis comparativo de las tendencias demográfcas subnacionales en América Latina y el Caribe. Río de Janeiro, Brasil: Asociación Latinoamericana de Población, 31–56, https://www.researchgate.net/publication/326132159_Convergencia_demografica_Analisis_comparativo_de_las_tendencias_demograficas_subnacionales_en_America_Latina_y_el_Caribe.

Caselli, G. (1995): The key phases of the European health transition. Polish Population Review (7), 73–102.

Caselli, G., Meslé, F., Vallin, J. (2002): Epidemiologic transition theory exceptions. Genus 58(1), 9–52, https://www.demogr.mpg.de/papers/workshops/020619_paper40.pdf.

Chesnais, J. (1986): La transition démographique. Etapes, formes, implications économiques. Paris: INED, Presses Universitaires de France, https://www.jstor.org/stable/1532931.

Coale, A. J. (1974): The history of the human population. Scientific American 231(3), 40–51, https://www.jstor.org/stable/24950164.

Frenk, J., Bobadilla, J. L., Stern, C., Frejka, T., Lozano, R. (1991): Elements for a theory of the health transition. Health Transition Review 1(1), 21–38, https://www.jstor.org/stable/40608615.

Gapminder. Life expectancy at birth (years) with projections [online]. [cit. 2021-08-23]. Stockholm, https://www.gapminder.org/data/documentation/gd004/.

Horiuchi, S. (1999): Epidemiological transitions in human history. In: United Nations (ed.). Health and mortality issues of global concern. New York: United Nations Population Division, Department of Economic and Social Affairs, 54–71.

Meslé, F., Vallin, J. (2000): Transition sanitaire: tendances et perspectives. Médecine/Sciences 16(11), 1161–1171, https://doi.org/10.4267/10608/1549.

Oeppen, J., Vaupel, J. W. (2002): Broken limits to life expectancy. Science 296 (5570), 1029–1031, https://doi.org/10.1126/science.1069675.

Omran, A. R. (1971): The epidemiologic transition: a theory of the epidemiology of population change. Milbank Memorial Fund Quarterly 49(4), 509–538, https://doi.org/10.2307/3349375.

Pavlík, Z. (1980): The theory of demographic revolution. European Demographic Information Bulletin 11(4), 130–139, https://doi.org/10.1007/BF02917743.

Pavlík, Z. (2004): Nejvýznamnější tendence světového populačního vývoje. Demografie 46(4), 230–234, https://dspace.cuni.cz/handle/20.500.11956/136765.

Rabušic, L. (2001): Kde ty všechny děti jsou?: porodnost v sociologické perspektivě. Praha: Sociologické nakladatelství.

United Nations (2019): World Population Prospects 2019 [online]. [Accessed 23. 8. 2021]. Online Edition, Rev. 1. Department of Economic and Social Affairs (DESA), Population Division. New York, https://population.un.org/wpp/Download/Standard/Population/.

Vallin, J., Meslé, F. (2004): Convergences and divergences in mortality: a new approach of health transition. Demographic Research 2, 11–44, https://doi.org/10.4054/DemRes.2004.S2.2.

Current global land systems classifications: comparison of methods and outputs

Aleš Hrdina*, Dušan Romportl

Department of Physical Geography and Geoecology, Faculty of Science, Charles University, Czechia
* Corresponding author: ales.hrdina@natur.cuni.cz

ABSTRACT
The anthropogenic impact on the functioning of natural systems and the concept of Anthropocene as a period of the human domination of the Earth has been widely discussed in literature in the past few decades. Consequently, several land systems classifications have been developed on a global scale to capture the diversity, intensity, and spatial distribution of the human suppression of natural stratification. This review presents the comparison of the most widely used complex global classifications, incorporating both natural conditions and the human influence on nature. Methods, input data, the number and type of output categories as well as their geographical extent and distribution are described and compared. The review will help potential users to find differences between available classifications and choose the right one for a particular use.

KEYWORDS
anthropogenic transformation; environmental stratification; global land use; human impact; land systems

Received: 11 October 2021
Accepted: 1 May 2022
Published online: 10 June 2022

Hrdina, A., Romportl, D. (2022): Current global land systems classifications: comparison of methods and outputs.
AUC Geographica 57(1), 48–60
https://doi.org/10.14712/23361980.2022.5

1. Introduction

The Earth is naturally stratified into specific zones, which have been classified in different ways by humans from ancient times. Humans have substantially changed this natural distribution by their actions, in the case of some regions so significantly that the original natural conditions have been completely suppressed in favour of anthropogenic factors (Vitousek et al. 1997). Therefore, several global classifications were presented to reflect the intensity of human influence covering a wide range of aspects of anthropogenic transformation. Most of the classifications are used as a spatial framework for assessing ecosystem or landscape processes (e.g. land cover / land use change, ecosystem services evaluation, ecosystem degradation etc.) and biodiversity monitoring (e.g. Ellis and Ramankutty 2008; Václavík et al. 2013). Some classifications were presented in order to describe the diversity and geographical differentiation of human pressure on the Earth (e.g. Letourneau et al. 2012).

In recent times of global climate and environmental change, understanding the different trends and impacts in specific land systems will be crucial in finding appropriate adaptation and mitigation measures. Existing global classifications may provide a useful spatial framework for such evaluation.

The aim of this review is to present selected global classifications, which are widely used and compare their methodology and results. Such an overview will help potential users in orientation and decision making, that is; which classification would fit a particular purpose of use.

2. Human domination of the Earth – development and geographical demonstration

People have been changing ecosystems, their processes and forms, for several million years (Goudie 2013). The oldest records (more than 3 million years ago) of human activity and technology have been found in various parts of Africa (Gosden 2003). The tools have become more sophisticated during the Stone Age (3.4 million years – ca. 4,000 BCE) and have enabled greater exploitation of natural resources. Other important factors were the development of communicative skills such as speech, and the discovery of the use of fire. Fire was one of the most powerful tools of environmental transformation. The Neolithic revolution (starting 10,000 to 8,000 BCE) has brought about many changes: the transition from a lifestyle of hunting and gathering to agriculture and settlement, the domestication of plants and animals, population growth, deforestation, irrigation etc. In the Holocene humans also began to mine ores and smelt metals (Goudie 2013). The Technological-Scientific Revolution and the development of modern industrial and urban civilizations have led to immense changes in the reshaping of ecosystems globally (Takács-Sánta 2004; Goudie 2013). The impact of human activities on the global environment rapidly increased (Crutzen 2002) and the number of ways in which humans are affecting the environment is multiplying (Vitousek et al. 1997). The 20th century was especially an epoch of very exceptional change (McNeill 2003).

The current period is called by some scientists, the Anthropocene (Crutzen 2002, Waters et al. 2016). The Earth is now more influenced by human activities than the forces of nature, according to a number of authors, anthropogenic transformation of the biosphere prevails (Vitousek et al. 1997; Crutzen 2002; Steffen et al. 2007; Ellis et al. 2010; Steffen 2010). Human impact is mainly reflected in land cover changes, therefore this information is often included in global classifications. However, the range of anthropogenic activities is much wider – e.g. geographical differentiation of population density, varied intensity of natural resource use, diverse intensities of domestic livestock, degradation of natural processes, etc. play important role as well in terms of natural systems alternation. Human activities are causing global biodiversity declines (Newbold et al. 2015), both inside and outside protected areas (Schulze et al. 2018), 75% of the planet's land surface is experiencing measurable human pressures (Venter et al. 2016; Williams et al. 2020; Ellis et al. 2021). Therefore, anthropogenic transformation of the natural systems cannot be simply ignored in modern global classifications. Human influence used to be simplified or ignored (Alessa and Chapin 2008; Ellis et al. 2010) and biomes were identified chiefly as a result of a combination of abiotic and biotic factors (Udvardy 1975; Olson et al. 2001; Bailey 2004, Higgins et al. 2016, Dinerstein et al. 2017). Several studies on environmental stratifications involving human influence have recently been published resulting in different spatially explicit classifications. The classifications result in the creation of global maps of anthropogenic biomes, anthromes, land-use systems, land systems, land system archetypes or world ecosystems (Ellis and Ramankutty 2008; Letourneau et al. 2012; van Asselen and Verburg 2012; Václavík et al. 2013; Sayre et al. 2020).

3. Global environmental classifications

3.1 Anthropogenic biomes

Ellis and Ramankutty (2008) presented the first global classification of terrestrial biomes based on an empirical analysis of direct human-nature interaction. The result of the analysis is a global map of anthropogenic biomes. A multi-stage empirical procedure was used for the identification and mapping of anthropogenic biomes, based on global data of

land use (percent area of pastures, crops, irrigated and rice), land cover (percent area of trees and bare earth) and population (Table 1). The analysis was executed at 5 arc minute resolution (5′ grid cells cover, i.e. 86 km^2 at the equator). The procedure first separated wild cells from anthropogenic cells based on the presence of human populations, pastures, and crops. The authors then categorized human-ecosystem interactions in anthropogenic cells into four classes according to population density. Dense class with high population intensity (more than 100 persons km^{-2}), residential class with substantial population intensity (10 to 100 persons km^{-2}), populated class with minor population (1 to 10 persons km^{-2}) and remote class with inconsequential population (less than 1 person km^{-2}). During the next step of cluster analysis using SPSS, natural groupings within the cells of each class were identified based on non-urban population density, percentage of urban areas, crops, pastures, irrigated lands, rice fields, tree cover and bare land. As the last step, the derived strata were organised into groupings based on their populations, land-cover and land-use characteristics; resulting in the 18 anthropogenic biome classes and 3 wild biome classes (Ellis and Ramankutty 2008).

Anthropogenic biome classes were classified into five basic groups: dense settlements, villages, croplands, rangelands and forested; wild biome classes belong to wildlands (Table 3). Dense settlements contain two biomes, 40% of people live here, the majority is urban population. This category covers 1.5 million km^2 and can be found especially in South and Southeast Asia, North America or in Western Europe. Villages include six biomes which also host 40% of people in the world but only 38% is urban. Village biomes cover 7.7 million km^2, and are most commonly found in Asia, where they cover more than a quarter of all land. They are also typical for regions of Europe or Africa. Croplands cover more than 27 million km^2 and host 15% of people (7% urban) in five biomes. In Europe croplands occupy almost half of all land; the residential irrigated cropland biome covers about 35%. Croplands are often also located in South and Southeast Asia, Latin America and Africa, covering about 25% of land in these areas. Rangeland biomes are the most extensive, covering nearly 40 million km^2, almost 30% of North and Latin America, Australia, New Zealand and Asia, but they are most common in Africa; (> 40%) especially in the Near East region (> 45%). Rangelands are divided into three different biomes, they account for less than 5 % of the global population. Forested biomes contain two classes: populated and remote forests, and cover 25 million km^2 of which more than 45% is covered with trees. Forested biomes contain only 0.6% of the global population and are typical for Latin America (40%) and Eurasia (25%). Wildlands occupy nearly 30 million km^2 (i.e. only 22% of Earth's ice-free land) and are located mainly in the Near East region (50%), North America, Australia and New Zealand (40%) and North Asia (30%) (Ellis and Ramankutty 2008).

Tab. 1 Datasets used for the classification of anthropogenic biomes.

Classification factor	Reference
Population	Dobson et al. (2000)
Pastures area	Ramankutty et al. (2008)
Crops area	Ramankutty et al. (2008)
Irrigated area	Siebert et al. (2007)
Rice area	Monfreda et al. (2008)
Tree cover	Hansen et al. (2003)
Bare earth	Hansen et al. (2003)

Tab. 2 Datasets used for the classification of anthromes.

Classification factor	Reference
Population density	Klein Goldewijk (2007)
Urban area	Klein Goldewijk (2007)
Cropland area	Klein Goldewijk (2007)
Pasture area	Klein Goldewijk (2007)
Irrigated area	Siebert et al. (2007)
Rice cover	Monfreda et al. (2008)
Land cover	Ramankutty and Foley (1999)

3.2 Anthromes

Ellis et al. (2010) used a new *a priori* anthrome classification algorithm built on standardized thresholds for classifying the same variables (Table 2) instead of the *a posteriori* anthrome classification used by Ellis and Ramankutty (2008). The new classification used the same basic classification levels but the system was simplified. Village classes were collapsed from six to four, croplands from five to four and wildlands from three to two. The forested level was broadened from two to four classes and named seminatural (Table 3). Ellis et al. (2010) also simplified the system interpretation by aggregating anthrome levels into three categories: used anthromes (dense settlements, villages, croplands, rangelands), semi natural anthromes and wildlands.

3.3 Land-use systems

Letourneau et al. (2012) proposed a new classification based on land-use systems, which represent specific combinations of interactions between humans and the natural environment. Land-use systems try to describe the heterogeneity of land cover and also land-use intensity; they are characterized by land cover, land use, population pressure and accessibility (Table 4). The spatial units of the analysis cover an area of less than 100 km^2 each (5 arc-minutes resolution). Multiple datasets were used in the classification: population density, land use / land cover data,

Tab. 3 List of classes of all classifications.

Classification	Category	Classes
Anthropogenic biomes	Dense settlements	1) Urban; 2) Dense settlements
	Villages	1) Rice villages; 2) Irrigated villages; 3) Cropped and pastoral villages; 4) Pastoral villages; 5) Rainfed villages; 6) Rainfed mosaic villages
	Croplands	1) Residential irrigated cropland; 2) Residential rainfed mosaic; 3) Populated irrigated cropland; 4) Populated rainfed cropland; 5) Remote croplands
	Rangeland	1) Residential rangelands; 2) Populated rangelands; 3) Remote rangelands
	Forested	1) Populated forests; 2) Remote forests
	Wildlands	1) Wild forests; 2) Sparse trees; 3) Barren
Anthromes	Dense settlements	1) Urban; 2) Mixed settlements
	Villages	1) Rice villages; 2) Irrigated villages; 3) Rainfed villages; 4) Pastoral villages
	Croplands	1) Residential irrigated croplands; 2) Residential rainfed croplands; 3) Populated rainfed cropland; 4) Remote croplands
	Rangeland	1) Residential rangelands; 2) Populated rangelands; 3) Remote rangelands
	Seminatural lands	1) Residential woodlands; 2) Populated woodlands; 3) Remote woodlands; 4) Inhabited treeless and barren lands
	Wildlands	1) Wild woodlands; 2) Wild treeless and barren lands
Land-use systems	Bare soils	1) Remote bare soils; 2) Accessible bare soils; 3) Populated areas covered by bare soils
	Cropland system	1) Accessible rainfed croplands; 2) Rainfed croplands with intensive livestock breeding; 3) Remote rainfed croplands; 4) Rice croplands with intensive bovines breeding; 5) Rice croplands with intensive bovines and monogastrics breeding; 6) Partly irrigated croplands with intensive livestock breeding; 7) Partly irrigated croplands with extensive livestock breeding; 8) Irrigated croplands with intensive livestock breeding; 9) Irrigated croplands with intensive bovines breeding
	Densely populated systems	1) Urban areas; 2) Villages or peri-urban area; 3) Villages and rice croplands; 4) Villages and irrigated croplands
	Forested systems	1) Sparse trees; 2) Populated areas with forests; 3) Remote forests
	Mosaic systems	1) Mosaic landscape; 2) Populated areas mosaic landscape
	Pastoral systems	1) Extensive pastures; 2) Intensive pastures with bovines and small ruminants; 3) Intensive pastures with bovines
Land systems	Cropland systems	1) Cropland extensive with few livestock; 2) Cropland extensive with bovines, goats and sheep; 3) Cropland extensive with pigs and poultry; 4) Cropland medium intensive with few livestock; 5) Cropland medium intensive with bovines, goats and sheep; 6) Cropland medium intensive with pigs and poultry; 7) Cropland intensive with few livestock; 8) Cropland intensive with bovines, goats and sheep; 9) Cropland intensive with pigs and poultry
	Mosaic cropland and grassland systems	1) Mosaic cropland and grassland with bovines, goats and sheep; 2) Mosaic cropland and grassland with pigs and poultry; 3) Mosaic cropland (extensive) and grassland with few livestock; 4) Mosaic cropland (medium intensive) and grassland with few livestock; 5) Mosaic cropland (intensive) and grassland with few livestock
	Mosaic cropland and forest systems	1) Mosaic cropland and forest with pigs and poultry; 2) Mosaic cropland (extensive) and forest with few livestock; 3) Mosaic cropland (medium intensive) and forest with few livestock; 4) Mosaic cropland (intensive) and forest with few livestock
	Forest systems	1) Dense forest; 2) Open forest with few livestock; 3) Open forest with pigs and poultry
	Mosaic (semi-)natural systems	1) Mosaic grassland and forest; 2) Mosaic grassland and bare
	Grassland systems	1) Natural grassland; 2) Grassland with few livestock; 3) Grassland with bovines, goats and sheep
	Bare systems	1) Bare; 2) Bare with few livestock
	Settlement systems	1) Peri-urban and villages; 2) Urban
Land system archetypes	–	1) Forest systems in the tropics; 2) Degraded forest/cropland systems in the tropics; 3) Boreal systems of the western world; 4) Boreal systems of the eastern world; 5) High-density urban agglomerations; 6) Irrigated cropping systems with rice yield gap; 7) Extensive cropping systems; 8) Pastoral systems; 9) Irrigated cropping systems; 10) Intensive cropping systems; 11) Marginal lands in the developed world; 12) Barren lands in the developing world
World ecosystems	–	431 classes; see Sayre et al. (2020)
IUCN Global ecosystem typology	Terrestrial	25 biomes and 108 ecosystem functional groups; see Keith et al. (2020)
	Subterranean	
	Freshwater	
	Marine	
	Atmospheric	

Tab. 4 Datasets used for the classification of land-use systems.

Classification factor	Reference
Bare soil area	Hansen et al. (2003)
Tree cover area	Hansen et al. (2003)
Build-up area	Elvidge et al. (2007)
Croplands area	Ramankutty et al. (2008)
Pastures area	Ramankutty et al. (2008)
Crop areas	Monfreda et al. (2008)
Irrigated areas	Siebert et al. (2005)
Sheep density	FAO (2007)
Goats density	FAO (2007)
Chicken density	FAO (2007)
Pigs density	FAO (2007)
Buffaloes density	FAO (2007)
Bovines density	FAO (2007)
Population density	Dobson et al. (2000)
Accessibility	Verburg et al. (2011)

livestock density and accessibility. Cropland data was not divided into several types in contrast with Ramankutty et al. (2008); livestock density data was converted to livestock unit densities according to FAO, which enabled the comparison of the densities of different types of livestock. Letourneau et al. used a two-step cluster analysis to identify particular land-use systems. Firstly, all the grid-cells were pre-grouped into many sub-clusters; secondly an algorithm grouped the sub-clusters into the optimal number of clusters according to the algorithm used. During the first stage of the clustering; wild areas, croplands or pastures were identified, then major categories of landscapes were determined. Each major category was further classified; the classification had 32 land-use systems, subsequently reduced to 24 classes (Letourneau et al. 2012).

Land-use system classes are grouped into six categories: densely populated systems (4 classes), cropland systems (9), pastoral systems (3), mosaic systems (2), forested systems (3) and bare soil systems (3). South America, Africa and Australia are dominantly covered by extensive pastoral land-use systems; in Europe, South America and New Zealand we can find intensive grazing systems; croplands are mainly found in Europe, SE Asia and North America. Densely populated systems are characterized by population densities above ca. 1000 inhabitants/km^2 (Letourneau et al. 2012). This classification is comparable with anthropogenic biomes (Ellis and Ramankutty 2008; Ellis et al. 2010).

3.4 Land systems

Van Asselen and Verburg (2012) claim that land use and land management were not represented adequately until the classification by Ellis and Ramankutty (2008). Relatively small, but important types of land use were not represented and mosaic landscapes were inaccurately characterized by a single homogeneous land cover type. Van Asselen and Verburg (2012) consider land-use intensity as a crucial characteristic of land systems and a main cause of environmental damage (Foley et al. 2005). Land cover, livestock and agricultural intensity data was used for classification of land systems (Table 5), population wasn't used as a classification criterion. Land cover variables were tree cover and bare soil cover (Hansen et al. 2003), cropland cover (Ramankutty et al. 2008) and built-up area (Schneider et al. 2009). Livestock data comes from FAO statistics (2007) and agricultural intensity is based on global data of Neumann et al. (2010). All data was transformed into spatial resolution of 5 arc-minutes in this study. For the classification and delineation of land systems, a hierarchical procedure was used (van Asselen and Verburg 2012).

The global land system classification map contains 8 categories. Cropland systems are divided into nine classes and cover about 8% of the world's land surface. They are characterized by an average cropland cover of ca. 70% and are distinguished based on agricultural intensity, and livestock type and intensity. 28% of the global population lives in this category. Extensive croplands can be found in Africa and India while intensive croplands are found in central-eastern US, Europe, SW Russia, in parts of China and India. The second category is called mosaic cropland and grassland systems, which contain five classes that all together cover 5% of the land surface and host 10% of the world's population. Extensive types occur mainly in Africa, whereas intensively managed systems are found in the United States, Europe or Argentina. Mosaic croplands and forest systems cover only 4% of the world's area, and 9% of the world's population lives in this area. These systems occur all over the world. Forest systems cover a much larger area of 21% of the world's land surface, but only 8% of the population can be found here. Dense forest systems have an average tree cover of about 80% and mostly include tropical forests or temperate forests at higher latitudes. Open forest systems (two different classes) have an average tree cover of about 55%. The next category, grassland systems cover 12% of the land surface and host 4.6% of the world's population. This category

Tab. 5 Datasets used for the classification of land systems.

Classification factor	Reference
Tree cover	Hansen et al. (2003)
Bare soil cover	Hansen et al. (2003)
Cropland cover	Ramankutty et al. (2008)
Build-up area	Schneider et al. (2009)
Livestock density	FAO (2007)
Efficiency of agricultural production	Neumann et al. (2010)

is divided into 3 classes, one natural**;** in tundra and two anthropogenic all over the world. Mosaic (semi-) natural systems are widely spread covering 24% of the world land surface, 8% of the population lives in the mosaic grassland and forest system, which occurs in Canada, Russia, South America, Central Africa and China, only 1.5% live in the second class – mosaic grassland and bare system. Settlement systems are subdivided into the urban, and peri-urban and village systems. They cover only 2% of the world's land surface, but 25% of people live here. Both classes can be found all over the world. The last category is named bare systems, and is subdivided into two classes; the average bare cover is 90%. Bare systems cover 1/4 of the land surface and host 5% of the world's population. These systems occur in the Sahara, Australia, western China, the Middle East, Mongolia, Kazakhstan etc. (van Asselen and Verburg 2012).

3.5 Land system archetypes

Mapping land systems with the incorporation of land-use intensity and land management is useful for a better understanding of the interactions and feedbacks between nature and people, measuring impacts, addressing global trade-offs of land-use change and developing better policies adapted to regional conditions (Foley et al. 2011; Seppelt et al. 2011; Václavík et al. 2013). In previous studies top-down approaches were used based on expert's rules or *a priori* classification**.** In the study of Václavík et al. (2013) a new approach was proposed for representing human-environment interactions, a bottom-up approach driven only by the data. Global land system archetypes were defined as unique combinations of environmental conditions, socioeconomic factors and land-use intensity; they were identified based on 32 indicators (Table 6). All datasets were derived for the period around the year 2005; spatial resolution was the same as in all previous studies – 5 arc-minutes. Land-use intensity was characterized by data on cropland and pasture (Klein Goldewijk et al. 2011) and their trends, use of N fertilizer (Potter et al. 2010), irrigation (Siebert et al. 2007), soil erosion (van Oost et al. 2007), yields and yield gaps for wheat, maize and rice (IIASA/FAO 2012), total production index and the human appropriation of net primary production (Haberl et al. 2007). Environmental conditions were characterised by 35 bioclimatic variables, from which 5 were selected for the final analysis (Kriticos et al. 2012), climate anomalies (Menne et al. 2009), NDVI mean and seasonality (Tucker et al. 2005), soil organic carbon (Batjes 2006) and species diversity of terrestrial mammals, birds, amphibians and reptiles from the IUCN database. Finally GDP, GDP from agriculture, the capital stock in agriculture (FAO), population density and its trend (CIESIN 2005), political stability (Kaufmann et al. 2010) and accessibility (Uchida and Nelson 2009) were used as socioeconomic factors. For the classification of land system archetypes, a self-organizing map algorithm (SOM) was used; an unsupervised neural network. The SOM analysis was conducted in R version 2.14.0. A 3 by 4 hexagonal plane was chosen as the two-dimensional output space. The final result was a map of global land system archetypes (Václavík et al. 2013).

Forest systems in the tropics represent the first archetype of a total of 12 archetypes. They cover ca. 14% of terrestrial ecosystems and they are determined mainly by climate. This archetype can be found in Latin America and the Amazon basin, West and Central Africa and in SE Asia. Degraded forest/cropland systems in the tropics cover only 0.35% of the world's land surface area; are characterized by enormous soil erosion and occur in Southeast Asia and Latin America. Boreal systems of the western world cover 14% of the world's land surface, it's an area of scarcely populated boreal forests and tundra. This LSA occurs mainly in Canada, Northern Europe, and Patagonia; or in higher elevations. Boreal systems of the eastern world occupy 20% of terrestrial ecosystems and are typical for Russia and Northeast China. Extensive cropping systems (11%) are defined by a high density of cropland and its increasing trend and the population density exceeding the global average. Extensive cropping systems occur in Eastern Europe, Sub-Saharan Africa, South America, India and China. Intensive cropping systems (5%) are also characterized by a high density of cropland, but it has decreased in recent decades. This land system archetype occurs in Western Europe, Eastern United States of America and Western Australia. Only 2% of terrestrial ecosystems are covered by irrigated cropping systems. The intense land-use pressure can be illustrated by a very dense population that has increased in the last 50 years. This archetype is typical for India, China or Egypt. Irrigated cropping systems with rice yield gap (only 1%) occur in economically very poor and also politically unstable regions such as Bangladesh, India and Southeast Asia. Pastoral systems (13%) are characterized by high densities of pastures and grasslands and are still scarcely populated. They are located in Central Asia, South and North Africa and Sahel, and in Latin America. High-density urban agglomerations cover only 0.1% of the world's land surface and values of its indicators are predominantly extreme, the population density is 7138 persons per km^2 etc. Marginal lands in the developed world (9%) have low values for indicators of land-use intensity, and the population density is only 6 people per km^2 and decreasing. This archetype occurs in Western USA, Australia or Argentina. The last land system archetype is called barren lands in the developing world and covers 11% of terrestrial ecosystems. It consists of mainly barren and desert areas characterized by low densities of cropland and pastures, extremely low primary production and an extreme climate. The population density is only 12 people per km^2, the countries are

Tab. 6 Datasets used for the classification of land system archetypes.

Classification factor	Reference
Temperature	Kriticos et al. (2012)
Diurnal temperature range	Kriticos et al. (2012)
Precipitation	Kriticos et al. (2012)
Precipitation seasonality	Kriticos et al. (2012)
Solar radiation	Kriticos et al. (2012)
Climate anomalies	http://www.ncdc.noaa.gov /cmb-faq/anomalies.php#grid
NDVI – mean	Tucker et al. (2005)
NDVI – seasonality	Tucker et al. (2005)
Soil organic carbon	Batjes (2006)
Species richness	http://www.iucnredlist.org /technical-documents/spatial-data
Cropland area	Klein Goldewijk et al. (2011)
Cropland area trend	Klein Goldewijk et al. (2011)
Pasture area	Klein Goldewijk et al. (2011)
Pasture area trend	Klein Goldewijk et al. (2011)
N fertilizer	Potter et al. (2010)
Irrigation	Siebert et al. (2007)
Soil erosion	Van Oost et al. (2007)
Yield for wheat	http://www.gaez.iiasa.ac.at/
Yield for maize	http://www.gaez.iiasa.ac.at/
Yield for rice	http://www.gaez.iiasa.ac.at/
Yield gap for wheat	http://www.gaez.iiasa.ac.at/
Yield gap for maize	http://www.gaez.iiasa.ac.at/
Yield gap for rice	http://www.gaez.iiasa.ac.at/
Total production index	http://faostat.fao.org/
HANPP	Haberl et al. (2007)
Gross domestic product	http://faostat.fao.org/
Gross domestic product in agriculture	http://faostat.fao.org/
Capital stock in agriculture	http://faostat.fao.org/
Population density	CIESIN (2005)
Population density trend	CIESIN (2005)
Political stability	http://www.govindicators.org
Accessibility	http://bioval.jrc.ec.europa.eu /products/gam/index.htm

poor and very politically unstable. Barren lands exist in regions of the Middle East, Saharan Africa, the deserts of Namibia and the Gobi and Atacama deserts (Václavík et al. 2013).

3.6 World ecosystems

Sayre et al. (2020) described a new set of maps of global ecosystems at a spatial resolution of 250 m (8 arc-seconds resolution). The map of terrestrial world ecosystems was derived from the objective development and integration of global temperature domains, global moisture domains, global landforms, and global vegetation and land use (Table 7).

Tab. 7 Datasets used for the classification of world ecosystems.

Classification factor	Reference
Global temperature domains	Fick and Hijmans (2017)
Global moisture domains	Trabucco and Zomer (2009)
Global landforms	Karagulle et al. (2017)
Global vegetation and land use	ESA (2017)

Temperature data come from the WorldClim version 2 (Fick and Hijmans 2017) database. Global temperature domains consist of six temperature classes (tropical, subtropical, warm temperate, cold temperate, boreal, and polar). World moisture domains are based on the value of the aridity index (AI) (Trabucco and Zomer 2009), and there are three classes (moist, dry, desert) designed. The world temperature domains layer and the world moisture domains layer were then combined to derive a world climate regions layer. With six temperature domains and three moisture domains, a total of 18 climate regions is possible (Sayre et al. 2020). The climate regions data were then combined with a world landforms data layer that is an aggregation of the global Hammond landforms layer (Karagulle et al. 2017) into four classes (mountains, hills, plains, and tablelands), extending the 18 climate region classes to 72 possible climate region and landform combinations, called world climate and terrain settings. In the end Sayre et al. (2020) combined this layer with the world vegetation and land cover data layer. The world vegetation and land cover layer contains forest, shrubland, grassland, cropland, sparsely or non-vegetated (bare) area, settlements, snow and ice, and water classes, and was derived from the global land cover data produced by the European Space Agency (ESA 2017). A combination of the previous 72 settings with the eight vegetation classes yields 576 total possible combinations of world ecosystems. A total of 431 world ecosystems were identified, and of these a total of 278 units were natural or semi-natural vegetation/environment combinations. The biggest classes of the classification are Tropical moist forest on plains, Tropical desert sparsely or non-vegetated on plains, Boreal moist forest on mountains, and Subtropical moist forest on mountains, all having more than 3 million km^2 (Sayre et al. 2020).

3.7 IUCN Global ecosystem typology

This typology (version 2.0) is created as a hierarchical classification. In its upper three levels, functional variation among ecosystems is represented, ecosystems are defined by their convergent ecological functions. In its lower three levels, compositional variation is represented, ecosystems with differing groups of species influencing those ecological functions are defined (Keith et al. 2020).

The top level of the classification consists of five global realms: terrestrial, but also subterranean,

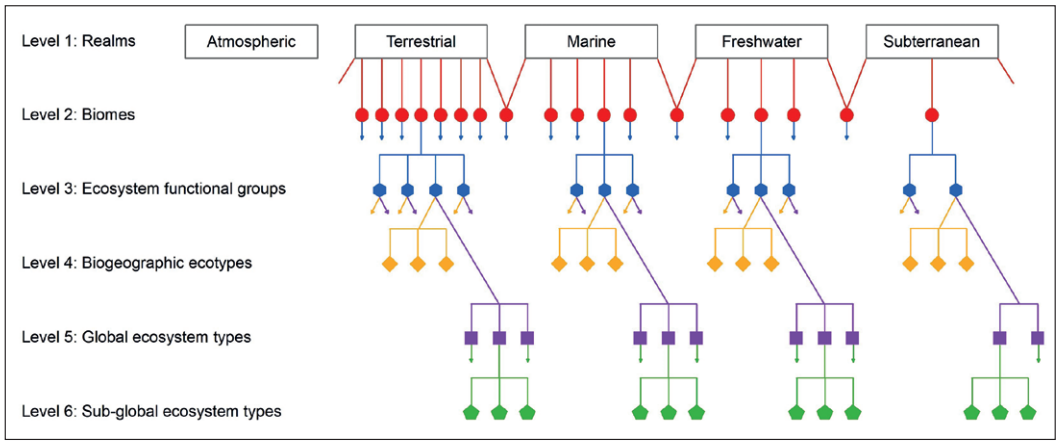

Fig. 1 Hierarchical structure of Global Ecosystem Typology.
Source: Keith et al. 2020

freshwater, marine, and atmospheric. Realms at the interface between contrasting environments are called transitional realms. At the second level, the classification defines 25 biomes ranging from tropical forests to several anthropogenic biomes. At the third level, the classification splits into 108 classes called Ecosystem Functional Groups (EFG). These three levels were developed from the top-down approach. The units of the fourth level are developed top-down by division of EFGs. In contrast, the fifth and sixth level facilitate integration of established local classifications into the global framework. Integration uses the bottom-up approach. The units at the fourth and fifth level are both nested with the third level units; they represent alternative pathways below the third level (Figure 1). Level four units are called Biogeographic ecotypes, they are ecoregional expressions of an EFG. Global ecosystem types create the fifth level of the classification, they are complexes of organisms, with similar ecological processes and their associated physical environment within an area occupied by an EFG, but with substantial difference in composition of organisms. And finally the sixth level – Sub-global ecosystem types are subunits or nested groups of subunits within a global ecosystem type, which exhibit more compositional homogeneity and resemblance to one another than global ecosystem types (Keith et al. 2020).

In the terrestrial realm can be found seven biomes: tropical-subtropical forests, temperate-boreal forests and woodlands, shrublands and shrubby woodlands, savannas and grasslands, deserts and semi-deserts, polar-alpine, and intensive land-use systems. These biomes are further divided into 34 EFGs. There are also transitional realms with terrestrial component: palustrine wetlands, shoreline systems, supralittoral coastal systems, anthropogenic shorelines, and brackish tidal systems comprising altogether a total of 16 EFGs (Keith et al. 2020).

4. Comparison and discussion of methods and outputs of global environmental classifications

Ellis and Ramankutty (2008), Ellis et al. (2010), Letourneau et al. (2012), Van Asselen and Verburg (2012) applied top-down approaches based on expert's rules or *a priori* classification, in contrast Václavík et al. (2013) used a bottom-up approach to reduce the level of subjectivity and also used a much

Tab. 8 Comparison of global environmental classifications.

Name	Authors	Number of categories		Number of classes	Resolution
Anthropogenic biomes	Ellis and Ramankutty (2008)	6		21	5 arc minutes
Anthromes	Ellis et al. (2010)	6		19	5 arc minutes
Land-use systems	Letourneau et al. (2012)	6		24	5 arc minutes
Land systems	Van Asselen and Verburg (2012)	8		30	5 arc minutes
Land system archetypes	Václavík et al. (2013)	–		12	5 arc minutes
World ecosystems	Sayre et al. (2020)	–		431	8 arc seconds
IUCN Global ecosystem typology	Keith et al. (2020)	5	25	108	30 arc seconds

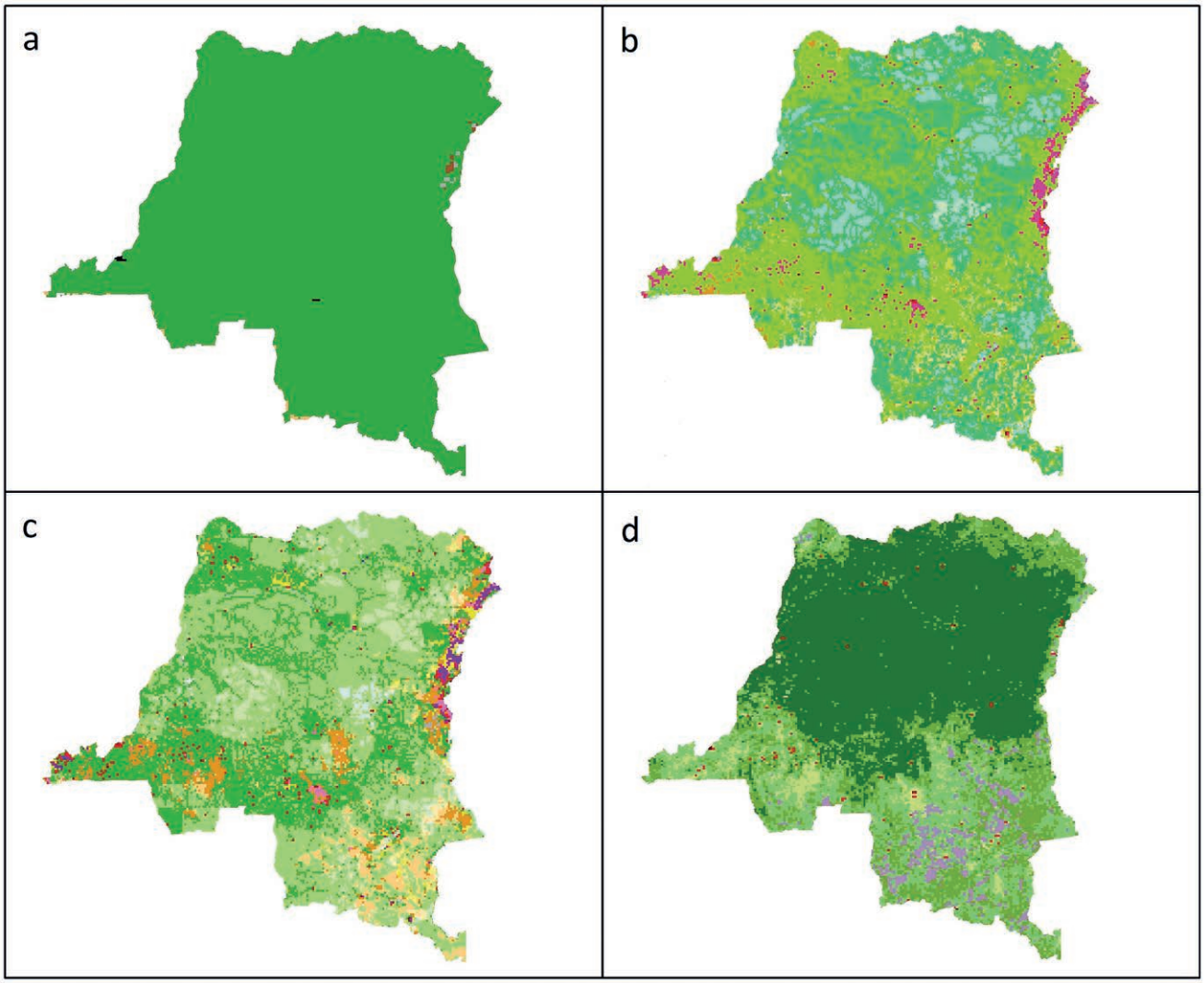

Fig. 2 Comparison of land system archetypes (a), anthropogenic biomes (b), anthromes (c) and land systems (d) on the example of The Democratic Republic of the Congo.

higher number of input classification factors (32) compared to the other studies (Tables 1–2, 4–6). All these classifications were executed at the same 5 arc minute resolution. Sayre et al. (2020) have taken the structural approach. They mapped and subsequently integrated different natural elements. World ecosystems were executed at the 8 arc seconds resolution. Keith et al. (2020) used the combination of top-down and bottom-up approaches, which serves to balance consistency with realism. The IUCN Global ecosystem typology was executed at the 30 arc seconds resolution. Anthropogenic biomes, anthromes, land-use systems and land systems all have a similar structure. They are grouped into six or eight categories respectively; each category is further divided into individual classes. Land system archetypes are completely different, there are 12 categories, which are not further divided. World ecosystems consist of 431 different classes. The IUCN Global ecosystem typology has five categories at the top level further divided into 25 classes and further into 108 units, etc. (Table 8).

Anthropogenic biomes, anthromes, land-use systems and land systems are suitable for further use on a wide range of scales, from global to regional; or a sub-regional scale. Land system archetypes are useful mainly on a global or continental scale (Figure 2).

On the other hand, land system archetypes present the most objective classification and they are based on much more different types of input data. World ecosystems and Global ecosystem typology are created at a much finer spatial resolution. They are useful especially for conservation management.

The availability of individual classifications including a link for download is shown in the following table (Table 9), classifications of Ellis and Ramankutty (2008), Ellis et al. (2010), Van Asselen and Verburg (2012), Václavík et al. (2013), Sayre et al. (2020) and Keith et al. (2020) are for those interested, freely available.

Tab. 9 Availability of global environmental classifications

Name	Authors	Data reference (link for download)
Anthropogenic biomes	Ellis and Ramankutty (2008)	Anthrome Data (https://ecotope.org/anthromes/data/)
Anthromes	Ellis et al. (2010)	Anthrome Data (https://ecotope.org/anthromes/data/)
Land-use systems	Letourneau et al. (2012)	N/A
Land systems	Van Asselen and Verburg (2012)	Global Land System classification data (https://www.environmentalgeography.nl/site/data-models/data/global-land-system-classification/)
Land system archetypes	Václavík et al. (2013)	Land system archetypes (https://www.ufz.de/index.php?en=37603)
World ecosystems	Sayre et al. (2020)	World ecosystems (https://rmgsc.cr.usgs.gov/outgoing/ecosystems/Global/)
IUCN Global ecosystem typology	Keith et al. (2020)	Global ecosystems (https://global-ecosystems.org/)

5. Summary

All the classifications show human-environment interactions, but each in a slightly different way. Interesting regional patterns, similarities on a global level and differences on a sub-national scale – can all be found here. Every classification provides a naturally generalized and simplified picture of a rather diverse reality. The best currently available datasets are used, but the quality and spatial resolution of all the input data are the limiting factors, moreover datasets often capture information for different periods. Many factors that could be very useful for classification aren't available or lack the necessary quality (Ellis and Ramankutty 2008; Letourneau et al. 2012; van Asselen and Verburg 2012; Václavík et al. 2013). Anthropogenic biomes, anthromes, land-use systems, land systems, land system archetypes, world ecosystems or whatever we want to call them, are useful in the better understanding of global human-environment interactions and land-use change impacts, identifying regions with similar policy demands, they can also help with the global change challenges and can be used as inputs for global land change models and other modelling.

Naturally, all classifications presented differ in the purpose of their development, complexity of input variables and range of use by both scientists, international institutions, government bodies and the general public. Anthropogenic biomes and anthromes (Ellis and Ramankutty 2008; Ellis et al. 2010), land-use systems (Letourneau et al. 2012), land systems (van Asselen and Verburg 2012) and land system archetypes (Václavík et al. 2013) have certainly had a significant impact, and each has been cited hundreds or thousands of times. Anthropogenic biomes and anthromes have become part of the Principles of Terrestrial Ecosystem Ecology and the National Geographic Atlas of the World, and have been incorporated into the IUCN Global ecosystem typology (Keith et al. 2020). These classifications have recently been used also in analysing long-term changes (Ellis et al. 2021). The most recent classifications with most likely future impact are, firstly, World ecosystems, the system devised by Sayre et al. (2020) for the Nature Conservancy and IPCC, a useful tool for the Convention on Biological Diversity's (CBD) Aichi Target 11, IUCN, FAO or IPBES. World ecosystems can be used in global conservation, global planning efforts. This system is data-derived with high spatial resolution. On the contrary, WWF Ecoregions (Olson et al. 2001, Dinnerstein et al. 2017) are expert-derived, coarse, and macroscale. And, secondly, the Global ecosystem typology (Keith et al. 2020) approved by the IUCN. Ecosystems of the new IUCN Red List of Ecosystems are classified according to the IUCN Global ecosystem typology, a framework based on ecosystem function and biodiversity.

All the classifications provide a complex global spatial framework incorporating both natural and human factors that influence the functioning of land systems. Therefore, they can be used for the monitoring of global change of land use, ecosystems and biodiversity dynamics, global conservation and much more.

Acknowledgements

Supported by the Charles University Grant Agency (GAUK) project No. 387115.

References

Alessa, L., Chapin, F. S. (2008): Anthropogenic biomes: a key contribution to earth-system science. Trends in ecology and evolution 23(10), 529–531, https://doi.org/10.1016/j.tree.2008.07.002.

Bailey, R. G. (2004): Identifying ecoregion boundaries. Environmental management 34(1), S14–S26, https://doi.org/10.1007/s00267-003-0163-6.

Batjes, N. H. (2006): ISRIC-WISE Derived Soil Properties on a 5 by 5 arcminutes Global Grid (Ver. 1.1), Report 2006/02. ISRIC – World Soils Information, Wageningen, https://www.isric.org/sites/default/files/isric_report_2006_02.pdf.

CIESIN (2005): Gridded Population of the World Version 3 (GPWv3): Population Density Grids. Socioeconomic Data and Applications Center (SEDAC)/Columbia University/Centro Internacional de Agricultura Tropical (CIAT), Palisades, NY, https://doi.org/10.7927/H4XK8CG2.

Crutzen, P. J. (2002): Geology of mankind. Nature 415(6867), 23, https://doi.org/10.1038/415023a.

Dinerstein, E., Olson, D., Joshi, A.,Vynne, C., Burgess, N. D., Wikramanayake, E., Hahn, N., Palminteri, S., Hedao, P., Noss, R., Hansen, M., Locke, H., Ellis, E. C., Jones, B., Barber, Ch. V., Hayes, R., Kormos, C., Martin, V., Crist, E., Sechrest, W., Price, L., Baillie, J. E. M., Weeden, D., Suckling, K., Davis, C., Sizer, N., Moore, R., Thau, D., Birch, T., Potapov, P., Turubanova, S., Tyukavina, A., de Souza, N., Pintea, L., Brito, J. C., Llewellyn, O. A., Miller, A. G., Patzelt, A., Ghazanfar, S. A., Timberlake, J., Klöser, H., Shennan-Farpón, Y., Kindt, R., Lillesø, J.-P. B., van Breugel, P., Graudal, L., Voge, M., Al-Shammari, K. F., Saleem, M. (2017): An ecoregion-based approach to protecting half the terrestrial realm. Bioscience 67(6), 534–545, https://doi.org/10.1093/biosci/bix014.

Ellis, E. C., Klein Goldewijk, K., Siebert, S., Lightman, D., Ramankutty, N. (2010): Anthropogenic transformation of the biomes, 1700 to 2000. Global Ecology and Biogeography 19(5), 589–606, https://doi.org/10.1111/j.1466-8238.2010.00540.x.

Ellis, E. C., Ramankutty, N. (2008): Putting people in the map: anthropogenic biomes of the world. Frontiers in Ecology and the Environment 6(8), 439–447, https://doi.org/10.1890/070062.

Ellis, E., Gauthier, N., Klein Goldewijk, K., Bird, R., Boivin, N., Diaz, S., Fuller, D., Gill, J., Kaplan, J., Kingston, N., Locke, H., Mcmichael, C., Ranco, D., Rick, T., Shaw, M., Stephens, L., Svenning, J.-Ch., Watson, J. (2021): People have shaped most of terrestrial nature for at least 12,000 years. Proceedings of the National Academy of Sciences 118 (17): e2023483118, https://doi.org/10.1073/pnas.202348311.

ESA (European Space Agency) (2017). Land cover CCI product user guide version 2.0. http://maps.elie.ucl.ac.be/CCI/viewer/download/ESACCI-LC-Ph2-PUGv2_2.0.pdf

FAO (2007). Gridded Livestock of the World, 141 p., FAO, Rome.

FAO – FAOSTAT, http://www.fao.org/faostat/en/#data.

Fick, S. E., Hijmans, R. J. (2017): WorldClim 2: new 1-km spatial resolution climate surfaces for global land areas. International Journal of Climatology 37, 4302–4315, https://doi.org/10.1002/joc.5086.

Foley, J. A., DeFries, R., Asner, G. P., Barford, C., Bonan, G., Carpenter, S. R., Chapin, F. S., Coe, M. T., Daily, G. C., Gibbs, H. K., Helkowski, J. H., Holloway, T., Howard, E. A., Kucharik, Ch. J., Monfreda, Ch., Patz, J. A., Prentice, C., Ramankutty, N., Snyder, P. K. (2005): Global consequences of land use. Science, 309(5734), 570–574, https://doi.org/10.1126/science.1111772.

Foley, J. A., Ramankutty, N., Brauman, K. A., Cassidy, E. S., Gerber, J. S., Johnston, M., Mueller, N. D., O'Connell, C., Ray, D. K., West, P. C., Balzer, C., Bennett, E. M., Carpenter, S. R., Hill, J., Monfreda, C., Polasky, S., Rockstrom, J., Sheehan, J., Siebert, S., Tilman, D., Zaks, D. P. M. (2011): Solutions for a cultivated planet. Nature 478, 337–342, https://doi.org/10.1038/nature10452.

Gosden, C. (2003). Prehistory: A Very Short Introduction. OUP Oxford, https://doi.org/10.1093/actrade/9780192803436.001.0001.

Goudie, A. S. (2013): The human impact on the natural environment: past, present, and future. John Wiley and Sons.

Haberl, H., Erb, K. H., Krausmann, F., Gaube, V., Bondeau, A., Plutzar, C., Gingrich, S., Lucht, W., Fischer-Kowalski, M. (2007): Quantifying and mapping the human appropriation of net primary production in earth's terrestrial ecosystems. Proceedings of the National Academy of Sciences of the United States of America 104 (31), 12942–12945, https://doi.org/10.1073/pnas.0704243104.

Hansen, M., DeFries, R., Townshend, J.R., Carroll, M., Dimiceli, C., Sohlberg, R. (2003): Vegetation Continuous Fields MOD44B. University of Maryland, College Park.

Higgins, S. I., Buitenwerf, R., Moncrieff, G. R. (2016). Defining functional biomes and monitoring their change globally. Global Change Biology 22(11), 3583–3593, https://doi.org/10.1111/gcb.13367.

Hijmans, R. J., Cameron, S. E., Parra, J. L., Jones, P. G., Jarvis, A. (2005): Very high resolution interpolated climate surfaces for global land areas. International journal of climatology 25(15), 1965–1978, https://doi.org/10.1002/joc.1276.

IIASA/FAO (2012): Global Agro-Ecological Zones (GAEZ v3.0) IIASA/FAO, Laxenburg, Austria/Rome, Italy.

IUCN – The IUCN Red List of Threatened Species, http://www.iucnredlist.org/technical-documents/spatial-data.

Jenkins, C. N., Pimm, S. L., Joppa, L. N. (2013): Global patterns of terrestrial vertebrate diversity and conservation. Proceedings of the National Academy of Sciences 110(28), E2602–E2610, https://doi.org/10.1073/pnas.1302251110.

Karagulle, D., Frye, C., Sayre, R. (2017): Modeling global Hammond landform regions from 250-m elevation data. Transactions in GIS 21(5), 1040–1060, https://doi.org/10.1111/tgis.12265.

Kaufmann, D., Kraay, A., Mastruzzi, M. (2010): The worldwide governance indicators: methodology and analytical issues. The World Bank Policy Research Working Paper Series, 5430. World Bank, http://hdl.handle.net/10986/3913.

Keith, D. A., Ferrer-Paris, J. R., Nicholson, E., Kingsford, R. T. (eds.) (2020): The IUCN Global Ecosystem Typology 2.0: Descriptive profiles for biomes and ecosystem functional groups. Gland, Switzerland: IUCN, https://doi.org/10.2305/IUCN.CH.2020.13.en.

Kier, G., Mutke, J., Dinerstein, E., Ricketts, T.H., Küper, W., Kreft, H., Barthlott, W. (2005): Global patterns of plant diversity and floristic knowledge. Journal of Biogeography 32(7), 1107–1116, https://doi.org/10.1111/j.1365-2699.2005.01272.x.

Klein Goldewijk, K., Beusen, A., van Drecht, G., de Vos, M. (2011): The HYDE 3.1 spatially explicit database of human-induced global land-use change over the past 12,000 years. Global Ecology and Biogeography 20(1), 73–86, https://doi.org/10.1111/j.1466-8238.2010.00587.x.

Kriticos, D. J., Webber, B. L., Leriche, A., Ota, N., Macadam, I., Bathols, J., Scott, J. K. (2012): CliMond: global high-resolution historical and future scenario climate surfaces for bioclimatic modelling. Methods in Ecology and Evolution 3(1), 53–64, https://doi.org/10.1111/j.2041-210X.2011.00134.x.

Letourneau, A., Verburg, P. H., Stehfest, E. (2012): A land-use systems approach to represent land-use dynamics at continental and global scales. Environmental Modelling

and Software 33, 61–79, https://doi.org/10.1016/j.envsoft.2012.01.007.

McNeill, J. R. (2003): Resource exploitation and overexploitation: a look at the 20th century. Exploitation and overexploitation in societies past and present. Münster: LIT Verlag, 51–60.

Menne, M. J., Williams, C. N., Vose, R. S. (2009). The US historical climatology network monthly temperature data, version 2. Bulletin of the American Meteorological Society 90(7), 993–1007, https://doi.org/10.1175/2008BAMS2613.1.

Mittermeier, R. A., Mittermeier, C. G., Brooks, T. M., Pilgrim, J. D., Konstant, W. R., Da Fonseca, G. A., Kormos, C. (2003): Wilderness and biodiversity conservation. Proceedings of the National Academy of Sciences 100(18), 10309–10313, https://doi.org/10.1073/pnas.1732458100.

Neumann, K., Verburg, P. H., Stehfest, E., Müller, C. (2010): The yield gap of global grain production: a spatial analysis. Agricultural Systems 103 (5), 316–326, https://doi.org/10.1016/j.agsy.2010.02.004.

Newbold, T., Hudson, L., Hill, S. et al. (2015): Global effects of land use on local terrestrial biodiversity. Nature 520**,** 45–50. https://doi.org/10.1038/nature14324.

Olson, D. M., Dinerstein, E., Wikramanayake, E. D., Burgess, N. D., Powell, G. V. N., Underwood, E. C., D'amico, J. A., Itoua, I., Strand, H. E., Morrison, J. C., Loucks, C. J., Allnutt, T. F., Ricketts, T. H., Kura, Y., Lamoreux, J. F., Wettengel, W. W., Hedao, P., Kassem, K. R. (2001): Terrestrial Ecoregions of the World: A New Map of Life on Earth. BioScience 51(11), 933–938, https://doi.org/10.1641/0006-3568(2001)051[0933:TEOTWA]2.0.CO;2.

Pimm, S. L., Jenkins, C. N., Abell, R., Brooks, T. M., Gittleman, J. L., Joppa, L. N., Raven, P. H., Robertsand, C. M., Sexton, J. O. (2014): The biodiversity of species and their rates of extinction, distribution, and protection. Science 344(6187): 1246752, https://doi.org/10.1126/science.1246752.

Potter, P., Ramankutty, N., Bennett, E. M., Donner, S. D. (2010): Characterizing the spatial patterns of global fertilizer application and manure production. Earth Interactions 14(2), 1–22, https://doi.org/10.1175/2009EI288.1.

Ramankutty, N., Evan, A. T., Monfreda, C., Foley, J. A. (2008): Farming the planet: 1. Geographic distribution of global agricultural lands in the year 2000. Global Biogeochemical Cycles 22(1): GB1003, https://doi.org/10.1029/2007GB002952.

Sanderson, E. W., Jaiteh, M., Levy, M. A., Redford, K. H., Wannebo, A. V., Woolmer, G. (2002): The human footprint and the last of the wild. BioScience 52(10), 891–904, https://doi.org/10.1641/0006-3568(2002)052[0891:THFATL]2.0.CO;2.

Sayre, R., Karagulle, D., Frye, C., Boucher, T., Wolff, N. H., Breyer, S., Wright, D., Martin, M., Butler, K., Van Graafeiland, K., Touval, J., Sotomayor, L., McGowan, J., Game, E. T., Possingham, H. (2020): An assessment of the representation of ecosystems in global protected areas using new maps of World Climate Regions and World Ecosystems. Global Ecology and Conservation 21: e00860, https://doi.org/10.1016/j.gecco.2019.e00860.

Schneider, A., Friedl, M. A., Potere, D. (2009): A new map of global urban extent from MODIS satellite data. Environmental Research Letters 4:044003, https://doi.org/10.1088/1748-9326/4/4/044003.

Schulze, K., Knights, K., Coad, L. et.al (2018): An assessment of threats to terrestrial protected areas. Conservation Letters 11(3): e12435, https://doi.org/10.1111/conl.12435.

Seppelt, R., Dormann, C. F., Eppink, F. V., Lautenbach, S., Schmidt, S. (2011): A quantitative review of ecosystem service studies: approaches, shortcomings and the road ahead. Journal of Applied Ecology 48(3), 630–636, https://doi.org/10.1111/j.1365-2664.2010.01952.x.

Siebert, S., Döll, P., Feick, S., Hoogeveen, J., Frenken, K. (2007): Global Map of Irrigation Areas Version 4.0.1. Johann Wolfgang Goethe University/Food and Agriculture Organization of the United Nations, Frankfurt am Main, Germany/Rome, Italy.

Steffen, W., Crutzen, P. J., McNeill, J. R. (2007): The Anthropocene: are humans now overwhelming the great forces of nature. AMBIO: A Journal of the Human Environment 36(8), 614–621, https://doi.org/10.1579/0044-7447(2007)36[614:TAAHNO]2.0.CO;2.

Steffen, W. (2010): Observed trends in Earth System behaviour. Wiley Interdisciplinary Reviews: Climate Change 1(3), 428–449, https://doi.org/10.1002/wcc.36.

Takács-Sánta, A. (2004): The major transitions in the history of human transformation of the biosphere. Human Ecology Review 11(1), 51–66, http://www.jstor.org/stable/24707019.

Trabucco, A., Zomer, R. J. (2009): Global aridity index (Global-Aridity) and global potential evapo-transpiration (Global-PET) geospatial Database. CGIAR consortium for spatial information, http://www.csi.cgiar.org.

Tucker, C. J., Pinzon, J. E., Brown, M. E., Slayback, D. A., Pak, E. W., Mahoney, R., Vermote, E. F., El Saleous, N. (2005): An extended AVHRR 8-km NDVI dataset compatible with MODIS and SPOT vegetation NDVI data. International Journal of Remote Sensing 26(20), 4485–4498, https://doi.org/10.1080/01431160500168686.

Uchida, H., Nelson, A. (2009): Agglomeration Index: Towards a New Measure of Urban Concentration. World Bank, Washington, DC, https://doi.org/10.1093/acprof:oso/9780199590148.003.0003.

Udvardy, M. D., Udvardy, M. D. F. (1975): A classification of the biogeographical provinces of the world (Vol. 8). Morges, Switzerland: International Union for Conservation of Nature and Natural Resources, http://fnad.org/Documentos/A%20Classification%20of%20the%20Biogeographical%20Provinces%20of%20the%20World%20Miklos%20D.F.%20Udvardy.pdf.

van Asselen, S., Verburg, P. H. (2012): A Land System representation for global assessments and land-use modeling. Global Change Biology 18(10), 3125–3148, https://doi.org/10.1111/j.1365-2486.2012.02759.x.

van Oost, K., Quine, T. A., Govers, G., De Gryze, S., Six, J., Harden, J. W., Ritchie, J. C., McCarty, G. W., Heckrath, G., Kosmas, C., Giraldez, J. V., da Silva, J. R. M., Merckx, R. (2007): The impact of agricultural soil erosion on the global carbon cycle. Science 318(5850), 626–629, https://doi.org/10.1126/science.1145724.

Václavík, T., Lautenbach, S., Kuemmerle, T., Seppelt, R. (2013): Mapping global land system archetypes. Global Environmental Change 23(6), 1637–1647, https://doi.org/10.1016/j.gloenvcha.2013.09.004.

Venter, O., Sanderson, E., Magrach, A. et al. (2016): Sixteen years of change in the global terrestrial human footprint and implications for biodiversity conservation. Nature Communications 7: 12558, https://doi.org/10.1038/ncomms12558.

Vitousek, P. M., Mooney, H. A., Lubchenco, J., Melillo, J. M. (1997): Human domination of Earth's ecosystems. Science 277(5325), 494–499, https://doi.org/10.1126/science.277.5325.494.

Waters, C. N., Zalasiewicz, J., Summerhayes, C. et al. (2016): The Anthropocene is functionally and stratigraphically distinct from the Holocene. Science 351(6269), https://doi.org/10.1126/science.aad2622.

Williams, B., Venter, O., Allan, J. et al. (2020): Change in terrestrial human footprint drives continued loss of intact ecosystems. One Earth 3(3), 371–382, https://doi.org/10.1016/j.oneear.2020.08.009.

The role of cohorts in the understanding of the changes in fertility in Czechia since 1990

Jiřina Kocourková, Jitka Slabá*, Anna Šťastná

Department of Demography and Geodemography, Faculty of Science, Charles University, Czechia
* Corresponding author: jitka.slaba@natur.cuni.cz

ABSTRACT
This article presents a detailed analysis of the fertility changes in Czechia since 1990 using the cohort approach and contributes to the overall understanding of the fertility postponement process. Because the timing of childbearing since 1990 has changed significantly, particular attention is devoted to the differences in the timing of fertility between cohorts. Data from the Human Fertility Database was analyzed via both standard (based on age-specific fertility rates) and advanced methods (postponement and recuperation indicators, parity progression ratio). Four groups of cohorts with specific fertility patterns were identified: 1965–1970, 1971–1976, 1977–1982, and 1983–1990. These groups were impacted by the political, economic and social transformation of the 1990s, the financial crisis of 2008–2012 and other socio-economic changes during the study period in different ways. While the 1965–1970 cohort was associated with the rapid occurrence of postponement, it still reflected the early fertility pattern. The 1971–1976 cohort was associated with the most intensive degree of postponement, the 1977–1982 cohort can be linked to the onset of the deceleration of the postponement process, and the 1983–1990 cohort appears to be the first to stabilize their fertility at later ages.

KEYWORDS
fertility patterns; Czechia; cohort analysis; postponement and recuperation; parity progression ratio

Received: 28 January 2022
Accepted: 13 June 2022
Published online: 29 June 2022

Kocourková, J., Slabá, J., Šťastná, A. (2022): The role of cohorts in the understanding of the changes in fertility in Czechia since 1990. AUC Geographica 57(1), 61–74
https://doi.org/10.14712/23361980.2022.6

1. Introduction

Following the Velvet Revolution of 1989, Czech society experienced a large number of changes. The most important processes comprised the transformation of the political system towards democracy and that of the centrally-planned economy to a market economy. These changes also influenced the reproductive behavior of Czech couples as indicated by trends in the level and timing of fertility (Kocourková and Fait 2011; Polesná and Kocourková 2016; Kurkin et al. 2017; Křesťanová and Kurkin 2020). The total fertility rate decreased markedly during the 1990s (from 1.91 in 1990 to 1.14 in 1999); while it has since recovered significantly, it remains below an average of two children per woman (TFR 1.66 in 2019; see Figure 1). Despite the decline in fertility, the ideal and planned family size has remained practically unchanged. Most Czech men and women, as with other Europeans, wish to have two children (Šťastná 2007; Rabušic and Chromková Manea 2013; Sobotka and Beaujouan 2014). The drop in the period fertility rate was accompanied by a gradual increase in the mean age of women at childbirth, which was particularly dramatic in the 1990s (see Figure 1). The period mean age of women at childbirth was 24.8 years in 1990 and 30.2 years in 2019. This increase was driven mainly by changes in the timing of fertility, i.e. by the delaying of fertility rather than by changes in the birth order composition (a decrease in third and higher order fertility) (Křesťanová 2016; Sivková and Hulíková Tesárková 2012).

The change in the mean age at motherhood has been considered by many researchers who have published on the topics of the postponement of fertility and later childbearing (see for example Sobotka 2017; Šprocha and Bačík 2020; Beaujouan 2020; Kocourková and Šťastná 2021, etc.). Generally, the fertility postponement process has been described as the consequence of value changes, the increasing individualization of society (Lesthaeghe 2010) and overall increasing economic uncertainty (Kohler, Billari, and Ortega 2002; Billingsley 2010). Recent studies on value-related changes have stressed the impact of education since it is becoming increasingly clear that the higher education of women has contributed significantly to the explanation of changes in fertility timing (Ní Bhrolcháin and Beaujouan 2012; Neels et al. 2017). The argumentation concerning the increasing role of the education effect on fertility timing also appears to be valid in the case of Czechia, where the proportion of students, in particular women, in tertiary education has been increasing gradually since 1990 (Czech Statistical Office 2014; Kurkin et al. 2017).

As regards economic uncertainty, the effect on fertility timing can be understood in two ways, as a temporal uncertainty related to the life stage (e.g. during study or at the outset of a career) or as a temporal uncertainty driven by macro-economic forces (e.g. an economic crisis). The postponement of fertility due to economic uncertainty leads to a temporary decline in period fertility rates. In Czechia, the effect of economic factors can be identified from 1990 onward (see Figure 1). Firstly, the drop in total fertility rates during the 1990s was related to the initial period of economic transition from 1990 to 1996 when Czech GDP declined beyond the stagnation level (Vltavská and Sixta 2015). Following a recovery in the period fertility rate in the 2000s, a further drop in fertility occurred after the start of the global financial crisis in 2008 (Kocourková et al. 2019). Interestingly, the total fertility rate initially stagnated and subsequently declined temporarily (see Figure 1). Since 2013, the total fertility rate has been increasing. The study of the effect of the financial crisis on the reproductive behavior of Czech women at the individual level determined that the experience of unemployment during the economic crisis led to the further unplanned postponement of first childbirth (Slabá 2020).

The events of the 1990s led to changes in Czechia that can easily be observed from the period perspective, and they have been subjected to analysis on a regular basis (see Křesťanová and Kurkin 2020). We expect that these period changes exerted a major influence on the respective birth cohorts and led to the transformation of their fertility behavior. Figure 1 shows that the cohort fertility rate has been decreasing continuously since the late 1950s cohorts. However, the continuous increase in the mean age of mothers at childbirth began later, i.e. with the 1966 cohort. There is currently a lack of a more detailed cohort analysis of fertility in Czechia. Recent studies indicate that the clarification of cohort differences can help us to understand long-term changes in fertility (Šťastná et al. 2017; Šťastná et al. 2019; Slabá 2020).

The aim of the study is to present a detailed analysis of fertility changes in Czechia over the last three decades using the cohort approach and to contribute to the overall understanding of the fertility postponement process. Whereas previous studies on fertility postponement and recuperation in Czechia (Sobotka et al. 2011; Šprocha 2014; Šprocha et al. 2018) have analyzed the underlying trends without the assessment of cohort differences, this paper aims to compare cohort differences in terms of the level and timing of fertility in more detail in order to identify the various "steps" in the transformation of reproductive patterns in Czechia. We take into account that each cohort has its own unique position in the course of history; thus, each cohort is differentiated from the other cohorts considered. The main focus of the study comprises the examination of birth parities and their role in changes in reproductive patterns. Parity is observed up to the third childbirth since the first, second and third births have made up more than 95% of total fertility since 1989. Accordingly, the main aim is to distinguish those groups of cohorts that exhibit

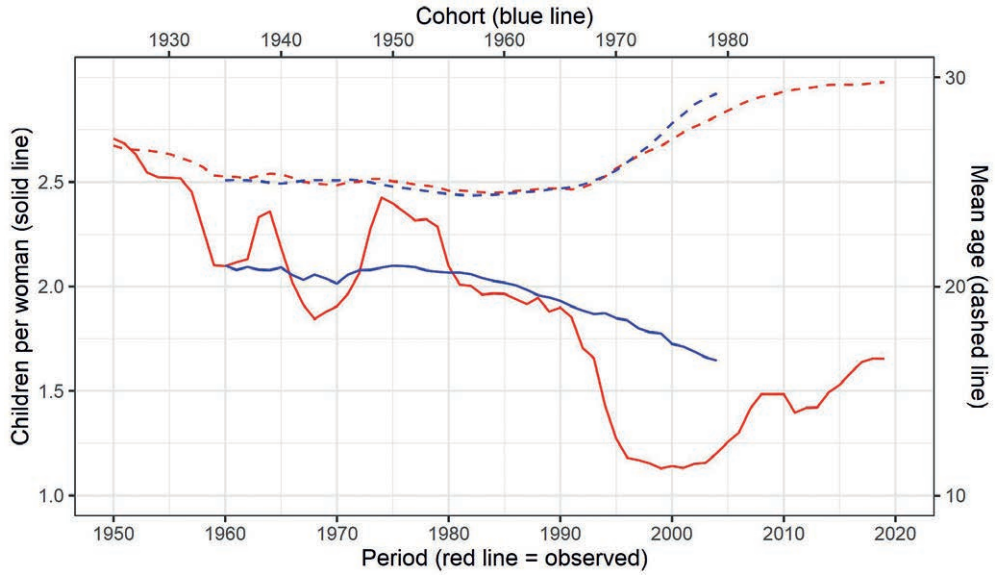

Fig. 1 Trends in the period and cohort fertility rates of women up to the age of 40, as well as in the period and cohort mean age of women at childbirth in 1950–2018 and for the generations from 1935 to 1978.
Notes: Both the fertility rates and the mean ages were computed for women up to the age of 40. The cohort fertility rates were shifted by 25 years (the 1965 generation corresponds to 1990 in the figure) as the mean age of women at childbirth before 1990.
Data: Human Fertility Database

specific fertility patterns since the transition to parenthood and parenthood itself are influential factors for the whole of adult life, which may well make a difference in terms of the social, political and economic features of each cohort group.

2. The cohort analytical approach and cohort differences in Czech society

The study of the cohort perspective aimed at enhancing the understanding of demographic processes and social changes is not a new approach. A paper on the cohort approach to the study of social changes was published as early as in the mid-1960s (Ryder 1965). Ryder considered cohort differentiation through social norms (the age at the completion of education or at first marriage), the impact of the size of the cohort on competitiveness during the life course (university entrance examination, the labor market) and the impact of contextual historical events. Wunsch et al. (2021) suggest that the cohort approach is applied when time trends are examined period by period and discussed in the causal perspective by taking into account the historical contexts of the periods considered.

The life trajectories of Czech women before 1989 were highly standardized with the almost universal transition into marriage and parenthood at a relatively low age (Sobotka et al. 2008). The political and economic change of the 1990s, however, led to the significant diversification of life trajectories (Bartošová et al. 2012). The opportunities for study, travel and other types of self-realization were significantly expanded. Therefore, intensive changes in social norms were observed in the 1990s in tandem with a decrease in marriage and fertility rates and an increase in the number of children born outside wedlock (Rabušic 2001). An example of the diversification of life trajectories is provided in Morávková and Kreidl (2017), who identified cohort differences in the partnership trajectories of solo mothers in terms of more recent cohorts having a higher chance of the transition to co-residential partnerships than older cohorts. They interpreted this development as the effect of a de-standardized life trajectory in which childbirth preceded cohabitation with the father of the child, and as the result of the significant de-stigmatization of 'solo-motherhood' compared to before 1989, both of which led to the easing of the settings of new co-residential partnerships.

As period fertility rates have become progressively distorted by timing shifts, the cohort approach has become increasingly appropriate in terms of the analysis of fertility transformation over the last two decades (Frejka and Calot 2001; Frejka 2011). The cohort approach views postponement and recuperation as being interconnected within the life course history. However, both the postponement and recuperation phases are subject to period effects, which differ since postponement and recuperation occur at different times. We acknowledge that changes in fertility are both cohort and period driven without discussing whether the cohort effects are more or less important than the period effects in terms of driving

the observed fertility trends. Sobotka et al. (2011) introduced a new analytical approach that served for the description of the intensity of the decline in fertility caused by postponement and subsequent recuperation from the cohort perspective. The application of this approach clearly illustrates the effect of fertility postponement on temporal declines in the period fertility rate.

The postponement process, which influenced the decrease in the period fertility rate, appears to have played a major role in fertility postponement in Czechia. The cohort analytical approach highlights the differences in fertility timing across cohorts. Moreover, it assists in the identification of which birth order was most postponed and which postponed children were born later, and the extent to which the probability of having an order-specific child has changed.

3. Data and Methods

All the analysis was conducted using R via R Studio statistical software (RStudio Team 2020). The data for Czechia was taken from the Human Fertility Database (Human Fertility Database 2020) using R package HMDHFDplus (Riffe et al. 2020).

3.1 Indicators of postponement and recuperation

The calculation of the following indicators is based on a paper by Sobotka et al. (2011). Following the example of previously conducted studies of the Czech population (Šťastná et al. 2017; Šprocha 2014), the benchmark cohort was set as the 1965 cohort since the continuous dynamic increase in the cohort mean age of mothers at first birth has been identified from the 1966 cohort onward. Postponement was measured via the cumulation of the fertility decline for the younger-aged mothers registered in these cohorts in comparison with the 1965 cohort. The cumulative postponement and recuperation indicators were based on the following equations (Sobotka et al. 2011):

[1] The *cumulative fertility rate of cohort* (F_c) based on the age-specific fertility rates (f_c) at age (x). The cumulating of age-specific fertility rates from the minimum age (12) to the maximum age (55) across a specific birth cohort results in the *complete cohort fertility rate* (*CCFR*).

$$F_C(y) = \sum_{x=12}^{y-1} f_c(x)$$

[2] The *difference* in the cumulative fertility rate between (F_c) (where c is the observed cohort of 1966 to 1990) and the benchmark cohort (F_{1965}).

$$F_c(y) - F_{1965}(y)$$

[3] The *age of the trough* (m) is the age at the maximum difference in age between the cumulative fertility rate of the observed cohort ($F_c(m)$) and the benchmark cumulative fertility rate ($F_{1965}(m)$). The trough age (m) may differ for each cohort as shown in detail in Appendix.

[4] The *indicator of postponement* (cumulative fertility decline) (P_c) is the difference between the cumulative fertility rate of the observed cohort ($F_c(m)$) and the benchmark cumulative fertility rate ($F_{1965}(m)$) at the age of the trough m between the observed cohort (c) and the benchmark cohort (*1965*).

$$P_c = \sum_{x=12}^{m-1} [f_c(x) - f_{1965}(x)] = F_c(m) - F_{1965}(m)$$

[5] The *indicator of recuperation* (cumulative fertility increase) (R_c) is then observed after the age of the trough (m). It serves for the measurement of the absolute cumulative increase in fertility between the trough age and the end age of the reproduction period.

$$R_c = \sum_{x=m}^{55} [f_c(x) - f_{1965}(x)]$$

[6] Finally, the *recuperation index* is computed as the proportion of recuperation of the cumulative fertility decline.

$$RI_c = {}^{R_c}/_{-P_c}$$

This paper considers the recuperation and recuperation index indicators up to the following ages: 35, 40 and 45.

3.2 Inter-cohort change in the cumulative fertility decline

The cumulative fertility decline (P_c) defines the maximum difference in the cumulative fertility between the benchmark and the observed cohort; hence, this value varies for each cohort. The inter-cohort change in the cumulative fertility decline (ICP_c) serves for the measurement of the absolute intensity of growth/decline between two adjacent cohorts (P_c).

[1] This is equal to the cumulative decline for the benchmark cohort.

$$ICP_{1965} - P_{1965}$$

[2] For the other cohorts it comprises the difference in the cumulative fertility decline between the observed cohort (P_c) and the cohort that is one year older (P_{c-1}).

$$ICP_C = P_c - P_{c-1}$$
$$= F_c(m) - F_{1965}(m) - \left(F_{c-1}(m) - F_{1965}(m)\right)$$
$$= F_c(m) - F_{1965}(m) - F_{c-1}(m) + F_{1965}(m)$$
$$= F_c(m) - F_{c-1}(m)$$

[3] The values for the inter-cohort change in the cumulative decline (ICP_c) are then smoothed out as the average of the three adjacent cohorts.

$$avg(ICP_c) = \frac{ICP_{c-1} + ICP_c + ICP_{c+1}}{3}$$

3.3 Cumulative growth in the mean age of women at childbirth

The cumulative growth (CG) for cohort (c) is based on the mean age of the cohort at childbirth computed for women up to the age of 40 (MAB). In contrast to the related benchmark, the cumulative growth exhibits a change in the mean age of the mother at childbirth. The benchmark cohort was set as the 1965 cohort for this reason. The indicator was computed as parity specific (i). The final available mean age at childbirth up to the age of 40 value related to the 1979 cohort.

$$CG_i(c) = \sum_{c=1965}^{c} (MAB_i(c) - MAB_i(c-1))$$

3.4 Parity progression ratio

The parity progression ratio describes the probability of having a child of a specific birth order, provided that the woman already holds the status of one child less than is the specific order. We computed the transition to a first child (from the status of childless), the transition to a second child (from the status of one child) and the transition to a third child (from the status of two children). The progression ratio was computed as the proportion of the cumulative fertility rate up to a specific age (for the purposes of this paper, up to the ages of 30, 35, 40 and 45).

[1] The parity progression (PP) from childlessness to the first child was equal to the first birth fertility. The $CCFR_p$ comprises the completed cohort fertility rate of a specific parity (birth order).

$$PP_1 = CCFR_1 = \sum_{x=12}^{y} f_1(x)$$

[2] The parity progression from one child to a second child was computed as the cumulative fertility rate of the second birth divided by that of the first birth.

$$PP_2 = CCFR_2/CCFR_1$$

[3] The parity progression from two children to a third child was computed as the cumulative fertility rate of the third birth divided by that of the second birth.

$$PP_3 = CCFR_3/CCFR_2$$

4. Results

4.1 Fertility postponement in the 1965–1990 cohorts

Aimed at identifying the various "steps" in the transformation of reproductive patterns in Czechia, we commenced with the analytical approach as proposed

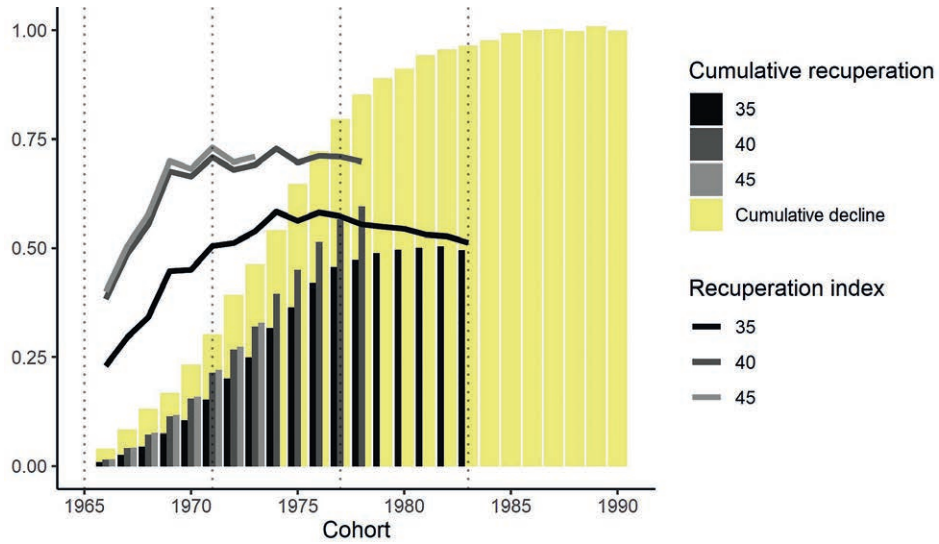

Fig. 2 Postponement and recuperation of fertility, cohort approach.
Note: Cohort 1965–1978 (1990), benchmark: the 1965 cohort; y axis = cumulative decline, cumulative recuperation, recuperation index/100.
Data: Human Fertility Database

Fig. 3 Inter-cohort changes in the decline in cumulative fertility.
Note: The gray line represents the observed change for each cohort; the red long-dashed line illustrates the three-year average.
Data: Human Fertility Database

by Sobotka et al. (2011) so as to analyze the dynamics of the postponement and recuperation of cohort fertility. The yellow columns in Figure 2 represent the cumulative fertility decline for each observed cohort compared to the benchmark cohort of 1965. The cumulative fertility decline increased continuously with each cohort, but slowed down gradually from the cohorts born after the mid-1970s onward. The difference in the cumulative fertility intensity between the 1965 and 1990 generations was 1.00 child.

The tempo of the cumulative fertility decline accelerated up to the 1970 cohort, with each subsequent generation experiencing a more intense reduction in fertility at younger ages than the previous generation (Figure 3). The tempo of the cumulative decline was highest for the 1971 to 1976 cohorts, for which, on average, the cumulative fertility at younger ages decreased for each subsequent generation by 0.08 children per woman compared to the previous generation. The growth in the cumulative decline slowed down between the 1977 and 1982 cohorts, and the cumulative fertility decline was close to zero for the 1983 cohort, thus indicating the cessation of postponement. Accordingly, four steps in the postponement transition process were identified based on the following cohorts: 1965–1970, 1971–1976,

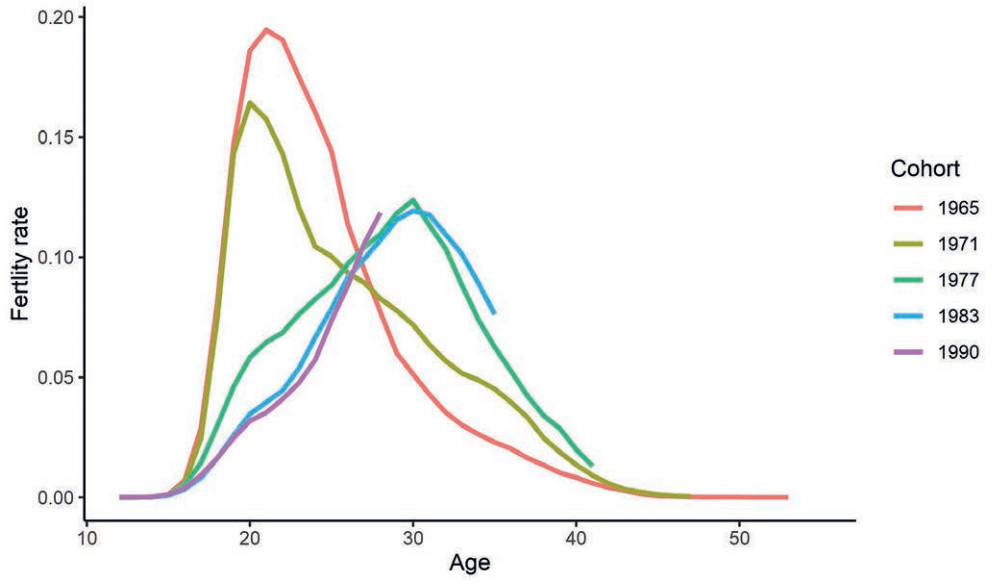

Fig. 4 Fertility rate age patterns for selected cohorts.
Data: Human Fertility Database

1977–1982, and 1983–1990. Finally, two main groups were differentiated: 1965–1982 (cohorts that were characterized by various postponement intensities) and 1983–1990 (cohorts that ceased further postponement).

Figure 4 presents the age-specific fertility rates of women for selected cohorts chosen so as to follow the previously identified fertility postponement stages: 1965, 1971, 1977, 1983 and 1990. The fertility of the 1965 cohort was concentrated mainly between the ages of 19 and 25 with a peak at the age of 21. The 1971 cohort appears to represent the first stage of the fertility postponement process, and is characterized by decreasing fertility rates at younger ages and increasing fertility rates over the age of 27; however, it continues to follow the previous early-fertility pattern. A completely different pattern was observed for the 1977 cohort, who shifted the dominance of their fertility to a median age of 30. Nevertheless, the fertility rates up to the age of 27 remained significant. Finally, a similar late-fertility pattern with significantly lower fertility up to the age of 28 was determined for both the 1983 and 1990 cohorts, thus confirming the stabilization of the postponement transition process.

4.2 The timing of fertility by birth order from the cohort perspective

In order to compare fertility across all the cohorts of interest in detail, Figure 5 presents the fertility rates of all the birth orders together and for the first, second and third childbirth. In the case of first childbirth, the dominant age category for the 1965–1970 cohorts comprised the 20–24 age group that featured a fertility rate decline of from 0.5 to 0.4. The second highest fertility was registered for the 15–19 age group. The distribution then changed significantly from the 1971 cohort onward. The first-child fertility of the 25–29 age group increased to above that of the 15–19 age group (from the 1974 cohort) and, subsequently, to above the formerly dominant 20–24 age group (from the 1977 cohort). Moreover, the importance of the 30–34 age group was reflected in its outstripping the fertility of the 20–24 age group from the 1981 cohort onward (see Figure 5).

A similar trend is evident with concern to second birth rates. Women between 20 and 24 lost their dominance, while women in the 30–34 age group exhibited an increasing second-birth fertility intensity (Figure 5). A shift in fertility is also evident with respect to third childbirth, with the 30–34 and 35–39 age groups becoming dominant from the 1971 generation onward (Figure 5).

As indicated by the above detailed analysis of cohort age-specific fertility rates, the fertility of each birth order was postponed progressively to later ages. The mean age of women at first birth increased from 22.5 years for the 1965 cohort to 27.4 years for the 1979 cohort (Figure 6). Similarly, the mean age of women increased from 25.8 to 30.6 for second births and from 29.0 to 32.7 for third births. However,

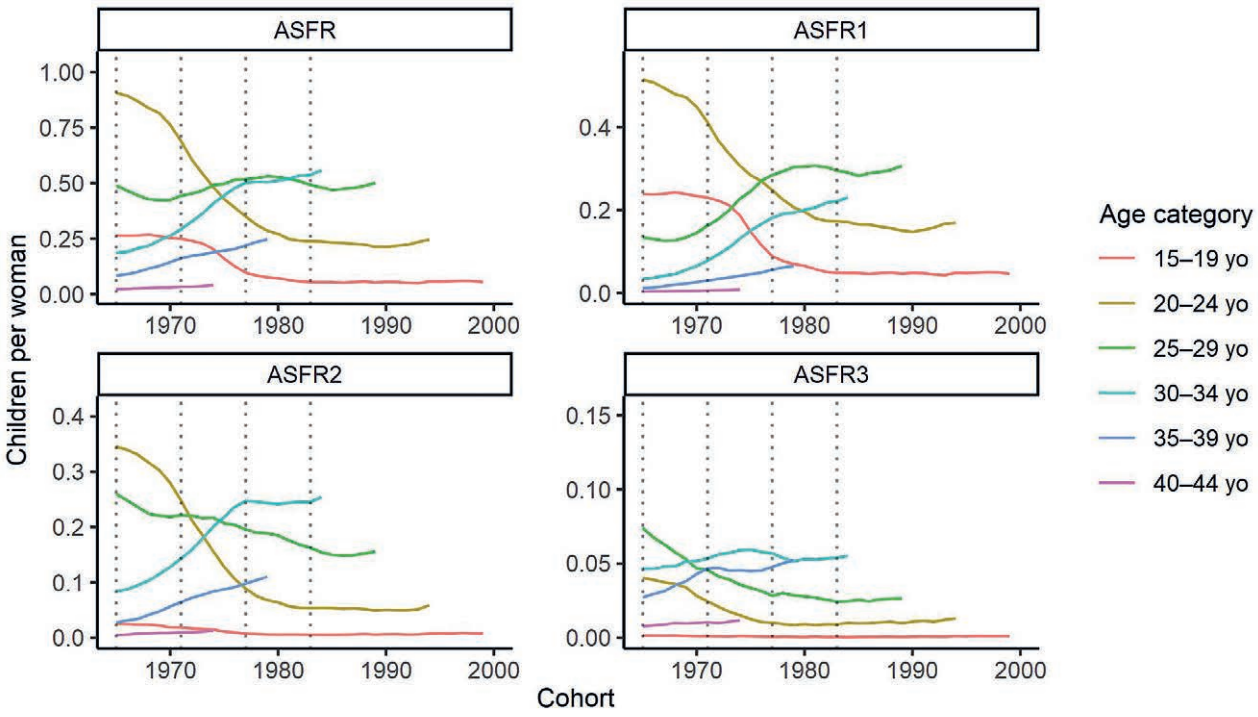

Fig. 5 Fertility rate cohort patterns for the five-year groups.
Note: Cohort 1965–2000. ASFR represents the rates for all the childbirth orders, ASFR1 represents first births, ASFR2 second births and ASFR3 third births.
Data: Human Fertility Database

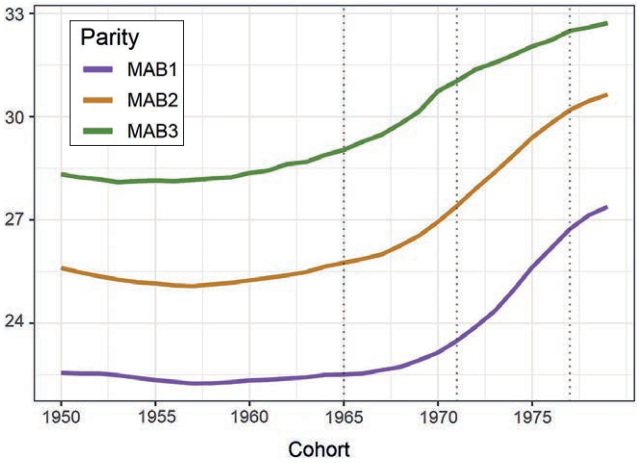

Fig. 6 Mean age of women at childbirth by parity, cohort 1950–1979.
Notes: The mean ages were computed for women up to the age of 40.
Data: Human Fertility Database

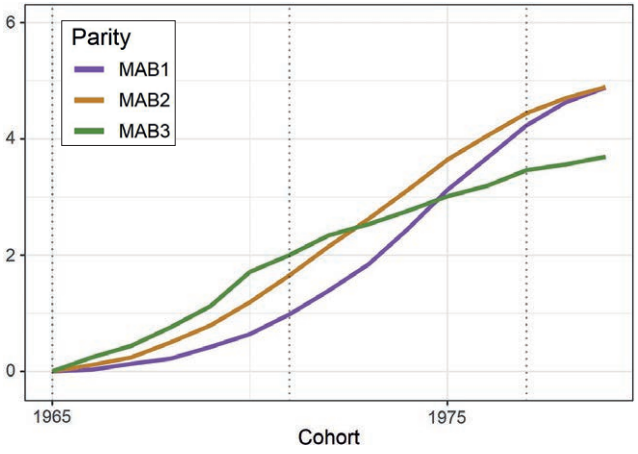

Fig. 7 Cumulative growth in the mean age of woman at childbirth (by parity).
Notes: Both the fertility rates and the mean ages were computed for women up to the age of 40. The vertical lines show the 1971 and the 1977 cohorts.
Data: Human Fertility Database

indications of such an increase were apparent for second- and third-order births as early as in the 1960–1964 cohorts. Therefore, Figure 7 was compiled so as to illustrate the cumulative increase in the mean age at childbirth by birth order from the 1965 benchmark cohort. While the postponement of third childbirth commenced earlier than that of the lower birth orders, the increase decelerated from the 1971 cohort onward. The cumulative first-order increase was slowest with respect to the 1971 cohort, whereupon the cumulative increase accelerated for both first- and second-order births and outstripped third-order births. A more intensive cumulative increase in first- and second-order births than for third-order births was evident for the 1977 to 1982 cohorts.

4.3 Fertility postponement and recuperation by birth order

Both the intensity and recuperation of postponement were examined, i.e. to what extent delayed childbearing was realized at older ages following the trough age. Overall, from the 1965 cohort to the 1971 cohort, the maximum difference between the cumulative fertility rates was 0.30 children per woman (the yellow column in Figure 2; the age of 27 represented the trough for the 1971 cohort, see the Appendix). 0.22 children per woman was born between the trough age and the age of 45 (the light gray column in Figure 2), thus indicating that 70% of postponed childbirths were recuperated (the light gray line in Figure 2). The dark gray and black columns and lines show the cumulative recuperation and recuperation indices up to the ages of 40 and 35, respectively. While the 1965–1970 cohorts registered a low but increasing recuperation index, the 1971–1976 cohorts registered a high and constant recuperation index up to the age of 40 of around 70%. The 1977–1982 cohorts experienced an intensifying cumulative fertility decline of up to 0.96 children (trough age = 26) accompanied by a later cumulative fertility increase (recuperation) of only 0.50 children per woman up to the age of 35. Thus, the recuperation index at the age of 35 decreased to just 53% (Figure 2).

The development of the cumulative decline, cumulative increase and recuperation indices differed according to the specific birth order (Figure 8). The cumulative fertility decline for the first-birth order reached a value of 0.42 children for the 1977 cohort and up to 0.56 children for the 1990 cohort. Although the recuperation index showed an increasing trend up to the 1969 cohort, it subsequently fluctuated at around 83% (the recuperation index up to the age of 40). In the case of second childbirths, the cumulative fertility decline was 0.36 children for the 1977 cohort and 0.43 children for the 1990 cohort. Therefore, the cumulative fertility decline due to postponement for the second childbirth was lower than for the first childbirth. The recuperation index for the second childbirth was also lower, i.e. 72% on average (up to the age of 40) for the 1971 to 1976 cohorts. The cumulative fertility decline was much lower for third-order births than for lower-order births. The maximum decline was 0.09 children per woman (the 1983 cohort). The average recuperation index value up to the age of 40 for the 1966–1976 generation was approximately 53%.

The progression ratios indicate the probability of transition to a subsequent child and were computed up to the ages of 30, 35, 40 and 45. The trends in the parity progression ratios once again highlight the postponement of fertility to later ages. As shown in Figure 9, the parity progression up to the age of 45 and 40 remained the same for these cohorts, while

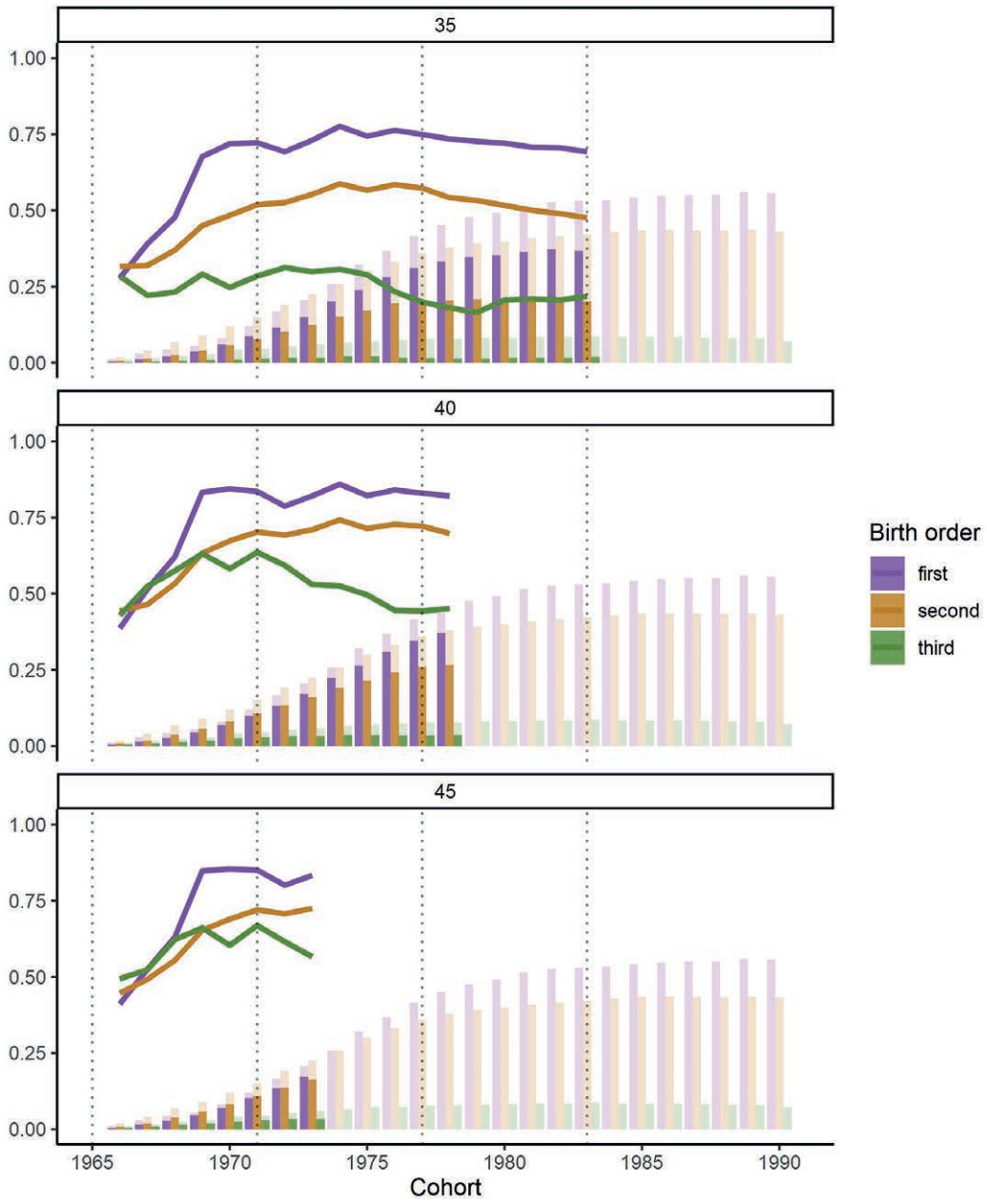

Fig. 8 Postponement and recuperation, cohort approach (parity comparison).
Note: 1965–1978 cohort (1990), benchmark: the 1965 cohort; y axis = cumulative decline (shaded columns), cumulative recuperation (colored columns), recuperation index/100 (lines).
Data: Human Fertility Database

the parity progression up to the age of 35 declined slightly, and the parity progression up to the age of 30 decreased significantly, especially with concern to the younger cohorts. Changes in the progression ratio up to the age of 30 illustrate the postponement of a significant amount of fertility to 30 years and older.

The highest progression ratio related to the transition from childlessness to a first child. The probability of having a first child by the age of 40 was still above 90% for the 1971 cohort and was close to 85% for the 1977 cohort (Figure 9). Changes in childbirth timing are more noticeable with concern to the parity progression trends up to the age of 30, which was 89% (i.e. only 4 percentage points lower than up to the age of 40) for the 1965 cohort and just 60% (i.e. 25 percentage points lower than up to the age of 40) for the 1977 cohort. The progression ratio to a first child decreased for the subsequent cohorts up to 1982 and stabilized at around 50% from 1983 onward.

A similar decline in the progression ratio up to the age of 40 was also evident between the 1965 and 1977 cohorts in the case of the transition to a second child (from 80% to 73%). However, the probability of having a second child decreased significantly when computed only to the age of 30 (from 71% for the 1965 cohort to 46% for the 1977 cohort, and to close

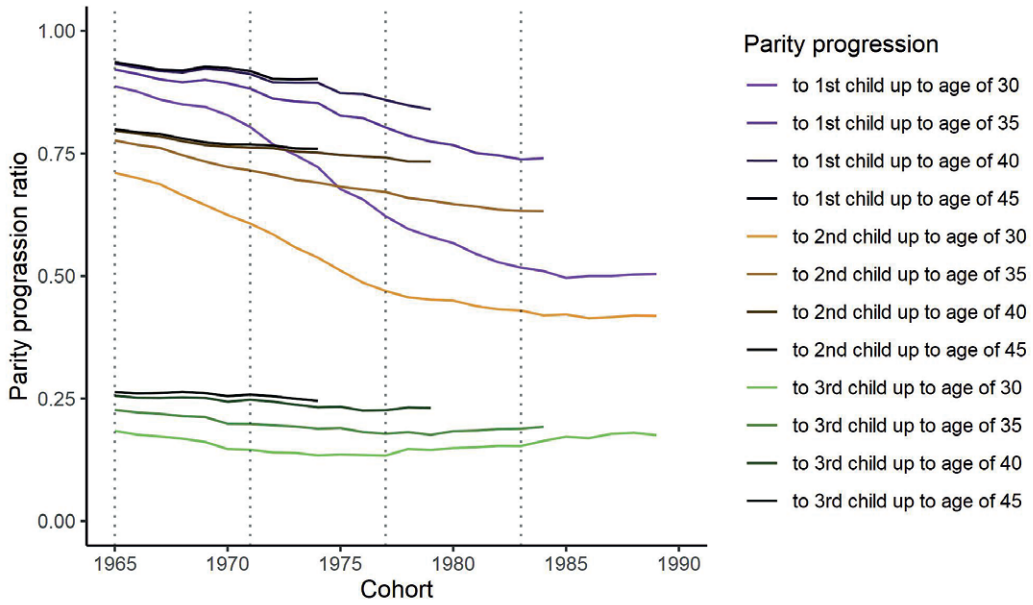

Fig. 9 Parity progression ratios.
Note: 1965–1990 cohort.
Data: Human Fertility Database

to 40% for the 1982 and subsequent cohorts). The progression ratio from the second to a third child did not change significantly, i.e. it stabilized at the much lower value of around 25%.

4.4 Defining cohort differences in fertility patterns

The aim of the above analysis was to identify detailed differences in fertility patterns across the four cohort groups.

The first cohort group (1965–1970) was characterized by the rapid commencement of the postponement process. Nevertheless, early fertility remained the typical pattern; the women in this cohort group mainly had a first child at the age of 20–24 (Figure 5), and the 15–19 age group was the second most fertile group. Up to the age of 45, the parity progression ratios to a first, second and third childbirth remained stable (92%, 78% and 23%, respectively). Nevertheless, the parity progression ratio up to the age of 30 decreased continuously between the 1965 and 1970 cohorts for both first and second births, thus indicating a gradual postponement of fertility toward the age of 30 and older (Figure 9). Interestingly, second childbirth postponement was more intense than first childbirth postponement (Figure 8), as confirmed by the trends evident in Figure 3 that show that the mean age at childbirth first began to accelerate with concern to higher-order births. The recuperation index for all the childbirth orders up to the age of 45 increased (85% for a first, 69% for a second and 60% for a third childbirth).

The second cohort group (1971–1976) was characterized by the most intensive rate of postponement. These women continued to have their first child predominantly at the age of 20–24; however, the fertility rate of this age group subsequently decreased at a constant rate. Conversely, fertility at the ages of 25–29 and 30–34 increased significantly (Figure 5). The progression ratio up to the age of 40 reflected a decrease in the probability of having a first, second or third child (Figure 9). While the recuperation index up to the age of 40 remained stable for both the first and second childbirth (82% for the first and 71% for the second), the third childbirth recuperation index decreased continuously from 64% to 45% (Figure 8).

The third (1977–1982) cohort group experienced a deceleration in fertility postponement. In 2020, these cohorts were approaching the end of their reproductive age, i.e. 38–43. These women predominantly had their first child aged 25–29, while the second most fertile age group in terms of first childbirth comprised the 30–34 age range (Figure 5). The parity progression ratios for the whole of the group can be observed only up to the age of 35 (Figure 9). The transition to a first child continued to decline with respect to these cohorts. The probability of having a first child up to the age of 35 was 80% for the 1977 cohort and 75% for the 1982 cohort. The probability of having a second child (in the case that the woman already had a first child) also slightly decreased from 67% to 64% between the 1977 and 1982 cohorts. Conversely, the progression rate to a third child up to the age of 35 increased slightly from 18% to 19% between these cohorts. The recuperation index up to the age of 35 decreased slightly for a first childbirth from 75% for the 1977 cohort to 71% for the 1982 cohort. A second child was recuperated by just 57% of the 1977 cohort and 49% of the 1982 cohort.

The fourth (1983–1990) cohort group indicated signs of the stabilization of postponement. In 2020, these women were aged 30 to 37 years, and thus had not reached the end of their fertility. The age-specific fertility rates revealed the dominance of a first childbirth at the age of 25–29. The main question concerns whether the 30–34 age group becomes dominant or not (Figure 5). The progression ratios for a first and second child up to the age of 30 were determined at the low levels of 50% for the first child and 42% for the second child (Figure 9). The recuperation index of these cohorts is not yet known.

5. Summary and discussion

This paper aims to assist in forming an understanding of the role of cohorts concerning fertility trends in Czechia. Cohort differences in terms of the fertility level and timing were compared in detail so as to identify the various "steps" in the transition of reproductive patterns in Czechia. The results served to distinguish four groups of cohorts with distinct demographic characteristics and fertility patterns: the 1965–1970 cohorts, 1971–1976 cohorts, 1977–1982 cohorts and 1983–1990 cohorts.

Four periods of significant change in economic development can be identified in recent Czech history, all of which were reflected in specific fertility trends. The period indicators clearly show that these periods differed in terms of the potential effect on fertility (Rychtaříková 2000; Kocourková 2009). We determined that these periods exerted particularly profound impacts on reproductive behavior from the cohort perspective. The application of the cohort approach allowed for the observation of differences in behavior between the cohorts that could not be identified via the period indicators. The various time occurrences were then projected to the behavior of each generation, thus contributing to the identification of the particularities of the various cohorts.

Firstly, the political and economic transformation which began in the early 1990s and influenced the whole of that decade led to a sharp drop in the period fertility (Rychtaříková 2000). This was the time at which the first (1965–1970) cohort experienced the key reproductive age of 20–30. Most of the women in these cohorts continued to have a first child early (mostly before the age of 24), and the probability of their having a second child was above 76%. Early childbearing continued to be the dominant reproductive pattern. Nevertheless, this was the first group for which signs were observed of the postponement of childbirth to later ages. The second (1971–1976) cohort group was more profoundly affected by the ambivalence and uncertainty of the 1990s, which led to their postponing childbearing to a much more significant extent. Thus, they are considered to be the initiators of changes in reproductive patterns; in other words, the transitional cohort group.

From 2000, the period fertility increased, which has often been explained via the creation of a more favorable population climate that reflected the positiveness of continuous economic growth (Kocourková 2009). GDP grew at an accelerating pace from 2003 and reached 6.1% in 2005 (Jahoda and Kofroň 2007) in tandem with the introduction of favorable family and housing policy measures. However, the positive socio-economic development affected the initiators of fertility postponement only marginally, as reflected in their failure to recuperate a significant part of delayed childbirths. Women in their mid-thirties are less receptive to improved family support measures if they lacked favorable conditions when they were in their late twenties or early thirties (Kocourková and Šťastná 2021). We determined that the probability of their having a first and second child up to the age of 40 had declined (from 91% for the 1970 cohort to 85% for the 1976 cohort, and from 71% for the 1970 cohort to 56% for the 1976 cohort, respectively). It was left for the subsequent (1977–1982) cohort group, who were in their late twenties or early thirties at that time, to fully take advantage of the more favorable conditions for starting a family. This cohort group was characterized by the formation of the late-fertility pattern.

The period 2008 to 2012 was dominated by the world financial crisis, which was reflected in the stagnation and a temporal decrease in period fertility. However, the crisis lasted for a relatively short time (at least in Czechia) and resulted only in the temporal stagnation of period fertility (Kocourková et al. 2019). Finally, the continuation of economic growth from 2013, accompanied by favorable family policies, acted to stimulate a further increase in period fertility (Šťastná et al. 2020). Accordingly, the 1983–1990 cohort group witnessed the stabilization of the late-fertility pattern, with the balanced contribution of the 25–29 and 30–34 age groups. Indeed, the further postponement of childbearing appears to have been prevented by recent developments in family policy, as suggested by the example of the effect of parental leave policies (Šťastná et al. 2020).

While we can reasonably expect that the current Covid-19 pandemic will exert an impact on reproductive behavior, it is still too early to reliably predict the extent thereof.

The postponement of childbearing significantly influences the life course. Older mothers are faced with circumstances and needs that differ from those of younger mothers. The former are more likely to experience difficulties becoming pregnant due to sub-fecundity (Schmidt 2010), thus leading to a higher demand for assisted reproduction treatment (Kocourková and Fait 2009). Moreover, fertility at later ages is often connected with career disruption in the case that the woman has already entered the labor market. However, the same is true for childbirth immediately

following the completion of tertiary education, with the resulting disruption of "up-to-date knowledge" and the devaluation of current investment in individual human capital. It has been estimated that the "motherhood penalty" in Czechia is around 7% (Žofková and Stroukal 2014). Aimed at reflecting these fertility patterns, the various challenges should be addressed via the introduction of the corresponding family policy strategies, and changes in fertility patterns should be considered a factor in terms of the future political and economic decision-making process.

Acknowledgements

The authors acknowledge the financial support provided by GACR, 2018-2020(/2021) (no. 18-08013S) "Transition towards the late childbearing pattern: individual prospects versus societal costs", and the Charles University UK UNCE/HUM/018 programme.

References

Bartošová, M., Pakosta, P., Fučík, P. (2012): Dlouhodobý vývoj v časování porodů a sňatků: obstojí individualizační teorie ve světle demografických dat? Sociologický časopis/Czech Sociological Review 48(2), 315–341, https://doi.org/10.13060/00380288.2012.48.2.05.

Beaujouan, É. (2020): Latest-Late Fertility? Decline and Resurgence of Late Parenthood Across the Low-Fertility Countries. Population and Development Review 46(2), 219–247, https://doi.org/10.1111/padr.12334.

Billingsley, S. (2010): The post-communist fertility puzzle. Population Research and Policy Review 29(2), 193–231, http://doi.org/10.1007/s11113-009-9136-7.

Czech Statistical Office (2014): Úroveň vzdělání obyvatelstva podle výsledků Sčítání lidu. Lidé a Společnost 30, https://www.czso.cz/documents/10180/20536250/17023214.pdf/7545a15a-8565-458b-b4e3-e8bf43255b12?version=1.1.

Frejka, T., Calot, G. (2001): Cohort reproductive patterns in low fertility countries. Population and Development Review 27(1), 103–132, https://doi.org/10.1111/j.1728-4457.2001.00103.x.

Frejka, T. (2011): The Role of contemporary childbearing postponement and recuperation in shaping period fertility trends. Comparative Population Studies 36(4), 927–958. https://doi.org/10.4232/10.CPoS-2011-20en.

Human Fertility Database (2020): Max Planck Institute for Demographic Research (Germany) and Vienna Institute of Demography (Austria). Available at www.humanfertility.org (data downloaded on 17. 01. 2022).

Jahoda, R., Kofroň, P. (2007): Domácnosti a sociální dávky v letech 2000 až 2005. [Households and social benefits between 2000 and 2005]. Praha: VUPSV výzkumné centrum Brno. 1–184.

Kocourková, J. (2009): The Current "Baby Boom" in the Czech Republic and Family Policy. Czech Demography 3, 10–21, https://www.czso.cz/documents/10180/23196876/kocourkova2011.pdf/1437d003-40cc-49b4-8ef0-7697e02c5c8d?version=1.0.

Kocourková, J., Fait, T. (2009): Can increased use of ART retrieve the Czech Republic from the low fertility trap? Neuroendocrinology Letters 30(6), 739–748, https://pubmed.ncbi.nlm.nih.gov/20038934.

Kocourková, J., Fait, T. (2011): Changes in contraceptive practice and the transition of reproduction pattern in the Czech population. The European Journal of Contraception & Reproductive Health Care 16(3), 161–172. https://doi.org/10.3109/13625187.2011.574750.

Kocourková, J., Šťastná, A., Černíková, A. (2019): Vliv ekonomické krize na úroveň plodnosti ve státech Evropské unie. Politická ekonomie 67(1), 82–104, https://doi.org/0.18267/j.polek.1230.

Kocourková J., Šťastná A. (2021): The realization of fertility intentions in the context of childbearing postponement: comparison of transitional and post-transitional populations. Journal of Biosocial Science 53, 82–97, https://doi.org/10.1017/S002193202000005X.

Kohler, H.-P., Billari, F. C., Ortega, J. A. (2002): The emergence of lowest-low fertility in Europe during the 1990s. Population and Development Review 28(4), 641–80, https://doi.org/10.1111/j.1728-4457.2002.00641.x.

Křesťanová, J. (2016): Analýza vývoje plodnosti na území České republiky po roce 1950 do současnosti za využití dekompozičních metod. Demografie 58(2), 142–58, https://www.czso.cz/documents/10180/33199357/clanek+3_krestanova.pdf/41543a79-f963-453b-80be-02fd4f6b238f?version=1.0.

Křeštanová, J., Kurkin, R. (2020): Populační vývoj v České republice v roce 2019 (Population development in the Czech Republic in 2019). Demografie 62(3), 159–181. https://www.czso.cz/documents/10180/123310412/13005320q3_159-181.pdf/21eae15b-0e30-4991-8240-ecb2fc91736e?version=1.1.

Kurkin, R., Šprocha, B., Šídlo, L., Kocourková, J. (2017): Ferility factors in Czechia according to the results of the 2011 census. AUC Geographica 52(2), 137–148, https://doi.org/10.14712/23361980.2018.14.

Lesthaeghe, R. (2010): The unfolding story of the second demographic transition. Population and Development Review 36(2), 211–51, https://doi.org/10.1111/j.1728-4457.2010.00328.x.

Morávková, H., Kreidl, M. (2017): Partnerské dráhy prvorodiček bez partnera ve společné domácnosti. Sociologický časopis/Czech Sociological Review 53(4), 565–591, https://doi.org/10.13060/00380288.2017.53.4.358.

Neels, K., Murphy, M., Ní Bhrolcháin, M., Beaujouan, É. (2017): Rising educational participation and the trend to later childbearing. Population and Development Review 43(4), 667–693, https://doi.org/10.1111/padr.12112.

Ní Bhrolcháin, M., Beaujouan, É. (2012): Fertility postponement is largely due to rising educational enrolment. Population Studies 66(3), 311–327, https://doi.org/10.1080/00324728.2012.697569.

Polesná, H., Kocourková, J. (2016): Je druhý demografický přechod stále relevantní koncept pro evropské státy? Geografie 121(3), 390–418, https://geografie.cz/media/pdf/geo_2016121030390.pdf.

Rabušic, L. (2001): Value Change and Demographic Behaviour in the Czech Republic. Sociologický časopis /Czech Sociological Review 9(1), 99–122, https://doi.org/10.13060/00380288.2001.37.11.15.

Rabušic, L., Chromková Manea, B. (2013): Velikost rodiny – postoje, normy a realita. Demografie 55(3), 208–219, https://is.muni.cz/repo/1123093/Demogradfie-3-2013.pdf.

Riffe, T., Boe, C., Goldstein, J., Hilton, J., Holzman, S. (2020): Read Human Mortality Database and Human Fertility Database Data from the Web, https://cran.r-project.org/web/packages/HMDHFDplus/index.html.

Ryder, N. B. (1965): The Cohort as a Concept in the Study of Social Change. American Sociological Review 30(6), 843–861, https://www.jstor.org/stable/2090964.

Rychtaříková, J. (2000): Demographic transition or demographic shock in recent population development in the Czech Republic? Acta Universitatis Carolinae Geographica 35(1), 89–102.

R Studio Team (2020): RStudio: Integrated development environment for R. Boston, MA: RStudio, PBC, http://www.rstudio.com/.

Schmidt, L. (2010): Should men and women be encouraged to start childbearing at a younger age? Expert Review of Obstetrics & Gynecology 5(2), 145–147, https://doi.org/10.1586/eog.09.77.

Sivková, O., Hulíková Tesárková, K. (2012): Dekompozice změn průměrného věku matky při narození dítěte v České republice od roku 1950. Demografie 54(3), 264–279, https://www.czso.cz/documents/10180/20555359/e-180312q3.pdf/62e9767a-5a61-40f3-baae-c0528427c1d7?version=1.0.

Slabá, J. (2020): Nezaměstnanost ženy jako příčina deklarovaného odkladu založení rodiny? Sociológia 52(2), 132–151, https://doi.org/10.31577/sociologia.2020.52.2.6.

Sobotka, T. (2017): Post-transitional fertility: the role of childbearing postponement in fuelling the shift to low and unstable fertility levels. Journal of Biosocial Science 49, S20–S45, https://doi.org/10.1017/S0021932017000323.

Sobotka, T., Šťastná, A., Zeman, K., Hamplová, D., Kantorová, V. (2008): A rapid transformation of fertility and family behaviour after the collapse of state socialism. Demographic Research 19(14), 403–454, https://dx.doi.org/10.4054/DemRes.2008.19.14.

Sobotka, T., Beaujouan, É. (2014): Two is best? The persistence of a two-child family ideal in Europe. Population and Development Review 40(3), 391–419, https://doi.org/10.1111/j.1728-4457.2014.00691.x.

Sobotka, T., Zeman, K., Lesthaeghe, R., Frejka, T. (2011): Postponement and Recuperation in Cohort Fertility: Austria, Germany and Switzerland in a European Context. Comparative Population Studies 36(2–3), 417–452, https://doi.org/10.12765/CPoS-2011-10.

Šprocha, B. (2014): Odkladanie a rekuperácie plodnosti v Českej republike a na Slovensku. Demografie 56(3), 219–233, https://www.czso.cz/documents/10180/20555387/13005314q3.pdf/d2fc4c66-582f-406e-81dd-59f4924f6a4b?version=1.0.

Šprocha, B., Bačík, V. (2020): Odkladanie rodenia detí a neskorá plodnosť v európskom priestore (Postponement of the childbirth and the late fertility in the European area). Demografie 62(3), 123–141, http://www.humannageografia.sk/clanky/demografie_sprocha_bacik_2020.pdf.

Šťastná, A., Slabá, J., Koucourková, J. (2017): Plánování, načasování a důvody odkladu narození prvního dítěte v České republice. Demografie 59(3), 207–223, https://www.czso.cz/documents/10180/46203816/stastna.pdf/0cf15559-1e0a-4b47-a7d6-e8faeb236404?version=1.0.

Šťastná, A., Slabá, J., Kocourková, J. (2019): Druhé dítě – důvody neplánovaného odkladu a časování jeho narození. Demografie, 61(2), 77–92, https://www.czso.cz/documents/10180/91917740/13005319q2_77.pdf/b0972342-7094-4feb-bf85-f0acb04e1f30?version=1.0.

Šťastná, A. (2007): Druhé dítě v rodině – preference a hodnotové orientace českých žen. Sociologický časopis 43(4), 721–745, https://sreview.soc.cas.cz/pdfs/csr/2007/04/04.pdf.

Šťastná, A., Kocourková, J., Šprocha, B. (2020): Parental Leave Policies and Second Births: A Comparison of Czechia and Slovakia. Population Research and Policy Review 39, 415–437, https://doi.org/10.1007/s11113-019-09546-x.

Wunsch, G., Russo, F., Mouchart M. (2021): Time and causality in the social sciences. Time & Society. First published online: September 17, 2021, https://doi.org/10.1177/0961463X211029488.

Vltavská, K., Sixta, J. (2015): A historical view on the development of Czech economy from 1970. Politická ekonomie 24(1), 105–122, https://doi.org/10.18267/j.pep.503.

Žofková, M., Stroukal, D. (2014): Odhad mzdové srážky za mateřství v České republice. Politická ekonomie 62(5), 683–700, https://doi.org/10.18267/j.polek.976.

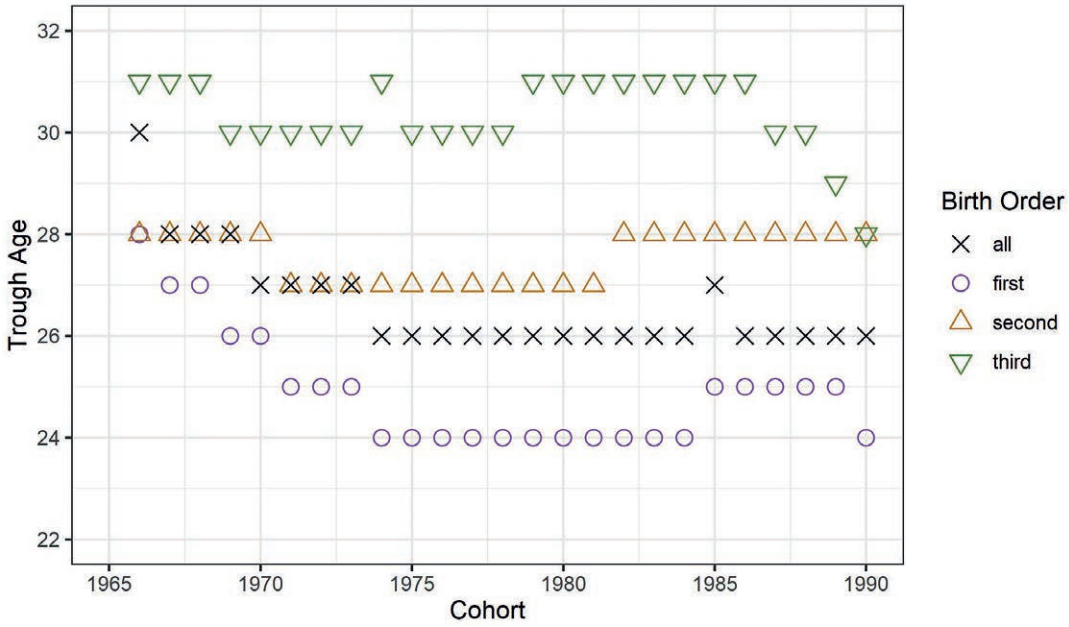

Appendix: Trough age.
Note: Cohort 1965–1990; benchmark: the 1965 cohort.
Data: Human Fertility Database

Analysis of movement and relationships between morphometric components of sand dunes (barchans) in the south-eastern of Iran

Mehdi Feyzolahpour[1,*], Rouholah Khodaie[1], Hasan Ghasemlu[2]

[1] University of Zanjan, Faculty of Humanities, Department of Geography, Iran
[2] University of Tabriz, Faculty of Planning and Environmental Sciences, Department of Geography and urban planning, Iran
[*] Corresponding author: feyzolahpour@znu.ac.ir

ABSTRACT

Morphology of barchan dunes plays a key role in the rate of movement of barchan dunes and accordingly, the areas that are in the path of barchan dunes can be identified. In this study, morphological parameters of eight barchan dunes in west Lut and movement were investigated. For this purpose, 8 parameters of windward slope length, back-to-wind slope length, right arm length, left arm length, length, width, right width and left width were measured in each barchan dune and Pearson correlation was calculated by SPSS software. In order to better understand the shape of barchan dunes, satellite images were extracted separately from google earth. The results of morphometry showed that barchan dune 6 was in the first place in terms of all morphometric factors. The right arm length to the width had the highest correlation (0.993). The back-to-wind slope length to the right arm length had the lowest correlation (0.815). The right arm length to the width had the highest coefficient of determination (0.9845). The movement during 2005–2019 was extracted from satellite images. It was found that until 2015, the highest movement belonged to barchan dune 3 (225.55 m) and during 2017–2019, the lowest movement belonged to barchan dune 6 (137.49 and 184.66 m). The highest movement during 2017–2019 was 288.24 and 307.67 m for barchan dune 5, respectively.

KEYWORDS

morphometry; correlation; coefficient of determination; movement; barchan dune; west Lut

Received: 28 July 2021
Accepted: 21 June 2022
Published online: 29 June 2022

Feyzolahpour, M., Khodaie, R., Ghasemlu, H. (2022): Analysis of movement and relationships between morphometric components of sand dunes (barchans) in the south-eastern of Iran. AUC Geographica 57(1), 75–84
https://doi.org/10.14712/23361980.2022.7

1. Introduction

About 80 million hectares of the Iranian plateau have very little vegetation and 12 million hectares are covered by barchan (Negaresh et al. 2008: 47). Different dune-like forms are found in deserts, which are classified into different groups by geologists. These depend on the amount of barchan available and the change in wind direction over the years (Brookfield et al. 2000; Bagnold 1941). The most well-known type of these shapes are barchan dunes, which are crescent-shaped and formed by the wind in the same direction over time. Barchan dune movement depends on wind speed and barchan dune height. The height of barchan dunes was between 1.5 and 10 m, while depending on the type, they were 40–150 m long and 30–100 m wide. Also, they have a slope between 8 and 20 degrees and lead to a sharp edge. This edge is located at the tip of the barchan dune and separates the sliding plate from the windward edge (Sauermann et al. 2000: 247). Barchan dune is one of the famous desert forms. These dunes cause deviating the wind due to their crescent shape. The factors affecting the crescent shape of barchan dunes follow nonlinear processes (Hersen 2004). Barchan dunes are formed in areas where there is not adequate barchan to completely cover the surface and the wind blows in the same direction for most of the year (Sauermann et al. 2003: 248). Barchan dunes are made of moving sand and move in the direction of the prevailing wind while maintaining their crescent shape. Therefore, movement is one of their most important features, so this obvious feature of barchan dune has turned it into a natural threat. Accordingly, it is necessary to pay attention to it as a risk factor. Although for more than 50 years geologists and geographers have measured barchan dunes and obtained data on their height, width, length, volume and movement rate, little is known about the morphological features of barchan dunes (Wiggs et al. 1996: 34). From a mathematical point of view, some are symmetrical shapes that are formed in the direction of the wind, but in nature, some factors such as unstable wind speed or the slope of the earth lead to their asymmetry. Simulations have also been performed to predict the evolution of barchan dunes (Howard and Morton 1978; Wippermann and Gross 1986; Anton and Vincent 1986; Anthonsen et al. 1996). Bagnold (1941) and Finkel (1978) presented the first concepts on barchan dunes and their morphological relationships in southern Peru. Then, many studies have been conducted on the morphology and movement of barchan dunes around the world (Lettau et al 1969; Ting Wang et al. 2007; Hesp et al. 1998; Gay 1999; Al-Harthi 2002; Daniell et al. 2007; Valle et al. 2008; Belrhiti et al. 2011; Hamdan

Tab. 1 Geographical location of eight barchan dunes in the study area.

Barchan number	Latitude	Longitude
Barchan No. 1	29° 59′ 49.55″ N	58° 07′ 05.97″ E
Barchan No. 2	29° 59′ 44.14″ N	58° 06′ 51.57″ E
Barchan No. 3	29° 59′ 40.63″ N	58° 06′ 57.34″ E
Barchan No. 4	29° 59′ 36.66″ N	58° 07′ 19.50″ E
Barchan No. 5	29° 59′ 33.52″ N	58° 07′ 29.89″ E
Barchan No. 6	30° 00′ 01.96″ N	58° 06′ 49.81″ E
Barchan No. 7	30° 00′ 05.11″ N	58° 07′ 05.30″ E
Barchan No. 8	29° 59′ 53.91″ N	58° 06′ 58.68″ E

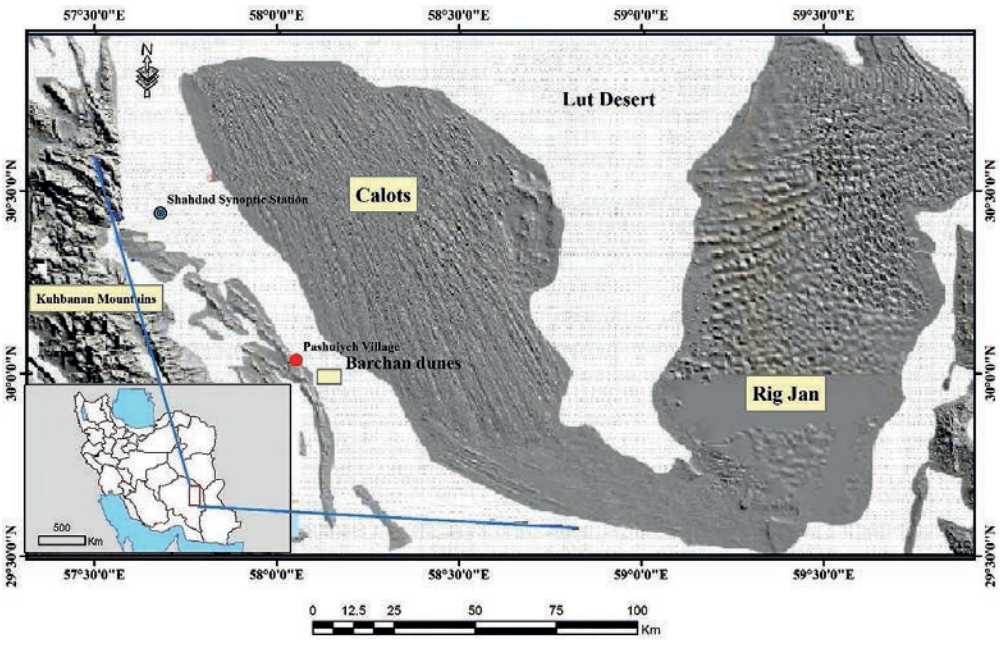

Fig. 1 Location of barchan dunes studied.

et al. 2015, 2016; Al Mutiry et al. 2016; Michel et al. 2018; Fu et al. 2019; Hu et al. 2019; Abdelkareem et al. 2020). In Iran, several studies have been conducted on the morphology of barchan dunes, especially barchans (Negaresh et al. 2008; Maghsoudi et al. 2018a, 2018b).

Barchan dune is one of the most common desert forms caused by the accumulation of barchan particles and wind erosion. According to the above, in this study, according to eight barchan dunes located in west Lut, the morphometric features, the relationships between them and the extent of their movement

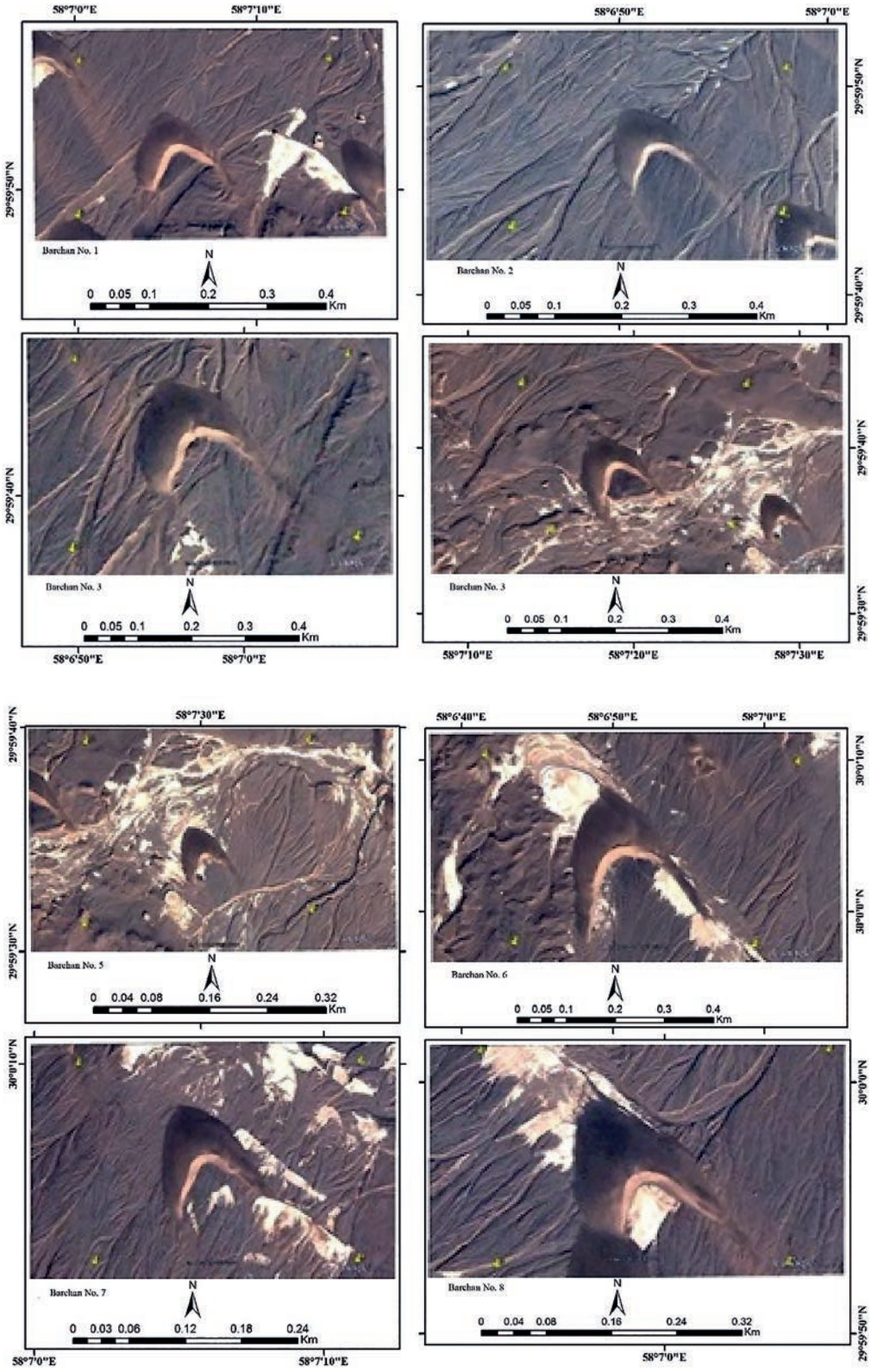

Fig. 2 Location of barchan dunes studied in Google earth image.

during 2005–2019 have been analyzed. It should be noted that Maghsoudi et al. in two studies investigated the morphometry of barchan dune and the movement of Pashuiyeh in west Lut, and the study area in this study is the same area in the study by Maghsoudi et al. However, the period studied for estimating the movement in the study by Maghsoudi et al. (2018a) was 1967–2005, while in the present study, the period 2005–2019 was investigated and it was attempted to complete the study by Maghsoudi (2018a). For the analysis of morphometric parameters of Barchan dune, Maghsoudi et al. (2018b) examined seven Barchan dunes in Pashuiyeh, which were different from eight barchan dunes in this study in Pashuiyeh. The novelty of this study is that so far, few studies have been conducted in the field of morphology and movement of barchan dunes in Iran and this study is one of the new studies in this field. Given that this region is newly registered as a natural monument in UNESCO cultural heritage, so the introduction of its features is very important.

2. Study area

The studied barchan dunes are located in Pashuiyeh village in Kerman Province and east of this city. This village is located at an altitude of 360 m above sea level. The barchan dunes are located to the east of Pashuiyeh village, and to the west are sediments from the Pleistocene.

3. Methodology

In this study, using google earth images, eight barchan dunes were identified in west Lut and Pashuiyeh village and were used as target barchan dunes in the analysis of morphometric relationships between certain parameters. In order to measure the length and average width of the barchan dunes, satellite images downloaded from google earth and during 3 days, the height of the barchan dunes was measured using GPS. In this way, first the absolute height of the area was measured by GPS and then the difference in height of the mentioned point with the barchan dune peak was measured. The morphometric parameters of barchan dunes included windward slope length (Lo), back-to-wind length (LS), right arm length (La), left arm length (Lb), length (L), width (W), left width (Wb) and right width (Wa). The position of the above parameters is shown in a schematic of barchan dunes.

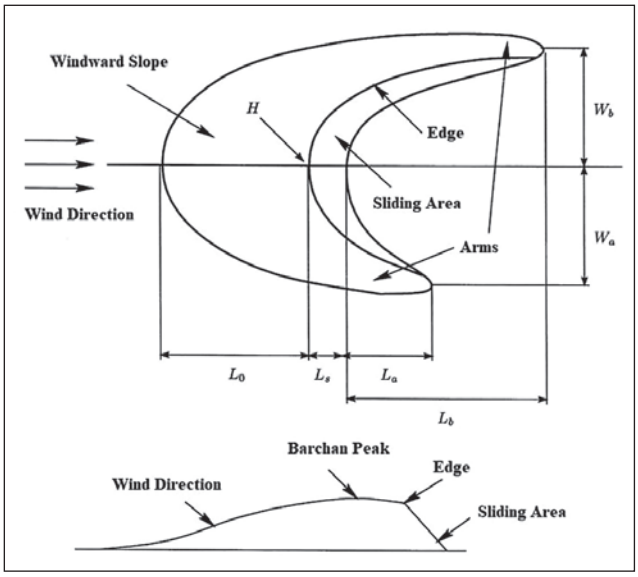

Fig. 3 Parameters used in morphometry of barchan dunes (Sauermann et al. 2000).

Among the above parameters, only the calculation of two parameters of length and width of barchan dunes requires the use of the following equations. This equation is also used to calculate the width of barchan dunes:

$$L = Lo + Ls + (La + Lb)/2$$

In this equation, La is the length of the right arm, L is the length of the barchan, Lo is the length of the windward slope, Lb is the length of the left arm, and Ls is the length of the leeward slope. This equation is also used to calculate barchan width:

$$W = Wa + Wb$$

In this equation, Wa is the right width and W and Wb are the barchan width and the left width. After estimating the above morphometric parameters, the relationship between the components was calculated using Pearson correlation by SPSS software and finally the values of coefficient of determination (R^2) were estimated by Origin 8 software and the wind direction and speed were drawn for the study area. Finally, using satellite images, the movement of the barchan dunes was measured during 2005–2019. In order to investigate the movement the barchan dunes, satellite images of google earth have been used. In this way, the images of 2005, 2017 and 2019 were first downloaded in digital form and by Arc GIS, the barchan dunes were drawn from the images.

4. Results and discussions

In this study, the morphometric properties of eight barchan dunes were measured and the morphometric components of windward slope, back-to-wind slope, right arm length, left arm length, length, width, left width and right width were estimated. Barchan dune 6 had the highest windward slope length (96.44 m) and Barchan dune 1 had only 28.93 m of windward slope length. Barchan dune 8 was in the second place in terms of the windward slope length (71.98 m). The

Tab. 2 Morphometric parameters calculated in eight studied barchan dunes to meter.

Row	Length of windward slope (Lo)	Length of leeward slope (Ls)	The length of the right arm (La)	The length of the left arm (Lb)	Length (L)	Width (w)	Left width (Wb)	Right width (Wa)
1	28.93	9.82	28.28	39.02	75.02	72.54	34.72	37.84
2	57.29	8.32	39.56	62.96	107.89	84.56	38.77	45.79
3	39.46	7.78	24.64	38.57	74.59	54.71	21.60	33.11
4	61.27	12.83	45.20	64.52	122.8	97.41	37.43	59.98
5	43.47	9.90	30.53	43.23	83.96	61.39	24.25	37.14
6	96.44	16.50	108.42	157.15	208.30	190.73	84.79	105.94
7	43.35	6.41	29.23	54.69	83.99	68.46	31.86	36.60
8	71.98	10.51	30.71	57.36	113.98	62.98	31.08	31.90

difference in windward slope length between these 8 barchan dunes was significant and about 43.05 m. Also, Barchan dune 6 had the highest back-to-wind slope length (16.5 m). Barchan dune 7 had the lowest back-to-wind slope length (6.41 m). Barchan dune 4 was in second place in terms of back-to-wind slope length (10.51 m). Barchan dune 6 had the highest right arm length (108.42 m) and Barchan dune 3 had the lowest right arm length (24.64 m). A significant difference was between the highest right arm length and the second one, which was for Barchan dune 4 (45.20 m). The reason for this is not clear, but this difference is more than double. In the meantime, it is observed that the differences in the right arm length were very close among other barchan dunes. This can be considered as an exception. Barchan dune 6, which was in the top position among 8 barchan dunes in terms of other morphometric components, was also in the first place in terms of the left arm length (157.15 m). Barchan dune 3 has the lowest left arm length (38.57 m). The exceptional width of Barchan dune 6 is still visible in the left arm length. For the length, which was calculated from the equation of the right and left arm length, Barchan dune 6 had the highest length (208.3 m). Barchan dune 3 had the lowest length (74.59 m). Barchan dune 3 had the lowest left width (21.6 m). Also, Barchan dune 6 had the highest width. Barchan dunes 1, 2, 4, 7 and 8 had very close values, but Barchan dune 6 had a significant difference in all morphometric parameters. Barchan dune 3 had the lowest width and Barchan dune 6 had the highest width (105.9 m). It can be said that almost all barchan dunes except Barchan dune 6 had the same right length relative to each other. For the width, which is obtained from the equation of left and right width, Barchan dune 6 had the highest width (190.7 m) and Barchan dune 3 had the lowest width (54.7 m).

In order to measure the wind direction and speed in the study area, the data of Shahdad synoptic station, which is 60 km away from the study area, had been used. The location of this station is shown in the map of the study area. The windrose diagram shows that most of the wind that blows in the study area has a speed of more than 11 meters per second and blows from the north. This explains the direction to the south of the barchan dunes.

In order to calculate the correlation between the barchan dune components, SPSS software and Pearson correlation method were used, the results of which are shown in Table 3. According to the data displayed in the Table above, the following results were obtained:

The windward slope length along with the length had the highest correlation (0.958). The back-to-wind slope length along with the length had a high correlation equal to 0.881. The right arm length had a high correlation of 0.993 and the left arm length had a correlation of 0.989. Also, the length along with the left arm length had a correlation equal to 0.977.

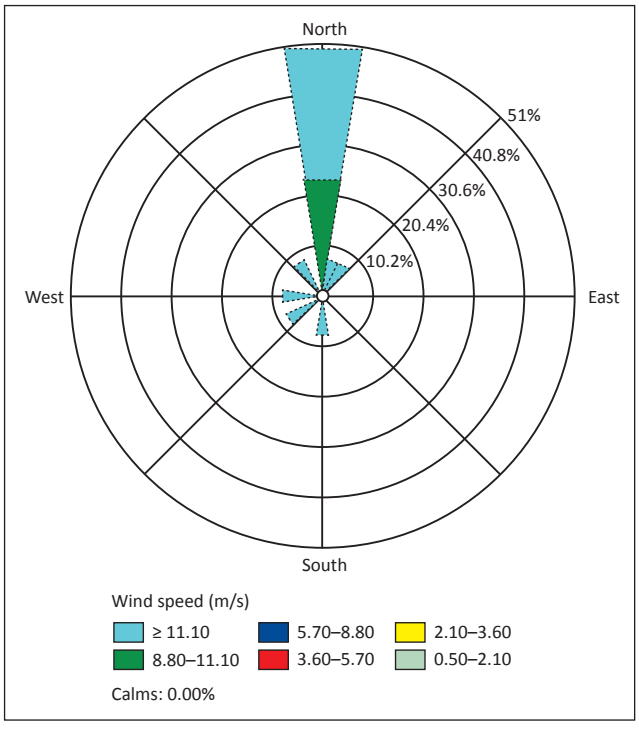

Fig. 4 The windrose diagram in the study area.

Tab. 3 Values of Pearson correlation between the factors used.

		Lo	Ls	La	Lb	L	Wa	Wb	W
Lo	Pearson Correlation	1	.858**	.873**	.900**	.958**	.825*	.875**	.856**
	Sig. (2-tailed)		.006	.005	.002	.000	.012	.004	.007
	N	8	8	8	8	8	8	8	8
Ls	Pearson Correlation		1	.859**	.815*	.881**	.872**	.816*	.856**
	Sig. (2-tailed)			.006	.014	.004	.005	.014	.007
	N		8	8	8	8	8	8	8
La	Pearson Correlation			1	.989**	.966**	.986**	.979**	.993**
	Sig. (2-tailed)				.000	.000	.000	.000	.000
	N			8	8	8	8	8	8
Lb	Pearson Correlation				1	.977**	.959**	.977**	.977**
	Sig. (2-tailed)					.000	.000	.000	.000
	N				8	8	8	8	8
L	Pearson Correlation					1	.943**	.943**	.952**
	Sig. (2-tailed)						.000	.000	.000
	N					8	8	8	8
Wa	Pearson Correlation						1	.960**	.992**
	Sig. (2-tailed)							.000	.000
	N						8	8	8
Wb	Pearson Correlation							1	.987**
	Sig. (2-tailed)								.000
	N							8	8
W	Pearson Correlation								1
	Sig. (2-tailed)								
	N								8

** Correlation is significant at the 0.01 level (2-tailed).
* Correlation is significant at the 0.05 level (2-tailed).

It was also observed that the right width along with width had a correlation of 0.992 and the width along with the right arm length had a correlation of 0.993. In the meanwhile, the windward slope length along with the right width had a slight correlation equal to 0.825 and the back-to-wind slope length along with the right arm length had a correlation equal to 0.815. Also, the right arm length along with the back-to-wind slope length had a correlation of 0.859. The correlation between the left arm length and the back-to-wind slope length was equal to 0.815. Finally, the correlation between length and back-to-wind slope length; right-width and windward slope length; left-width with back-to-wind slope length, and width and windward and back-to-wind slope length was 0.881, 0.825, 0.816 and 0.856, respectively. The results of Pearson correlation showed that the highest correlation of 0.993 was observed between the width and the length of the right arm and the lowest correlation was observed between the back-to-wind slope length and the left arm length.

The values of coefficient of determination (R^2) were estimated for 7 factors with the highest correlation as follows. According to the obtained values, it is observed that the highest coefficient of determination (0.9845) belongs to the width and length of the right arm and the lowest coefficient of determination (0.7666) belongs to the length of the back-to-wind slope length. The relationship between width and left width (0.9813) in terms of the highest coefficient of determination was in the second place. At this stage, using the parameters mentioned in the relevant Table, the regression equation was calculated among the factors that had the highest correlation and coefficient of determination with respect to each other.

Using the components of mean, standard deviation and Pearson correlation coefficient, the linear regression equation was calculated between the factors that had the highest correlation with each other. The above values are shown in the Table below.

Finally, the movement of barchan dunes was calculated during 2005–2019. The reason for using these time periods was the adaptation of the Gregorian calendar data with the solar calendar in Iran. In addition, the special attention of state officials in matters related to villages during these periods has led to an emphasis on these years. Studies have shown an inverse relationship between movement rate and the

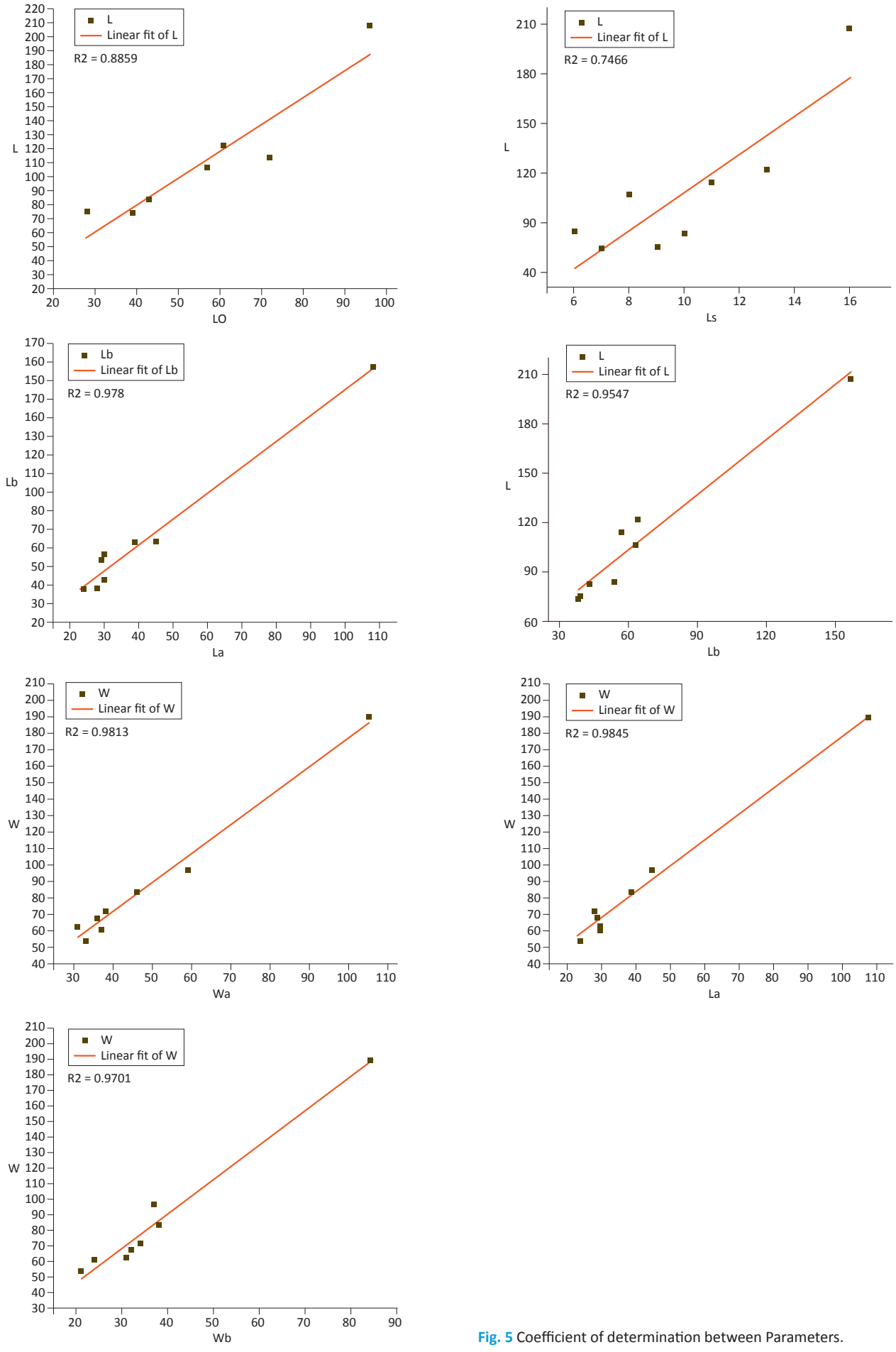

Fig. 5 Coefficient of determination between Parameters.

Tab. 4 Statistical values of components used for morphometric analysis of barchan dunes.

Statistical parameters	Minimum	Maximum	Total	Average	Standard deviation	Variance	Skewness	Kurtosis
Lo	39.46	96.44	459.48	57.4350	19.23524	369.994	1.331	1.505
Ls	6.41	16.50	81.97	10.2463	3.17907	10.106	1.085	1.282
La	24.64	108.42	336.57	42.0713	27.61851	762.782	2.523	6.631
Lb	38.57	157.15	517.50	64.6875	38.74336	1501.048	2.438	6.393
L	74.59	208.30	870.53	108.8163	44.18772	1952.555	1.939	4.221
Wa	31.90	105.94	388.30	48.5375	24.88598	619.312	2.199	4.985
Wb	21.60	84.79	304.48	38.0600	19.80148	392.099	2.314	5.988
W	54.71	190.73	692.78	86.5975	44.24161	1957.320	2.332	5.794

Tab. 5 Pearson correlation coefficient, determination coefficient and regression equations of barchan dunes.

Correlated factors	Pearson correlation coefficient	Coefficient of determination	Regression equation
Lo and L	0.958	0.8859	Lo = 0.41 L + 12
Ls and L	0.881	0.7466	Ls = 0.06 L + 3.46
La and W	0.993	0.9845	La = 0.6 W − 10.4
La and Lb	0.989	0.9780	La = 0.7 Lb − 3
L and Lb	0.977	0.9547	L = 1.13 Lb + 36.6
Wa and W	0.992	0.9813	W = 1.74 Wa − 2.2
Wb and W	0.987	0.9701	W = 2.17 Wb + 3.5

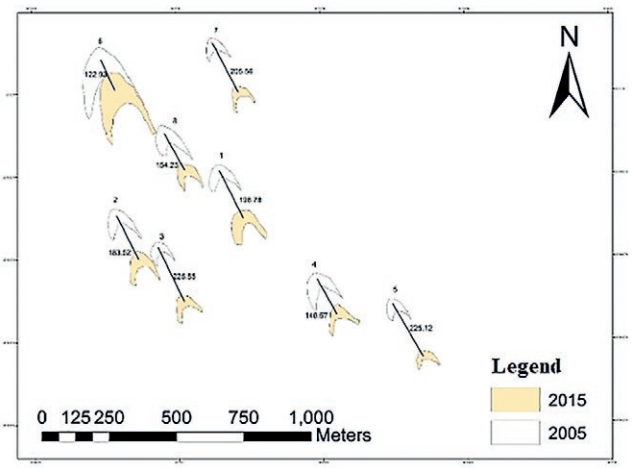

Fig. 6 Barchan movement rate from 2005 to 2015.

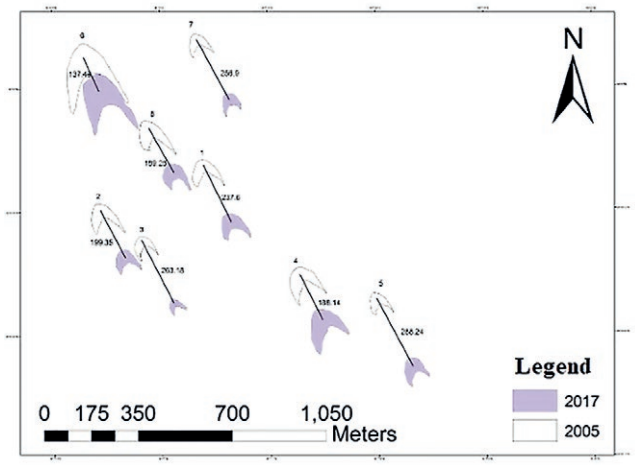

Fig. 7 Barchan movement rate from 2005 to 2017.

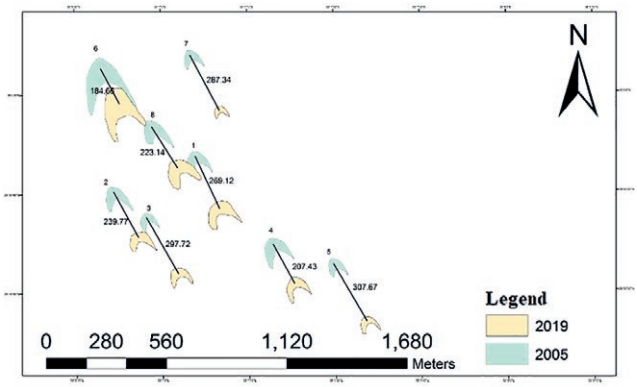

Fig. 8 Barchan movement rate from 2005 to 2019.

size of the barchan dune. The movement values for each barchan dune during the period mentioned in the Table are displayed and extracted from satellite images.

5. Conclusion

The study area is located west Lut. This area is the main place of density of barchan dunes in west Lut. In this study, the morphometric factors of barchan dune 8 have been investigated. First, the morphometric properties of the barchan dunes such as slope length were analyzed and then Pearson correlation was calculated for these factors by SPSS software. Finally, after estimating the coefficient of determination, the regression equation was estimated for the factors that had the highest correlation. According to the results of the measurements of barchan dunes, it was found that a significant difference was

Tab. 6 Movement of barchan dunes since 2005 to 2015, 2017, and 2019.

Row	The rate of movement from 2005 to meters	Barchan No. 1	Barchan No. 2	Barchan No. 3	Barchan No. 4	Barchan No. 5	Barchan No. 6	Barchan No. 7	Barchan No. 8
1	The rate of movement to 2015	198.78	183.52	225.55	148.57	225.12	122.93	205.56	154.23
2	The rate of movement to 2017	237.60	199.35	263.18	188.14	288.24	137.49	256.90	189.28
3	The rate of movement to 2019	269.12	239.77	297.72	207.43	307.67	184.66	287.34	223.14

in the size of the components of barchan dunes relative to each other. In the meantime, Barchan dune 6 among 8 barchan dunes studied had the highest windward slope (96.44 m). The same barchan dune had the highest back-to-wind slope (16.5 m). The longest right arm was 108.42 m for Barchan dune 6. The right arm length was significant compared to the other 7 barchan dunes, so that in some barchan dunes it even reaches five times. The same barchan dune had the highest left arm length (157.15 m). Barchan dune 6 had the highest length (about 208.3 m). Also, Barchan dune 6 had the highest width, and left and right width (190.73, 84.79 and 105 m). According to the calculation of Pearson correlation between the parameters, it is observed that the left arm length and width has the highest correlation (0.993) and the back-to-wind slope length and width had the lowest correlation (0.815). At the next stage, the coefficient of determination was calculated for the parameters that had the highest correlation. The results showed that the right arm length to the width had a coefficient of determination equal to 0.9845. This was the highest among other factors. Finally, regression equations were estimated for the cases where the coefficient of determination was calculated. The rate of movement during 2005–2019 was extracted from satellite images. It can be seen that until 2015, the highest movement belonged to Barchan dune 3 (225.55 m) and the lowest movement belonged to Barchan dune 6 (122.93 m). During 2017–2019, the lowest movement belonged to Barchan dune 6 (137.49 and 184.66 m) and during 2017–2019, the highest movement belonged to Barchan dune 5 (288.24 and 307.67 m). Therefore, it was observed that during 2015–2019, the rate of movement in Barchan dune 6 has increased significantly.

References

Abdelkareem, M., Gaber, A., Abdalla, F., Kamal El- Din, G. (2020): Use of Optical and Radar remote sensing satellites for identifying and monitoring active/ inactive landforms in the driest desert in Saudi Arabia. Geomorphology 362(1), 107–197, http://doi.org /10/1016/j/geomorph.2020.107197.

Al-Harthi, A. (2002): Geohazard assessment of sand dunes between Jeddah and Al- Lith western Saudi Arabia. Environmental Geology 42, 360–369, https://doi.org /10.1007/s00254-001-0501-z.

Al-Mutiry, M., Hermas, E. A., Al-Ghamdi, K. A., Al-Awaji, H. (2016): Estimation of dune migration rate north Riyadh city, KSA, using spot 4 panchromatic image. Journal of African Earth Science 124, 258–269, https://doi.org /10.1016/j.jafrearsci.2016.09.034.

Anthonsen, K. L., Clemmensen, L. B., Jensen, J. H. (1996): Evolution of a dune from crescentic to parabolic form in response to short-term climatic change – Rabjerg-Mile, Skagen-Odde, Denmark. Geomorphology 17(1–3), 63–77, https://doi.org/10.1016/0169-555X(95)00091-I.

Anton, D., Vincent, P. (1986): Parabolic dunes of the Jafurah desert, Eastern province, Saudi Arabia. Journal of Arid Encironments 11(3), 187–198, https://doi.org/10.1016 /S0140-1963(18)31205-9.

Bagnold, R. A. (1941): The physics of Blown Sand and Desert Dunes. Methuen, London.

El belrhiti, H., Douady, S. (2011): Equilibrium versus disequilibrium if barchans dunes. Geomorphology 125(4), 558–568, https://doi.org/10.1016/j.geomorph .2010.10.025.

Brookfield, M. E., Ahlbrandt, T. S. (2000): Eolian sediments and Processes. Elsevier Science.

Daniell, J., Hughes, M. (2007): The morphology of barchan-shaped sand banks from western Torres Strait, northern Australia. Sedimentary Geology 202(4), 638–652, https://doi.org/10.1016/j.sedgeo.2007.07.007.

Finkel, H. J. (1959): The barchans of southern Peru. Journal of Geology 67(6), 614–647, https://doi.org/10.1086 /626622.

Fu, T., Wu, Y., Tan, L., Li, D., Wen, Y. (2019): lmaging the structure and reconstructing the development of a barchan dune using ground-penetrating radar. Geomorphology 341, 192-202, https://doi.org /10.1016/j.geomorph.2019.05.014.

Gay, S. P. (1999): Observations regarding the movement of barchan sand dunes in the Nazca to Tanaca area of southern Peru. Geomorphology 27(3–4), 279–293, https://doi.org/10.1016/S0169-555X(98)00084-1.

Hamdan, M. A., Refaat, A. A., Abu Anwar, E., Shallaly, N. A. (2015): Source of the Aeolian dune sand of Toshka area, south eastern western Desert, Egypt. Aeolian Research 17, 275–289, https://doi.org/10.1016/j.aeolia .2014.08.005.

Hamdan, M. A., Refaat, A. A., Abdel Wahed, M. (2016): Morphologic characteristics and migration rate assessment of Barchan dunes in the southeastern Western desert of Egypt. Geomorphology 257, 57–74, https://doi.org/10.1016/j.geomorph.2015.12.026.

Hersen, P. (2004): On the crescentic shape of barchan dunes. European Physical Journal B 37, 507–514, https://doi.org/10.1140/epjb/e2004-00087-y.

Hesp, P. A., Hastings, K. (1998): Width, height and slope relationships and aerodynamic maintenance of barchans.

Geomorphology 22(2), 193–204, https://doi.org/10.1016/S0169-555X(97)00070-6.
Howard, A. D., Morton, J. B., Gad-E1-Hak, M., Pierce, D. B. (1978): Sand transport model of barchan dune equilibrium. Sedimentology 25(3), 307–338, https://doi.org/10.1111/j.1365-3091.1978.tb00316.x.
Hu, F., Yang, X., Li, H. (2019): Origin and morphology of barchan and linear clay dunes in the shuhongtu Basin, Alashan plateau, China. Geomorphology 339, 114–126, https://doi.org/10.1016/j.geomorph.2019.04.014.
Lettau. K., Lettau. H. (1969): Bull Transport of Sand by the Barchans of the Pampa de La Joya in Southern Peru. Zeitschrift für Geomorphologie 13, 182–195.
Maghsoudi, M., Mohamadi, A., Khanbabaei, Z., Mahboobi, S., Baharvand, M., Hajizadeh, A. (2018a): Reg movement monitoring and Barchans in West of Lot region (Pashoeyeh), Quantitative Geomorphological Research 5(4), 176–189.
Maghsoudi, M., Baharvand, M., Mahboobi, S., Khanbabaei, Z., Mohammadi A. (2018b): Analysis of Barchan morphology in the west of Loot desert using morphometric features. Geographical Research on Desert Areas 6(1), 175–197, https://doi.org/10.29252/grd.2018.1247.
Michel, S., Avouac, J.-P., Ayoub, F., Ewing, R. C., Vriend, N., Heggy, E. (2018): Comparing dune migration measured from remote sensing with sand flux prediction based on weather data model, attest cuse in Qatar. Earth and Planetary Science Letters 497, 12–21, https://doi.org/10.1016/j.epsl.2018.05.037.
Negaresh, H., Latifi, L. (2008): geomorphological Analysis of Dunes Drifting process in the East of Sistan plain During recent draughts, Geography and Development 6(12), 43–60, https://doi.org/10.22111/GDIJ.2008.1242.
Sauermann, G., Rognon, P., Poliakov, A., Herrmann, H. J. (2000): The shape of the barchan dunes of Southern Morocco. Geomorphology 36(1–2), 47–62, https://doi.org/10.1016/S0169-555X(00)00047-7.
Sauermann, G., Andrade Jr., J. S., Maia, L. P., Costa, U. M. S., Araújo, A. D., Herrmann, H. J. (2003): Wind velocity and sand transport on a barchan dune. Geomorphology 54(3–4), 245–255, https://doi.org/10.1016/S0169-555X(02)00359-8.
Wang, Z.-T., Tao, S.-CH., Xie, Y.-W., Dong, G.-H. (2007): Barchans of Minqin: Morphometry. Geomorphology 89(3–4), 405–411, https://doi.org/10.1016/j.geomorph.2006.12.014.
del Valle, H. F., Rostagno, C. M., Coronato, F. R., Bouza, P. J., Blanco, P. D. (2008): Sand Dune Activity in North-eastern Patagonia. Journal of Arid Environments 27(4), 411–422, https://doi.org/10.1016/j.jaridenv.2007.07.011.
Wiggs, G. F. S., Livingstone, I., Warren, A. (1996): The role of streamline curvature in sand dune dynamics: evidence from field and wind tunnel measurement. Geomorphology 17(1–3), 29–46, https://doi.org/10.1016/0169-555X(95)00093-K.
Wippermann, F. K., Gross, G. (1986): The wind-induced shaping and migration of an isolated dune: A numerical experiment. Boundary-Layer Meteorology 36, 319–334, https://doi.org/10.1007/BF00118335.